AMERICAN UNIVERSITY OF BEIRUT

OPTIMAL DESIGN AND FEASIBILITY STUDY OF UTILITY-SCALE SOLAR POWER PLANTS IN LEBANON

by
RAND TAREK KAASSAMANI

A thesis
submitted in partial fulfillment of the requirements
for the degree of Master of Science
to the Department of Mechanical Engineering
of the Maroun Semaan Faculty of Engineering and Architecture
at the American University of Beirut

Beirut, Lebanon
April 2025

AMERICAN UNIVERSITY OF BEIRUT

OPTIMAL DESIGN AND FEASIBILITY STUDY OF UTILITY-SCALE SOLAR POWER PLANTS IN LEBANON

by

RAND TAREK KAASSAMANI

Approved by:

Dr. Joesph Zeaiter, Associate Professor Baha and Walid Bassatne Department of Chemical Engineering and Advanced Energy	Advisor
Dr. Nessreen Ghaddar, Professor Department of Mechanical Engineering	Member of Committee
Dr. Fouad Azizi, Associate Professor Baha and Walid Bassatne Department of Chemical Engineering and Advanced Energy	Member of Committee

Date of thesis defense: April 9, 2025

ACKNOWLEDGEMENTS

I would like to express my sincere gratitude to my advisor, Dr. Joseph Zeaiter, for his continuous guidance and support throughout my research. I would also like to thank my committee members, Dr. Nessreen Ghaddar and Dr. Fouad Azizi, for generously providing suggestions and constructive feedback to improve my work.

I am also grateful to my family, especially my parents, husband, and children. This journey would not be possible without their unwavering support. Their belief in me has kept my spirits high and motivated me to excel and succeed in this journey.

ABSTRACT
OF THE THESIS OF

Rand Tarek Kaassamani for Master of Science
Major: Energy Studies

Title: Optimal Design and Feasibility Study of Utility-Scale Solar Power Plants in Lebanon

Lebanon's crisis in 2019 has led to a near collapse of its energy sector, leaving the population to rely on private diesel generators and decentralized solar PV systems to meet the basic electricity needs. However, these temporary solutions are unsustainable in the long term, especially without a regulatory framework or incentives to support the development of a reliable, secure, and diversified energy sector. There is an urgent need to explore cleaner, more sustainable energy solutions that align with Lebanon's commitments under the Paris Agreement. Henceforth, it is essential to perform a comprehensive evaluation of the feasibility and impact of utility-scale solar PV and CSP power plant deployment given Lebanon's high solar potential.

This study aims at identifying the most promising sites for utility-scale solar power plants in Lebanon for future development, while predicting the electrical yield and cost of generating electricity of at the chosen site. A comparative analysis will be performed between a solar PV farm with BESS and parabolic trough and power tower CSP power plants using molten salt as HTF. The technical performance and cost of the systems modeled will be evaluated, using the following criteria: system efficiency, annual electrical yield, and levelized cost of electricity. The proposed plants have been designed with the same nameplate capacity of 50MW.

A comprehensive feasibility analysis was conducted using SAM by NREL. After performing parametric analysis and optimization of the modeled CSP plants, results showed that the performance of the power tower system is maximized at SM of 2.6 and 13h TES, while the parabolic trough system performs best with an SM of 2.4 and 6h TES. The technical and economic comparison of the optimized CSP plants and the solar PV farm with 8h BESS showed that the power tower CSP plant generates the highest annual energy generation (241.8GWh) with a capacity utilization factor of 55.21%. However, the PV farm had the highest solar to electric efficiency at 22.82% and the lowest required land area of 203 acres among the proposed power plants. Economically, the power tower CSP plant had the lowest LCOE at 14.85cents/kWh, with the parabolic trough power plant and PV farm following (18.81 cents/kWh and 26.98 cents/kWh respectively).

Lastly, this study shows that the selection of the optimal solar power plant in Lebanon depends on priorities set by the government, investors, and policy makers. Moreover,

this study provides useful guidelines for policymakers and investors and facilitates the transition towards a more sustainable and diverse energy sector in Lebanon.

Keywords: CSP plant, PV farm, utility-scale solar power plants, renewable energy, solar energy, parabolic trough, power tower, optimization, feasibility, SAM software, energy sector, Lebanon.

TABLE OF CONTENTS

ACKNOWLEDGEMENTS 1

ABSTRACT 2

ILLUSTRATIONS 8

TABLES 11

ABBREVIATIONS 12

INTRODUCTION 14

1.1. The Current Status of the Lebanese Electricity Sector 14

1.2. Solar Energy Potential in Lebanon 17

1.3. Statement of Research Problem 18

1.4. Purpose of the Study and Research Question 19

1.5. Overview of Paper Methodology and Content 19

LITERATURE REVIEW 21

2.1. Types of Utility-scale Solar Plants: Key Concepts, Market Trends, and Global Deployment 21

2.1.1. Utility-scale Solar PV Farms 21

2.1.2. CSP Plants 22

2.1.3. Global Deployment Status: Solar PV Farm vs CSP 24

2.1.4. Market Trends of Solar PV Farm vs CSP 26

2.1.5. Comparison between Solar PV Farms and CSP Plants 28

2.2. Framework of Utility-scale Solar Plants in Lebanon 31

2.2.1. Financial Model of Utility-scale Solar Projects in Lebanon 31
2.2.2. PPA Model in Power Projects 32
2.2.3. Political Challenges 33
2.2.4. Public Involvement and Social Challenges 34

2.3. Selected Studies Relevant to the Research 35

2.4. Gaps in Existing Knowledge 40

METHODOLOGY 42

3.1. Research Methodology 42

3.1.1. Selection of the Financial Model in SAM 42
3.1.2. Site Specific Parameters and Meteorological Data 44
3.1.3. Design of Utility-Scale Solar PV and CSP Power Plants 46
3.1.4. Optimization Analysis for CSP Power Plants and Simulation of Solar PV Farm 48

3.2. SAM software by NREL 49

3.3. Limitations in Implementation 50

DESIGN OF UTILITY-SCALE SOLAR POWER PLANTS 52

4.1. Site Selection and Solar Resource Data 52

4.2. Modeling and Design of 50MW CSP Plant 56

4.2.1. Selection of Common Design Points 56
4.2.2. Solar Field and Receiver Design of Proposed CSP Power Plants 58
4.2.3. HTF and Thermal Energy Storage System 62
4.2.4. Solar Field Control of CSP Power Plants 65
4.2.5. Power Cycle Modeling of the CSP Power Plant 66
4.2.6. Efficiency of the CSP Plant 67
4.2.7. CSP Plant Optimization Approach 68

4.3. Design of 50MW PV Farm 68

4.3.1. Characteristics and Design Parameters of the PV Modules 69
4.3.2. Inverter Characteristics and Design Parameters 70
4.3.3. BESS Design Parameters 71

4.4. Economic Modeling for Solar PV and CSP Power Plants 72

RESULTS AND DISCUSSION 76

5.1. Optimization Results of CSP Plant 76

5.1.1. Optimization Analysis of Parabolic Trough CSP Plant 77
5.1.2. Optimization Analysis of Power Tower CSP Plant 80

5.2. Performance Analysis of the CSP Plants 84

5.2.1. Technical Analysis of Proposed CSP Plants 85
5.2.2. Economic Evaluation of CSP Plants 88

5.3. Performance Analysis of the PV Plant with BESS 89

5.3.1. Technical Analysis of the PV Plant 89
5.3.2. Economic Analysis of the PV Plant 90

5.4. Comparison between PV and CSP Plants 91

5.4.1. Electrical Energy 91
5.4.2. Comparative Efficiency and Land Utilization of the Proposed Plants 93
5.4.3. Economic Assessment of the Proposed Plants 96

5.5. Performance Assessment and Key Outcomes 97

CONCLUSION 100

6.1. Summary of findings 100

6.2. Insights and Recommendations 102

APPENDIX I 105

APPENDIX II.....107

APPENDIX III 108

APPENDIX IV 111

APPENDIX V.....113

REFERENCES 115

ILLUSTRATIONS

Figure

1. Estimated electricity demand in Lebanon since 2017 (BouKather, 2023). 15
2. Generation Capacities in 2018. Source: Adapted from (Ayoub et al., 2021) 16
3. Types of Solar CSP Technologies. Source: (World Bank, 2021) 23
4. Total capacity of CSP plants installed. Source: Adapted from IEA (2025) 25
5. Total capacity of CSP plants installed. Source: Adapted from (IRENA, 2024a) 26
6. Global weighted average of utility-scale solar PV costs, capacity factor, and LCOE. Source: (IRENA, 2024b) 27
7. Global weighted average of CSP costs, capacity factor, and LCOE. Source: (IRENA, 2024b) 28
8. Average land use of solar energy technologies. Source: (Yang, 2024) 29
9. Simplified schematic diagram of utility-scale solar PV farm with Li-ion battery storage assessed in this study 35
10. Simplified schematic diagram of CSP technologies assessed in this study. Adapted from (Hossain et al., 2024) 35
11. Financial Models in SAM for utility-scale solar power plants. 43
12. Screenshot from Global Atlas for Renewable Energy tool for site selection 45
13. Screenshot from NSRDB tool to obtain meteorological data for selected sites . 46
14. SAM modeling process 46
15. Selected locations of the CSP plant in Lebanon 53
16. Average temperature at the two selected sites. Source: NRSDB Database 54
17. GHI and DNI at Site 1. Source: NRSDB Database 55
18. GHI and DNI at Site 2. Source: NRSDB Database 55
19. PDF/CDF of direct beam irradiance (DNI) for Site 1 57
20. Selection of mean temperature (Design point temperature) at Site 1 58
21. Typical model of heliostat positioning and receiver tower for 50MW plant 60
22. Receiver thermal power directed to receiver tower (MWt) 61
23. TES thermal losses 62

24. Monthly energy produced of parabolic trough CSP plant using Theminol VP-1 vs Hitec solar salt as HTF. 64

25. PV Module Characteristics 69

26. Inverter Characteristics 71

27. Manual dispatch strategy for the BESS 72

28. Parametric analysis on real discount rate 74

29. Variation of capacity factor based on different SMs for parabolic trough CSP plant 77

30. Variation of energy concentration based on different SMs for parabolic trough CSP plant 78

31. Variation of LCOE based on different SMs for parabolic trough CSP plant 79

32. Annual energy and LCOE trend with varying TES hours for parabolic trough CSP plant 80

33. Variation of capacity factor based on different SMs for power tower CSP plant 81

34. Variation of energy concentration based on different SMs for power tower CSP plant 82

35. Variation of LCOE based on different SMs for power tower CSP plant 83

36. Annual energy and LCOE trend with varying TES hours for power tower CSP plant 84

37. Monthly energy generated from parabolic trough vs power tower CSP plant ... 85

38. Performance comparison of power tower and parabolic trough CSP power plants 86

39. Comparison of CSP plants: power plant and solar field efficiency 87

40. Annual after-tax cashflow of the proposed CSP plants 88

41. Monthly energy generated for PV solar farm + BESS 89

42. Annual after-tax cashflow of the proposed PV plant with Li-ion battery storage 90

43. Annual energy produced and capacity factor for the proposed solar power plants 92

44. Cumulative energy produced by PV and CSP plants 93

45. Solar to electric efficiency of the solar power plants 94

46. Land use factor of the proposed PV and CSP plants 96
47. Lebanon’s DNI Map. Source: Global Solar Atlas 105
48. Lebanon’s GHI Map. Source: Global Solar Atlas 106
49. Electrical Transmission Network in Lebanon. Source: EDL 107
50. Selected PV module datasheet 113
51. Selected inverter datasheet 114

TABLES

Table

1. Site Specific Parameters. Source: (IRENA, 2025) 53
2. Economic results of solar PV and CSP power plants 96
3. Summary of key technical and economic results..... 98
4. Design Parameters of 50MW Parabolic Trough CSP plant..... 108
5. Cost Parameters of 50MW Parabolic Trough CSP Plant 109
6. System Design Parameters of 50MW Power Tower CSP Plant..... 109
7. Cost Parameters of 50MW Power Tower CSP Plant..... 110
8. Characteristics of the PV module, inverter, and battery 111
9. System Design Parameters of 50MW solar PV Farm..... 111
10. Cost Parameters of 50MW Solar PV Farm..... 112

ABBREVIATIONS

BESS	Battery Energy Storage Systems
CSP	Concentrating Solar Power
DNI	Direct Normal Irradiation
EDL	Electricite Du Liban
EPC	Engineering, procurement, and construction
GHG	Greenhouse gases
GHI	Global Horizontal Irradiation
GWh	Gigawatt-hour
HFO	Heavy Fuel Oils
HTF	Heat Transfer Fluid
IEA	International Energy Agency
IPCC	Intergovernmental Panel on Climate Change
IRENA	International Renewable Energy Agency
kW	Kilo Watt
LCEC	Lebanese Center for Energy Conservation
LCOE	Levelized cost of electricity
MW	Megawatt
NCC	Net Capital Cost
NEEAP	National Energy Efficiency Action Plan
NPV	Net Present Value
NREAP	National Renewable Energy Action Plan
NREL	National Renewable Energy Laboratory

NSRDB	National Solar Radiation Database
PPA	Power Purchase Agreement
PV	Photovoltaic
SAM	System Advisor Model - NREL
SM	Solar Multiple
TES	Thermal Energy Storage

CHAPTER 1

INTRODUCTION

1.1. The Current Status of the Lebanese Electricity Sector

The energy crisis in Lebanon dates to the 1980s. Since then, the country has not been able to cover its energy demand, resulting in regular and daily blackouts. The crippling energy crisis worsened by its dependency on fuel imports because of the devaluation of Lebanese currency over the past five years. As a result, the electricity sector collapsed, and power cuts worsened. Blackouts that used to last for three to six hours could now leave entire areas with no more than two hours of state power a day.

The lack of affordable and reliable electricity has had a rippling effect on economic and social welfare, causing limited economic growth and constrained productivity. Due to frequent blackouts, citizens were forced to rely on expensive, polluting, and unsubsidized private community-based generators. It was estimated that in 2018 private diesel generators filled the gap by supplying 1200MW while EDL supplied 1800MW. Following the total collapse of the electricity sector, EDL production fell by 500-600MW in 2021, barely providing 1-3 hours of electricity per day with chronic blackouts (Ayat, 2021). In addition, lifting the diesel subsidies in 2021 led to a sharp increase in the tariff of private diesel generators, ranging between 50-100$ cents/kWh. Consequently, the average demand for electricity dropped further to 52% in 2022 as compared to 2019 due to unaffordability of soaring electricity prices to more than half of the Lebanese population, as shown in Figure 1 (BouKather, 2023).

The collapse of the electricity sector has also caused a surge in decentralized solar applications where solar production capacity reached an estimate of 690MW in 2022, as

shown in Figure 1. Despite the lack of favorable policies and regulatory frameworks and encouraging financial incentives, solar installations represented a 7-fold increase since the start of the crisis (BouKather, 2023).

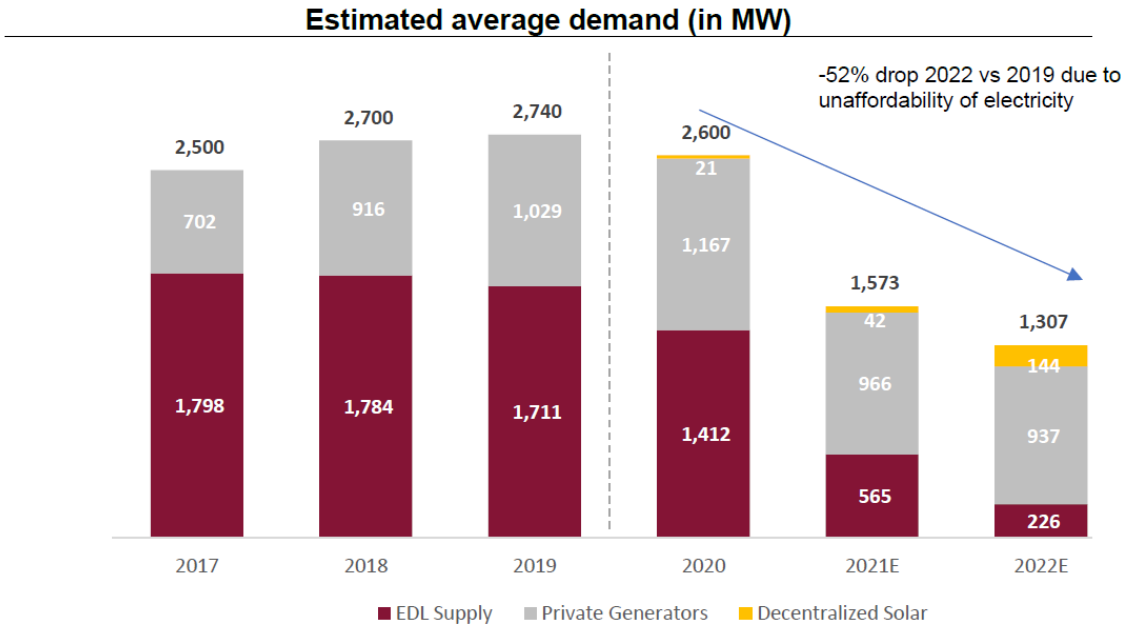

Note: Solar production assumes a 21% annual average capacity factor, an installed capacity of 200MW for 2021 and 690MW for 2022.

Figure 1. Estimated electricity demand in Lebanon since 2017 (BouKather, 2023).

The crisis in Lebanon's electricity sector have resulted in heavy financial burdens on both the government and consumers. The levelized cost of energy (LCOE) varies significantly across different energy sources in the country. Figure 2 shows the electricity generation costs in Lebanon in 2018 (Ayoub et al., 2021). The lowest generation costs are for the hydropower plants, with costs ranging between 2.65 and 3.97 cents/kWh. On the other hand, thermal and combined cycle power plants using heavy fuel oil and diesel oil have generation costs ranging between 13 to 21.44 cents/kWh.

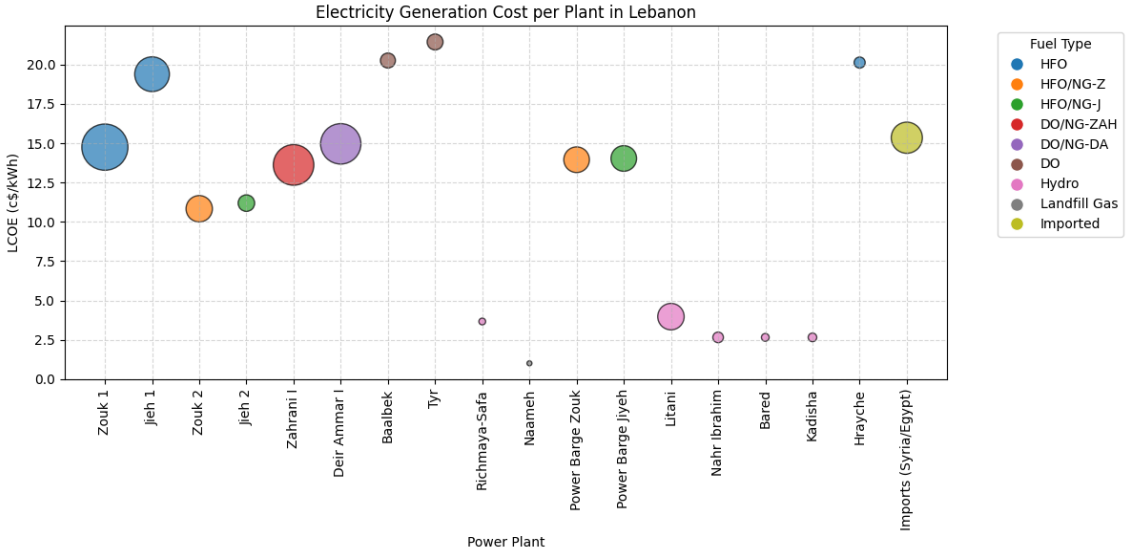

Figure 2. Generation Capacities in 2018. Source: Adapted from (Ayoub et al., 2021)

According to the Global Carbon Atlas, the energy sector in Lebanon is the main contributor to GHG emissions, accounting for more than 79% of the total emissions. And on top, due to the heavy use of private generators following EDL collapse, pollution levels increased by 300% by year 2021 (Ayat, 2021). The proposed solutions to date in response to the collapse of EDL do not address the long-term sustainability of the sector. Therefore, it is necessary to reform the electricity sector through rebalancing EDL financials to secure investments across the sector to provide affordable, sustainable, and clean energy and allow an increased deployment of renewables with a clear regulatory framework and financial incentives. The integration of large-scale renewable energy plants in the Lebanese energy sector is crucial to diversify the energy mix and pave the way forward to achieve reliability and energy security. On March 2019, Lebanon ratified the Paris Agreement and committed to achieve 30% of its power demand from renewable energy by 2030 and set the GHG reduction target to 31% (UNFCC, 2020). While efforts have primarily focused on solar photovoltaic (PV)

power, Concentrated Solar Power (CSP) technology presents an untapped opportunity due to Lebanon's high solar irradiation levels. Considering the above, solar energy generation technologies present a possible contribution to the future energy mix in Lebanon while reducing CO_2 emissions significantly.

1.2. Solar Energy Potential in Lebanon

Lebanon is a Mediterranean country characterized with an average of 300 sunny days and a yearly average solar irradiation of 2,200 kWh/m2. The high solar radiation level makes it interesting to explore this resource abundantly, relying on solar energy as a renewable energy resource (See APPENDIX I). Solar PV power and solar thermal or CSP generation are two types of utility-scale solar converting solar energy to electricity (Yang, 2024). The deployment of solar PV farms and CSP takes several criteria into consideration, of which:

- *Availability of solar resources:* Utility-scale solar PV farms require site locations with a global horizontal irradiance (GHI) of 1700kWh/m2/year. However, a direct normal irradiance (DNI) larger than 2000kWh/m2/year is required for CSP plant deployment.
- *Land availability, use, and terrain conditions:* CSP plants require the availability of large, accessible, and unpopulated land, excluding environmentally sensitive lands. Also, flat terrains and lower elevations are preferred to minimize shading and optimize the placement of the PV modules or heliostats.
- *Water availability:* Unlike solar PV farms, CSP plants require significant amounts of water for cooling purposes, depending on the technology used.

According to a study done by Berjawi et al. (2016), around 148m^2 of Lebanon's total area are suitable areas for utility-scale solar PV with promising technical and economic viability and least social and environmental drawbacks. Alternatively, a study done by CEDRO (2013) on the CSP potential in Lebanon mentioned that more than 76% of the total land area of Lebanon is subject to more than 2000kWh/m^2 DNI. Moreover, 42% of the total land area of Lebanon are categorized as scrubland, grassland, and bare soils, of which 28% have a land slope of less than 1%. These results show that Lebanon has a significant potential for both utility-scale PV and CSP deployment.

Therefore, it is interesting to perform a comparative analysis between solar PV farms and CSP technologies and their possible integration into the existing energy infrastructure in Lebanon.

1.3. Statement of Research Problem

Following the Lebanese crisis in 2019, there was a huge surge in decentralized solar applications despite lacking a regulatory and financial framework (BouKather, 2023). Current applications in solar energy focus on decentralized solar PV after the collapse in the Lebanese electricity sector. However, a comprehensive evaluation of the feasibility of utility-scale solar plants in Lebanon has not been assessed yet. Existing studies are either global or specific to regions with developed infrastructure and policy frameworks, such as the Gulf Region and North America. There is a gap in research that examines large scale solar plants' applicability and potential in Lebanon's unique climatic, economic, and political context. This research aims to fill these gaps by

providing a technical and economic assessment of both PV farms and CSP power plants in Lebanon.

1.4. Purpose of the Study and Research Question

The primary purpose of this study is to explore the performance of utility-scale solar plants in Lebanon. In this context, this study aims at identifying the most promising site for solar plants in Lebanon for future development, while predicting the electrical yield and cost of generating electricity of at the chosen site. Additionally, a comparative analysis will be performed between a solar PV farm with battery energy storage systems (BESS) and parabolic trough and power tower CSP power plants using molten salt as heat transfer fluid (HTF). The technical performance and cost of the systems modeled will be evaluated, using the following measures: system efficiency, annual electrical yield, and levelized cost of electricity. The power plants studied will have a nameplate capacity of 50MW to ensure a fair comparison. This capacity was chosen instead of 100MW due to land constraints, limited water resources, and high initial investment requirements. Additionally, a 50MW plant allows for a phased deployment strategy once the power plant's feasibility is proven.

Particularly, this study aims to answer the following research question:

- What is the optimal design and technical economic feasibility of implementing utility-scale solar power plants in Lebanon?

1.5. Overview of Paper Methodology and Content

Chapter 2 of this paper contains a literature review on both technologies, solar PV and CSP power plants, in addition to the global deployment status and the latest

market trends. Also, a review on the framework of utility-scale solar power plant implementation in Lebanon will be discussed. Chapter 3 will explain the research methodology implemented to model the solar PV farms and CSP plants within the scope of this study. Chapter 4 will explore the methodology followed to optimize the 50MW CSP plants and select the optimal design parameters. In addition, this chapter will also explore key design parameters for the solar PV farm. Then, Chapter 5 will discuss the results of the simulations done and perform a comparative technical economic assessment of the performance of the solar plants studied. Finally, Chapter 6 wraps up the paper with some conclusions and recommendations.

CHAPTER 2

LITERATURE REVIEW

In this chapter, a review of the literature on solar PV farms and CSP technologies, market trends, and global deployment will be presented. The data sources include published research articles in peer-reviewed journals, referred books, and published dissertations. The first section includes key concepts of solar PV and CSP technologies, the global deployment of solar generation projects during the past years, and the latest market trends concerning average installed costs, capacity factor, and LCOE. The second section touches on the framework of utility-scale solar projects in Lebanon and addresses the political and public involvement and social challenges that arise due to these projects. The third section of this chapter highlights previous literature works that were developed on utility-scale solar projects and assesses the technical and economic potential of these technologies. It concludes by addressing the gap in existing literature on implementing these projects in Lebanon thus providing a sound rationale for conducting this study.

2.1. Types of Utility-scale Solar Plants: Key Concepts, Market Trends, and Global Deployment

Electricity generation from solar energy involves two main technologies: Concentrated Solar Power (CSP) and Photovoltaic (PV) systems (Yang, 2024).

2.1.1. Utility-scale Solar PV Farms

Utility-scale solar PV farms refer to plants larger than 1MW in capacity and are designed to feed directly onto the electrical grid, unlike distributed solar PV systems

connected for local consumption (LCEC, 2016). The main components of solar PV farms mainly include the solar PV modules and mounting structures, inverters, balance of system (BOS) – which consists of wiring, connectors, monitoring systems, and power conditioning equipment – energy storage systems for grid stability and dispatchability, and finally the transformers and substations to step up voltage for transmission and integration into the electrical grid (IEA, 2011).

2.1.2. CSP Plants

Unlike PV technology which harnesses sunlight in the form of direct and indirect irradiation, CSP technologies generate electricity by reflecting, concentrating, and collecting direct normal irradiation (DNI) from the Sun to convert it to high-temperature heat. CSP technologies consist of three stages: (i) solar field consisting of mirrors, reflectors, or heliostats that concentrate sunlight and a receiver that collects the concentrated heat; (ii) power block consisting of a steam turbine and electric generator for power generation; and (iii) a thermal conversion block for heat transfer and an optional heat storage system to store the collected heat to be utilized during periods where solar irradiance can't be collected and therefore allowing longer operating hours of power generation (Yang, 2024).

There are four main configurations of solar CSP technologies, depending on the configuration of the solar collectors placed in the field. The concentration is either to a line, or linear focus, as in parabolic trough and linear Fresnel reflector, or to a point, or point focus, as in parabolic dish and solar power tower. Figure 3 illustrates the four CSP configurations (Yang, 2024).

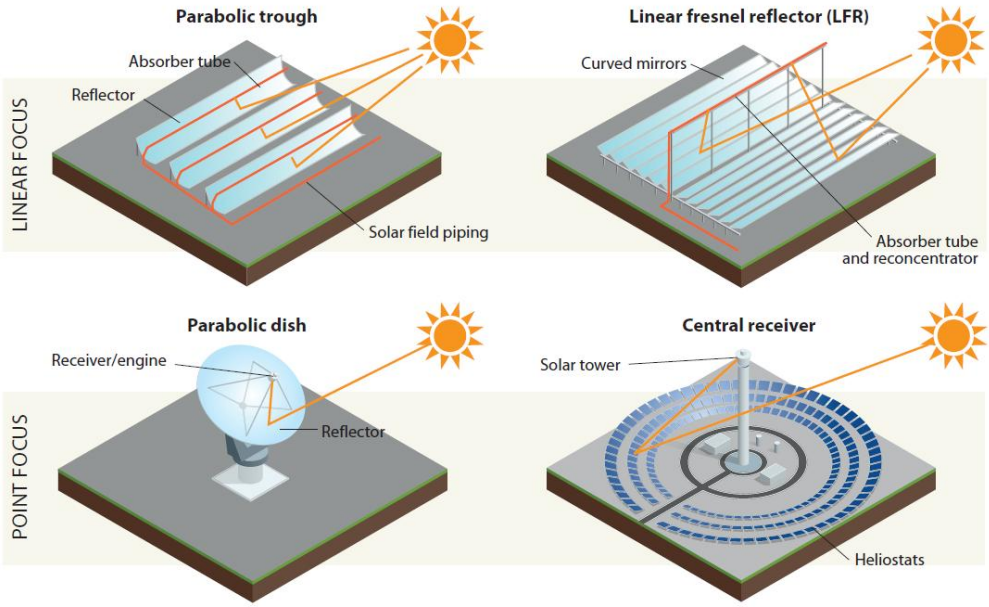

Figure 3. Types of Solar CSP Technologies. Source: (World Bank, 2021)

Parabolic trough systems are the predominant technology of CSP plants deployed to date, with a total market share of 72% (IRENA, 2024a). The solar field of the parabolic trough systems consists of parabolic shaped reflectors which concentrate direct sunlight onto a receiver tube that runs along the focal point of the trough. The receiver tube is made up of two concentric tubes. The inner tube channels the flow of the heat transfer fluid and is made up of stainless steel with a highly absorptive, low-emission coating, while the outer tube is glass with anti-reflective coating. Vacuum is created in the annular space between the inner and outer tubes thus improving the overall performance of the collector and reducing heat losses. The heat transfer fluid flowing in the receiver tube absorbs the concentrated heat and then transfers it to the power block where steam is generated to drive the turbine. The heat transfer fluid is then returned to the absorber tube after being cooled and condensed. The generation efficiency of parabolic trough collectors is typically 37.4% if thermal oil is to be used as heat transfer fluid. However, this efficiency could be significantly improved to 42.7%

while using molten salt as both heat transfer fluid and storage medium. The operating temperatures of the collectors are in the range of 150 to 400℃ and would reach 530℃ if molten salt is used as heat transfer fluid (IRENA, 2016; Yang, 2024).

Solar Power Tower, or central receiver systems, consist of a field of heliostats that surround a central receiver mounted on top of a tower. The receiver absorbs the concentrated sunlight and transfers it to a working fluid, such as molten salt, which in turn generates steam and drives the turbine to produce electricity. Heliostats vary in size ranging from $1m^2$ to $160m^2$. Larger heliostats have a higher power output but require stronger structures. However, for smaller heliostats, a larger number is required to generate the same output power. A solar tracking system changes the position of the heliostats to allow sun tracking during the day. The receiver is the core of the tower system and is designed to minimize heat losses while absorbing the incident irradiance under flux conditions. The solar heat absorbed by the receiver is then transferred to the thermal storage fluid, which in turn is used to generate steam and drive a turbine. The temperature of the heat transfer fluid reaches 565℃. The deployment of power tower plants accounts for 21% of the total CSP powerplant deployment worldwide (IRENA, 2024a). The corresponding technology is slightly less mature than parabolic trough collectors, however, the technology holds the promise of higher efficiencies and significantly lower costs with R&D advancements (IRENA, 2024a; Yang, 2024).

2.1.3. Global Deployment Status: Solar PV Farm vs CSP

According to IEA (2025), the installed capacity of utility-scale solar PV farms increased from 112GW in 2015 to 1,226GW in 2024, with an average annual growth rate of 23%, as shown in Figure 4. Alternatively, the rate of deployment of solar PV

farms differs significantly from the deployment rate of CSP plants. According to IRENA (2024a) renewable energy data statistics, the installed capacity of CSP projects grew from 419MW in 2000 to 6.9GW in 2023, as shown in Figure 5. The most significant growth in CSP installations was from 2008 to 2014, with an average annual growth rate of 33%. However, CSP expansion slowed down after 2014, with an average annual growth rate of 5% from 2014 to 2023. As per IRENA (2024a) renewable energy statistics, CSP deployment increased 1.5 folds from 2015 until 2024. However, solar PV installments increased 10 times during the same period.

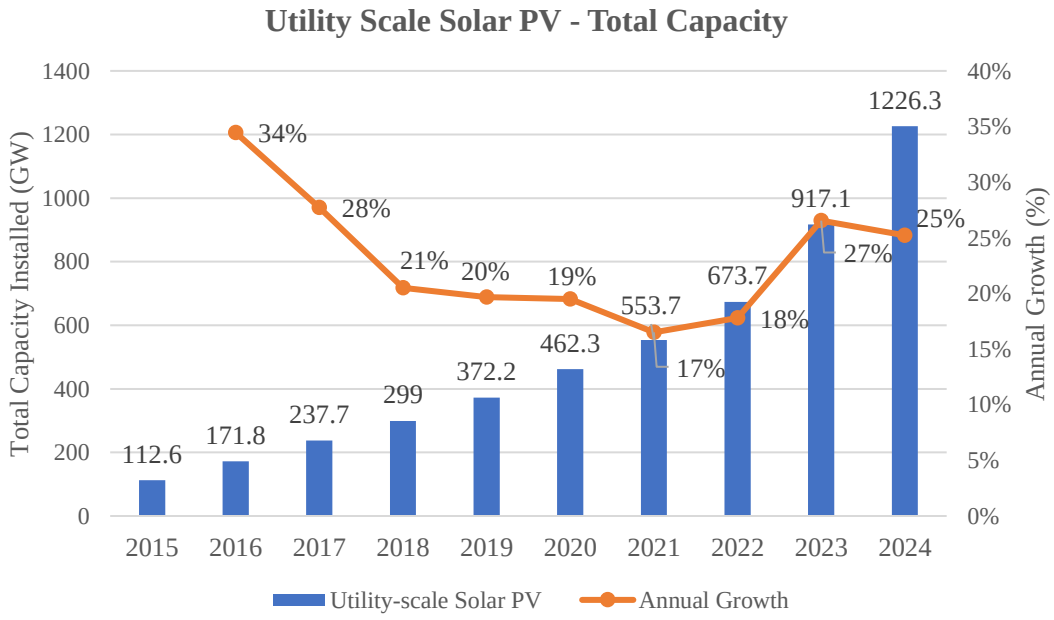

Figure 4. Total capacity of CSP plants installed. Source: Adapted from IEA (2025)

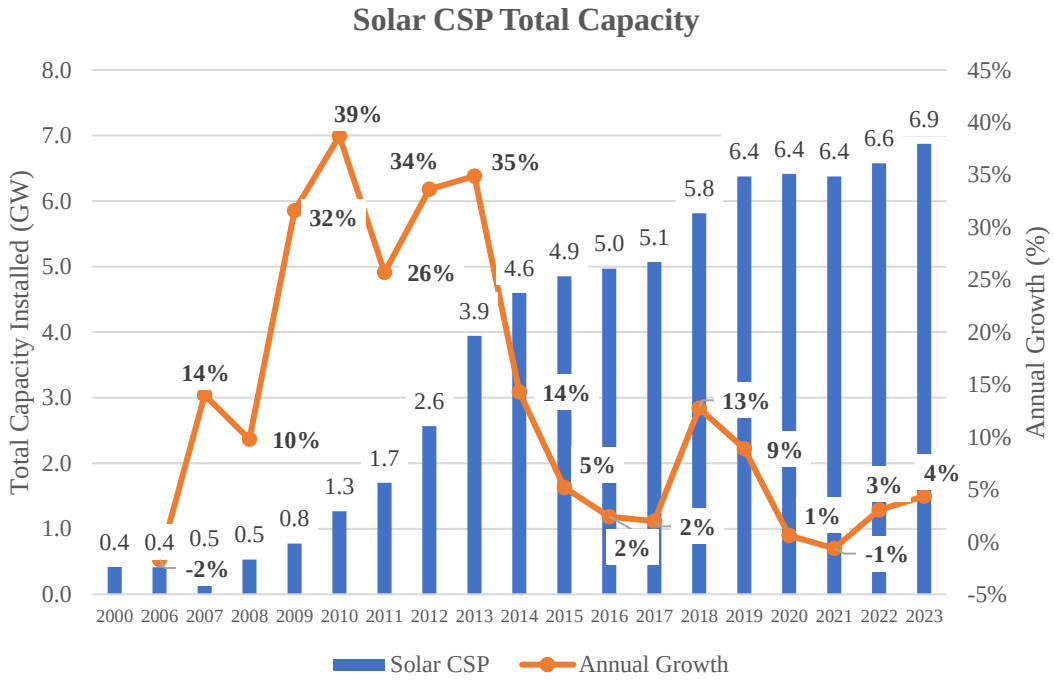

Figure 5. Total capacity of CSP plants installed. Source: Adapted from (IRENA, 2024a)

2.1.4. Market Trends of Solar PV Farm vs CSP

The cost of renewable electricity has significantly decreased since 2010 to present. This decline is mainly driven by advancements in technology, economies of scale, more competitive supply chains, and increased developer expertise. Solar PV costs have dropped by 86%, whereas CSP costs declined by 53%. As shown in Figure 6 and Figure 7, the total installed costs of solar PV without battery storage reached 758$/kW, while the installed costs for CSP plants reached 6,589$/kW in 2023 (IRENA, 2024b).

The global weighted average capacity factor of utility-scale solar PV without battery storage increased from 13.8% in 2010 to 16.2% in 2023. The increasing trend is a result of multiple interacting factors, including advanced tracking mechanisms of solar collectors, project location, solar resource availability, the growing use of bifacial modules, and advancements in the inverter loading ratio. On the other hand, the

capacity factor of CSP plants has been also increasing since 2010 from 30% to reach 42% in 2020, as shown in Figure 7. This decrease has been driven by several factors, of which improvements in technology, continuous R&D, decline in costs of energy storage, and an increase in the number of hours of storage. For instance, the excellent solar resource at Cerro Dominador CSP project location recorded a high capacity-factor of 80% in 2021 (IRENA, 2024b).

The global average LCOE of utility-scale solar PV plants without battery storage declined by 90%, from 0.46$/kWh in 2010 to 0.044$/kWh in 2023. This decrease was mainly due to the sharp decrease in module and inverter costs. The LCOE of CSP plants also witnessed a decline from 0.38$/kW in 2010 to 0.117$/kW in 2023. The major factor contributing to this decrease was installed costs reduction and continuous improvements in technology and thermal energy storage (IRENA, 2024b).

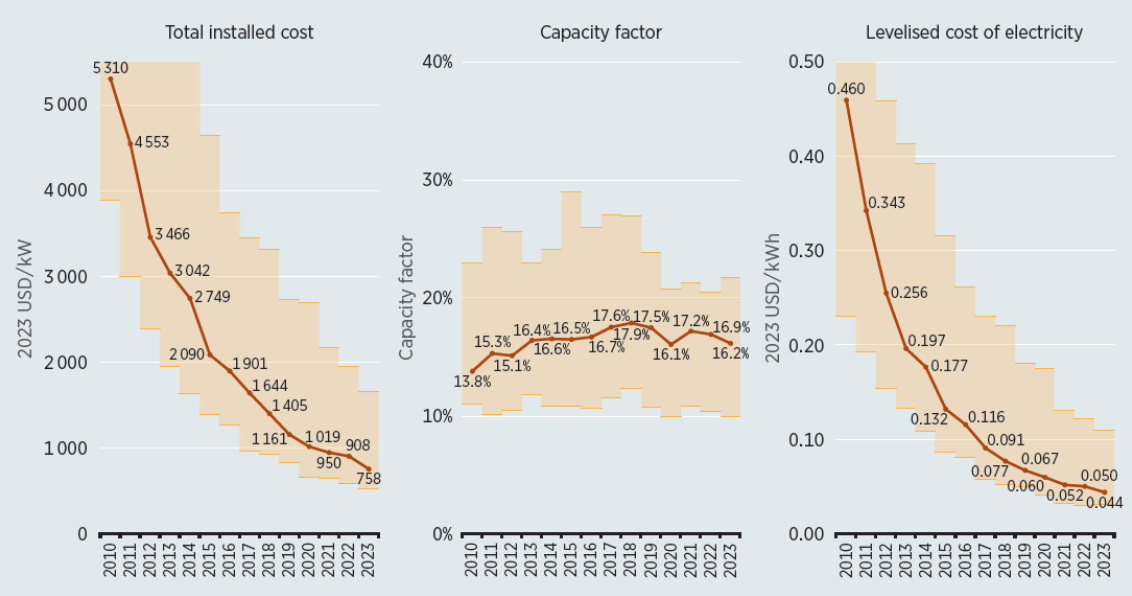

Figure 6. Global weighted average of utility-scale solar PV costs, capacity factor, and LCOE. Source: (IRENA, 2024b)

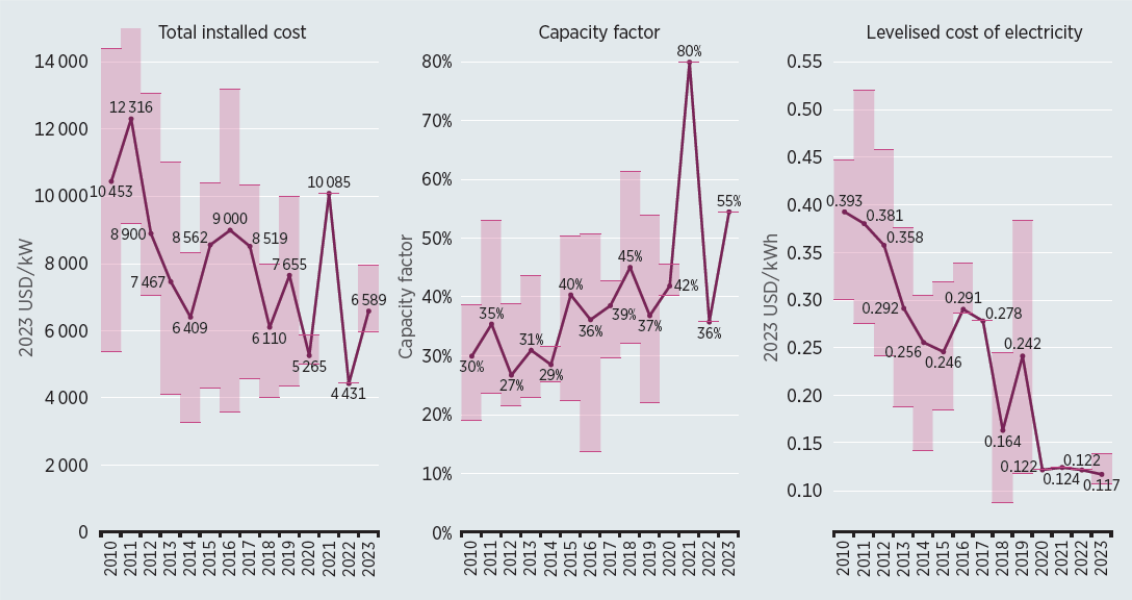

Figure 7. Global weighted average of CSP costs, capacity factor, and LCOE. Source: (IRENA, 2024b)

2.1.5. Comparison between Solar PV Farms and CSP Plants

One major challenge that both utility-scale solar PV farms and CSP power plants face is the high land area requirement. Utility-scale solar PV farms require much larger land than that of distributed solar PV. As for solar CSP plants, they are only cost-effective and efficient if they are deployed at a large scale. In geographically dense and populated countries, the limited land availability and high land prices complicate the process of siting and permission for land use. Siting permissions for land use and environmental review are usually a complicated process that takes a few years to complete because of the land constraints mentioned, the consequent environmental and ecological footprint and the significant water use.

Figure 8 shows the average land use of solar energy by technology. An average solar CSP plant requires 10acres/MW of power generation capacity, which is more demanding than solar PV farms that require 6 to 8 acres/MW. The Linear Fresnel CSP

plant has the lowest land footprint of 4.5acres/MW compared to 9.5 acres/MW and 10 acres/MW for parabolic trough and power tower CSP technologies. The difference is mainly due to the compact mirror arrangement of Linear Frensel collectors, which reduces spacing requirements compared to parabolic trough and power tower systems. In contrast, the parabolic trough solar collectors need wider spacing to accommodate their curvature and tracking mechanism, whereas the heliostats of power tower CSP plants are significantly larger and require significant spacing gaps to prevent shading and blocking (Yang, 2024).

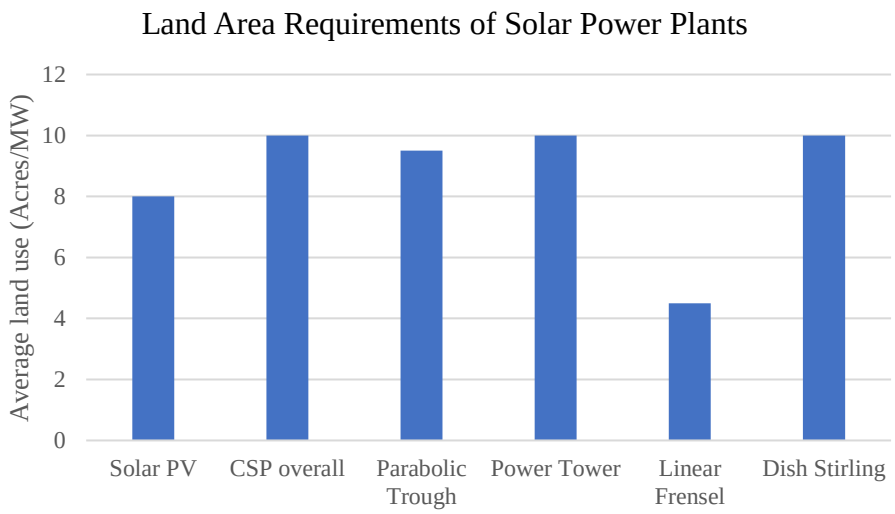

Figure 8. Average land use of solar energy technologies. Source: (Yang, 2024)

One advantage of CSP plants over solar PV farms is the energy storage. Till now, the expansion of solar power technologies is still limited by the current insufficient storage capacities worldwide. However, CSP projects are characterized by high thermal energy storage capacity, better grid stability, high-temperature heat generation, and dispatchable power. CSP technologies have the potential to be

justifiable and competitive in the energy landscape as the technology advances and economies of scale are reached. Heat storage systems integrated with CSP projects allow storage of excess heat, to be dispatched later at periods of low sunset, high demand, or after sunset. In addition, the high temperatures reached by CSP plants yield better thermodynamic efficiency in heat generation and energy storage, making CSP more suitable than PV in industrial processes (Yang, 2024).

While solar power accounts for a total of 25% of the global energy generation, of which 24% comes from solar PV, while solar CSP accounts for only 1%. The advancement in solar CSP applications has been running slower than that of solar PV, due to additional challenges that are discussed below (Yang, 2024).

- *High CSP Installation Costs:* The total installed costs of solar CSP were 10,082$ USD/kW in 2010, almost double the cost of solar PV at 5,124$ USD/kW. However, by 2022, the costs of solar PV dropped by 83% to reach 876$ USD/kW. On the other hand, the total installed costs of solar CSP were reduced by only 58%, reaching 6,589$ USD/kW (Khan et al., 2024).
- *High CSP water use:* CSP plants operate in locations where the DNI is usually very high, usually over 2000kWh/m2/year, and so the potential sites for deployment are usually deserts. Accordingly, the challenge of water availability for power generation is a major concern. Hence freshwater availability is a major factor considered before investing in large-scale deployment of CSP.
- *Ecological Challenges:* Solar heat and CSP plants have a major impact on the environment and ecological footprint, causing bird deaths, endangering wildlife habitats, inducing water pollution, and worsening water shortages. Therefore,

CSP projects often attract media attention and public opposition, leading to complicated environmental and siting approvals.

2.2. Framework of Utility-scale Solar Plants in Lebanon

2.2.1. Financial Model of Utility-scale Solar Projects in Lebanon

Unlike the distributed solar PVs, solar PV farms and CSP power plants are large-scale renewable energy projects and sell power by bulk. Therefore, due to the significant investment cost and long-term operational nature of these plants, securing a stable revenue stream is important for the project's feasibility. The financing mechanism must facilitate long-term contracts between the electricity producer and the purchaser, which is the Lebanese electrical utility company EDL. These agreements secure the project's financing, mitigate market risks, and guarantee a steady cash flow for the duration of the contract.

In 2011, the Lebanese Council of Ministers approved the National Energy Efficiency Action Plan (NEEAP) 2011-2015. NEEAP is a nationwide sectoral document aiming at achieving the declared objectives of the Lebanese Government about energy. NEEAP promoted the development of solar CSP plants in its seventh initiative, as it stated the following:

> "This initiative aims to start the development and promote the generation of electricity through the execution of Photovoltaic (PV) and Concentrated Solar Power (CSP) farms" (LCEC, 2012)

In 2017, the Lebanese Ministry of Water and Energy launched the National Renewable Energy Action Plan (NREAP) 2016-2020. NREAP presented strategic planning on the renewable energy sector in Lebanon by setting quantitative objectives to be achieved through deploying renewable energy. The Action Plan has set a target of

installing 150MW of large centralized solar PV farms and 50MW target of installing CSP plants by the end of the year 2020 according to a realistic scenario (LCEC, 2016).

In line with NREAP 2016-2020, the Lebanese Center for Energy Conservation (LCEC) considers that utility-scale solar plants connected to the Lebanese national grid or micro-grids must have a capacity equal or larger than 1MW. In this regard, NREAP explicitly states that all the output of utility-scale solar plants will be exported to the national grid, and not for local consumption, under a clear long-term power purchase agreement (PPA) with private investors. However, decentralized solar PV connected to facility's local consumption are categorized under distributed generation and follow the Decentralized Renewable Energy Law No. 318/2023 which was ratified by the Lebanese Parliament on 14 December 2023.

2.2.2. PPA Model in Power Projects

The procurement process of private public partnership (PPP) for large scale power projects is usually done through bids initiated by the government, which follows a transparent tender process. After bidders submit their offer and qualification documents, the winner is awarded the contract, referred to as power purchase agreement (or PPA).

A PPA is a foundational document for most power projects and facilitates the process of selling and purchasing electricity. The PPA outlines all financial terms between the two parties, the power producer company and the buyer (often the state-owned utility company), and these conditions include tariff adjustment, payment stream, and the responsibilities of both parties.

Under the PPA conditions, the buyer must pay the agreed tariff according to a scheme agreed upon by both parties. For instance, tariff rates can be flat or can increase

with time. In turn, the power producer company develop, finance, design, build, operate and maintain the power plant in alignment with the PPA conditions and applicable law in the country, and deliver the agreed amount of power in accordance with the PPA (US Department of Commerce and African Development Bank, 2013).

2.2.3. Political Challenges

A stable political environment plays a decisive role in the deployment of renewable energy projects. This is not the case of Lebanon, which has a long history of political instability that in turn increases the risk for investment in new technologies. As a result, funding from major financial sources becomes stalled, limiting investment opportunities for renewable energy projects. Additionally, Lebanese decision makers in governments and municipalities show a significant lack of political will regarding sustainable development and environmental issues. As such, due to challenging security problems and political instability in the country, the government does not prioritize the deployment of renewable energy. Besides, given the long development period for power projects, and prior to entering into long term agreements such as PPAs, the Lebanese government should work on the laws and policies that impact those investments to make them clear, consistent, and predictable throughout the project lifetime. The absence of a clear national strategy for renewable energy development and the lack of political will, where each political party has a different agenda, poses significant challenges on the development of renewable energy projects and deters private investors.

2.2.4. Public Involvement and Social Challenges

The limited financial mechanisms and lack of awareness are two key challenges for the growth of renewable energy in developing countries. It is mandatory to expose citizens to the improved value of green technologies over the past decade and the benefits that these projects bring to the whole community. In Lebanon, the lack of awareness on the benefits and feasibility of utility-scale solar projects is a challenge that needs to be addressed since it leads to public resistance. Moreover, even if there is a general trend towards acceptance in the Lebanese community, a major challenge that often faces these projects is the phenomenon known as "Not in my backyard (NIMBY)", which is the opposition of such projects near the peoples' homes due to perceived negative impacts. This phenomenon is very challenging when it comes to acquiring land from landowners, given that utility-scale solar projects require a vast amount of land. On the other hand, as has been discussed in a study done by Yuan et al. (2011), social acceptance of renewable energy projects is greatly influenced by the public's trust towards the developer. This is not the case for Lebanon, where the government has not been able to deploy feasible electricity generating plants. In addition, delays in such projects are very common. Henceforth, there is a lack of trust from the public's side in the government and its ability to implement such projects. Another major concern that the public usually has in such projects is the environmental impact on the surrounding, given that the implementation of large-scale projects changes the surrounding natural environment and social conditions. Therefore, this issue needs to be addressed through a thorough environmental and social impact assessment and shared with the public prior to the deployment of the project.

2.3. Selected Studies Relevant to the Research

This research paper will examine power generation from solar PV technology, alongside two types of CSP technologies: parabolic trough and power tower, as illustrated in Figure 9 and Figure 10 respectively.

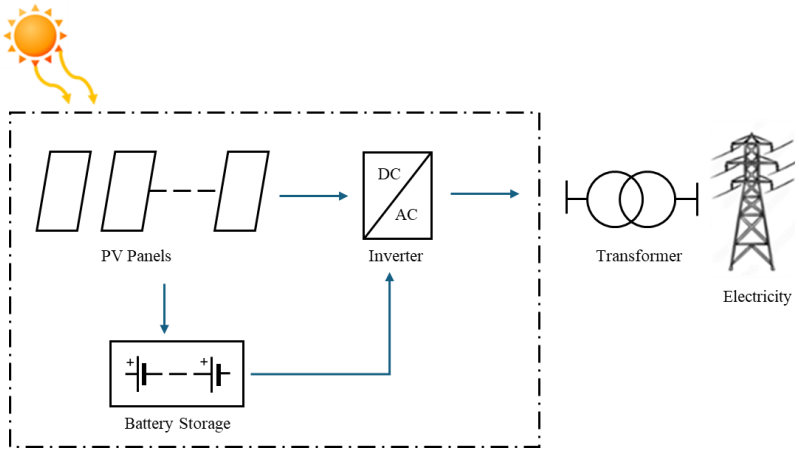

Figure 9. Simplified schematic diagram of utility-scale solar PV farm with Li-ion battery storage assessed in this study

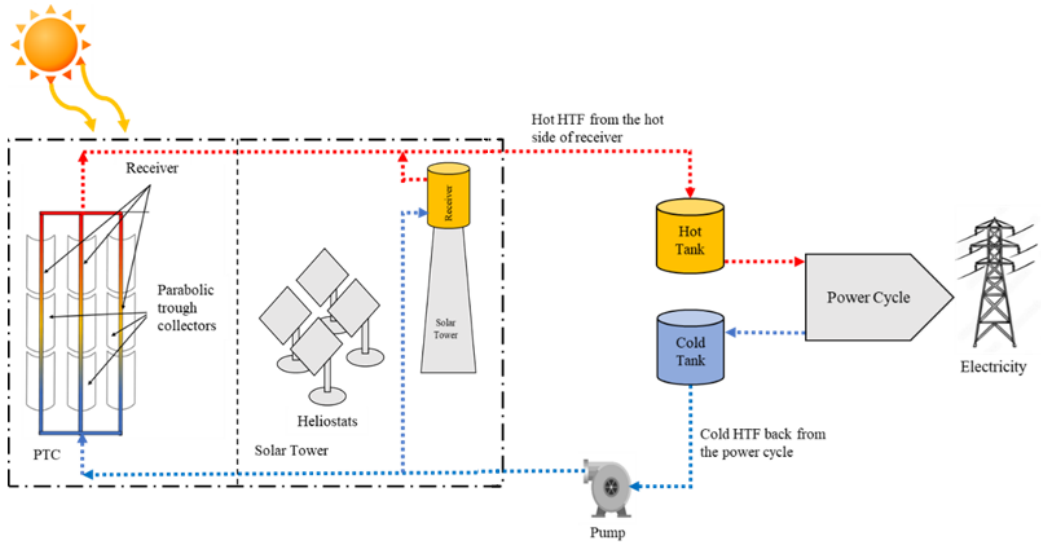

Figure 10. Simplified schematic diagram of CSP technologies assessed in this study. Adapted from (Hossain et al., 2024)

Several articles explored the technical and economic feasibility of CSP power plants as compared to other renewable energy generating technologies. Khan et al.

(2024) conducted an economic feasibility study and assessed the cost competitiveness and deployment potential of the four CSP technologies. Key economic parameters were assessed in this study, which are capital costs, capacity factors, operating expenses, and LCOE. Upon comparing CSP with solar PV and onshore wind technologies, the LCOE for CSP was the highest, averaging 0.12$/kWh in 2022, despite the 69% reduction between 2010 and 2022. On contrary, the LCOE of solar PV and onshore wind recorded 0.049$/kWh and 0.033$/kWh respectively. Moreover, installation costs dropped by 50%, to reach a range of 3000$ - 11000$ per kW, in addition to 20$ - 60$ per kW if thermal energy storage is to be added. Also, operation and maintenance (O&M) costs range from 12$ - 15$ per kW currently, however, they remain 2 to 4 times higher than O&M costs of solar PV and onshore wind. Additionally, the capacity factor has increased from 30% to 50% due to larger storage capacities and higher operating temperatures. Finally, Khan et al. (2024) emphasizes on the importance of design optimizations, ongoing innovations, and introducing financing mechanisms and incentives to support CSP maturation and cost reduction.

Another study conducted by Darbha et al. (2023) determined the potential of different CSP technologies in USA. However, the results of the study can be applied to locations of similar DNI worldwide. The simulations were done using SAM software on three different CSP technologies (power tower, parabolic trough, and linear Frensel systems) across eight different locations across the US and at four different storage capacities (0, 4, 8, and 12 hours). Results showed that the annual energy generation of CSP technology highly depends on the location and the DNI. For instance, the power tower had the highest annual energy generation for 6 out of the 8 sites studied. In

addition, results showed that an 8-to-12-hour storage system produces higher energy levels than 4 storage hours.

In another study, Poole (2017) performed a comparative study for parabolic trough and power tower CSP technologies using molten salt as HTF. Simulation was done across six different sites in South Africa for the two technologies. Simulation results showed that careful consideration is required when choosing between CSP technologies for a given location, where the feasibility and LCOE highly depend on the solar resource and the tariff structure available. Optimization analysis was done to determine the highest possible energy generation with the lowest possible cost for both plants. Results showed that parabolic trough plants and power tower plants have three main differences in performance. The first difference is the solar field efficiency, where parabolic trough collectors have higher solar field efficiency than the heliostat field. The second difference is in the receiver thermal efficiency. Thermal losses are higher in parabolic trough plants due to recirculation of HTF overnight to prevent freezing, whereas power tower receiver is drained when not in operation limiting these losses. As a result, power towers have higher efficiency. Finally, power tower plants have a consistent solar field efficiency throughout the year, while parabolic trough plants suffer from large seasonal variations in efficiency. Consequently, higher thermal energy is available during summer than winter, so storage is filled and hence the subsequent dumping of solar energy in parabolic trough plants.

In another study, Ahmad and Zeeshan (2022) conducted an optimization analysis on power tower and parabolic trough CSP plants under three different climatic conditions, temperate, semi-arid and sub-tropical zones. Both dry cooling and wet cooling systems were assessed. Optimizations were done by SAM software to select the

key design parameters such as the solar multiple (SM) and thermal energy storage (TES) hours to determine the best performance across different system configurations. Results showed that wet cooled power tower systems had the best performance in the three regions, offering 5–6% lower cost of electricity production and 3–7% higher electricity generation potentials.

The impact of hybrid wet/dry cooling on CSP plant performance was also examined by Wagner and Kutscher (2010). The study was performed to examine the performance of dry cooling and hybrid (parallel) wet/dry cooling combinations with the traditional wet-cooled model as a baseline. Since parabolic troughs are more sensitive to fluctuations in cooling conditions, the plant was analyzed to determine the maximum impact of alternative cooling configurations. As compared to the wet-cooling system, a hybrid system with 10% wet-cooling will not be practical since it adds complexity for limited performance improvement. An approach of 50% hybrid system reduces water use by 52% at the cost of a 1.67% penalty on performance. Dry cooled system saves 100% of the total annual water use as compared to the baseline at the expense of 2.45% reduction in performance. It is worth mentioning that CSP plants with dry cooling are of special interest in arid regions with limited water availability despite the performance penalties.

A detailed technoeconomic assessment of three different CSP technologies: power tower, parabolic trough, and Linear-Frensel was conducted by Hossain et al. (2024) in a more recent study. The studied CSP plants have the same nameplate capacity at 100MW. This study aims at finding the optimum CSP technology for the climate of Bangladesh using SAM software from NREL. Results showed that parabolic trough plant generates the maximum annual energy (345.3GWh) and has the highest efficiency

(18.61%) compared to other technologies. However, power tower configuration has the lowest LCOE (6.18 cents/kWh) whereas the Linear-Frensel system required the least land area among the three systems. This is a major advantage for Linear-Frensel systems, especially in highly populated areas. Finally, this study presented a detailed approach to optimize and perform a techno-economic analysis of different CSP plants in any location worldwide to evaluate their feasibility.

In recent years, utility-scale solar PV farms have been a key focus of research focusing on improving technologies, enhancing efficiencies, and reducing costs. A comparative analysis was carried out for PV and parabolic trough CSP plants by Awan et al. (2019), evaluating both technical and economic performance. In their study, a 100MW parabolic trough CSP plant, using synthetic oil as HTF and molten salt for thermal storage, was compared to a PV plant with no storage with same nameplate capacity. The electrical output and capacity utilization were higher for the parabolic trough CSP plant (45.4% vs 30.2% for PV), producing 33.3% more energy at the best site. However, the CSP plant had significantly higher costs, with a net capital cost 4.5 times greater and an LCOE 2.73 times higher than that of a PV farm.

Liu et al. (2022) conducted techno-economic feasibility study of solar power plants considering PV/CSP coupled with electrical/thermal energy storage systems. In this study, a multi-objective optimization approach was followed. Results showed that given the current economic scenarios, TES provides better reliability and is more economically feasible compared to BESS. Hence, CSP integration into the PV system is a feasible option for improving reliability.

Another recent study conducted by Imam et al. (2024) assessed the land suitability and techno-socio-economic feasibility of solar PV and wind energy in Saudi Arabia.

The optimal locations for large-scale PV deployment were identified using GIS spatial analysis. Results showed that large-scale PV plants are viable at PPA rates above 32.8$/MWh, compared to 26.1$/MWh for wind farms and 50.6$/MWh for hybrid solar PV-wind farms.

2.4. Gaps in Existing Knowledge

The contribution of this paper consists of assessing the technical and economic feasibility of implementing utility-scale solar power plants for power production in Lebanon. A detailed and thorough assessment of a utility-scale solar power plant in Lebanon in addition to modeling, optimization, and detailed comparison between solar PV farms and CSP plants is not available in the literature, to the best of my knowledge. This study aims to address the gap and perform a detailed feasibility assessment of solar PV farm and two CSP systems, parabolic trough and power tower, for grid-connected large-scale energy generation at a chosen site in Lebanon as per site requirements. The two CSP powerplants using molten salt as HTF, in addition to solar PV farm with BESS, of similar nameplate capacity of 50MW, will be designed and modeled. The proposed power plants will be compared regarding system efficiency, annual electrical yield, and levelized cost of electricity. Moreover, a similar approach used in the study done by Hossain et al. (2024) will be used for optimizing the design parameters of the CSP plant, including design point DNI, solar multiple (SM), and thermal energy storage (TES) hours. The main objective is to obtain maximum energy generation and plant efficiency with the lowest LCOE possible. This study will play a major role in guiding policy decisions and infrastructure planning for future energy generation in Lebanon to

ensure energy diversification and reach the 30% renewable energy target agreed upon in the Paris Agreement.

CHAPTER 3

METHODOLOGY

3.1. Research Methodology

The purpose of this study is to explore the optimal design and feasibility of implementing utility-scale solar powerplants in Lebanon. A systematic review of literature on related technology and worldwide applications has been made to have a better understanding of the powerplant's performance. This study will adopt a quantitative approach, relying on secondary data analysis to evaluate the technical and economic feasibility of CSP plants in Lebanon using SAM software by NREL.

3.1.1. Selection of the Financial Model in SAM

The System Advisor Model (SAM) is a software tool used to model the performance and financial feasibility of renewable energy systems. The first step to investigate the technical, economic and financial feasibility of renewable energy projects in SAM is to choose a suitable financial model depending on the project type and adhering to the policies and regulations in the given country. SAM provides multiple financial modeling options to fully evaluate the project's feasibility under different ownership and revenue structures. To model utility-scale solar power plants, the available financial models are shown in Figure 11 and include (NREL, 2024a):

- Power Purchase agreement (PPA) model, where the proposed system is connected to the grid and generates revenues through power sales. In this financial model, the project may be owned and operated by a single owner or by a partnership involving a flip or leaseback arrangement.

- Merchant plant, which is similar to PPA model, however, the power generated by the system is sold at market prices that can vary over the project's lifetime.
- LCOE calculator, which uses a simple fixed-charge rate (FCR) method to calculate a project's LCOE. The FCR is the revenue per amount of investment required to cover the investment cost. It is typically used in early stages of a project's feasibility analysis before having detailed information about the project's costs and financial structure.

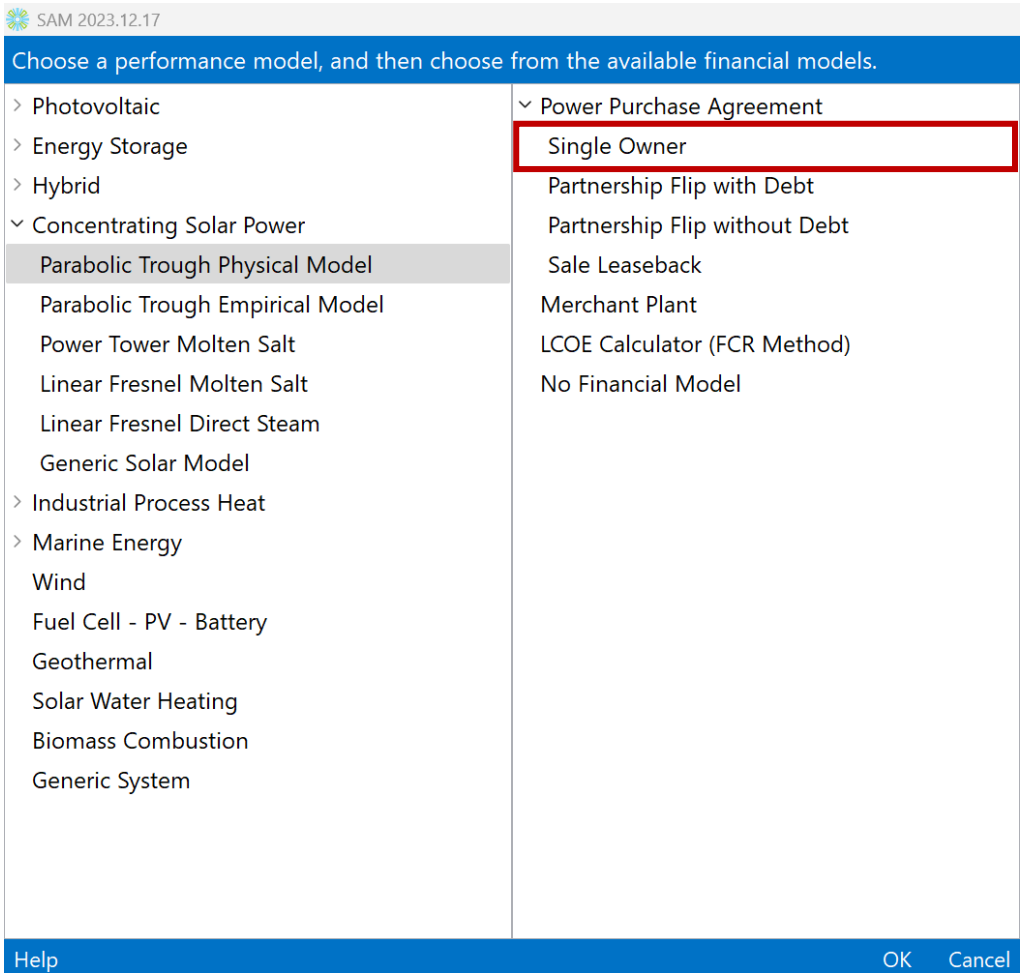

Figure 11. Financial Models in SAM for utility-scale solar power plants.

Referring to section 2.2 on the financial framework of utility-scale solar PV plants in Lebanon, and in line with NREAP 2016-2020, the output of the proposed power plants will be exported to the grid under a clear PPA with private investors. Therefore, the PPA model – single owner financial model will be selected as a financial model to perform the simulations in SAM.

3.1.2. Site Specific Parameters and Meteorological Data

The potential sites for CSP implementation will be short-listed based on the site requirements identified in previous literature works. Next, the selected site specifications such as the resource data, proximity to transmission network, population density, and land features are determined using the Global Atlas for Renewable Energy. The Global Atlas for Renewable Energy is an online tool developed by IRENA to assess site-specific renewable energy potential. The users select the location for the potential site and the type of renewable energy technology, such as solar, wind, geothermal, bioenergy and hydropower. The tool provides access to a wide range of geospatial datasets, including solar irradiance, wind speed, population information, land features, and grid network and infrastructure, as shown in Figure 12.

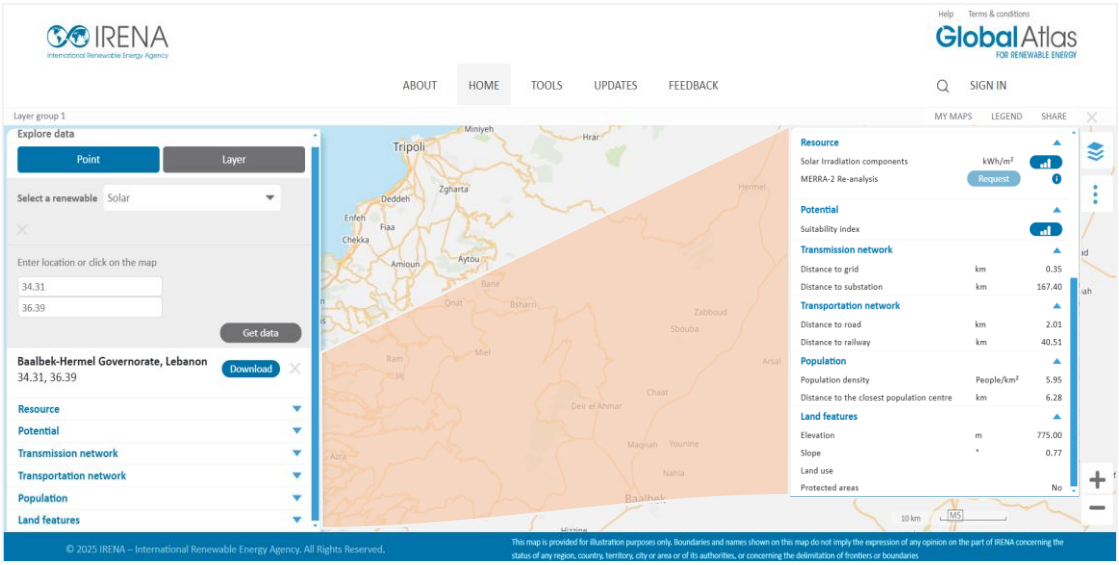

Figure 12. Screenshot from Global Atlas for Renewable Energy tool for site selection

After assessing site specific parameters, the meteorological data, such as DNI data, wind data and ambient temperature data, required to perform an annual simulation at selected sites are determined from NSRDB by NREL. The data generated is used for simulations of the proposed power plants at the selected sites. The NSRDB provides reliable hourly and half-hourly values of meteorological data in addition to the three most common measurements of solar radiation: global horizontal, direct normal and diffuse horizontal irradiance. The datasets include attributes of solar irradiance DNI and GHI, dry-bulb and wet-bulb temperature, wind speed, and other atmospheric parameters crucial for assessing site-specific conditions as shown in Figure 13. The data obtained is then integrated with SAM to accurately model energy production, performance, and financial feasibility of the proposed renewable energy systems.

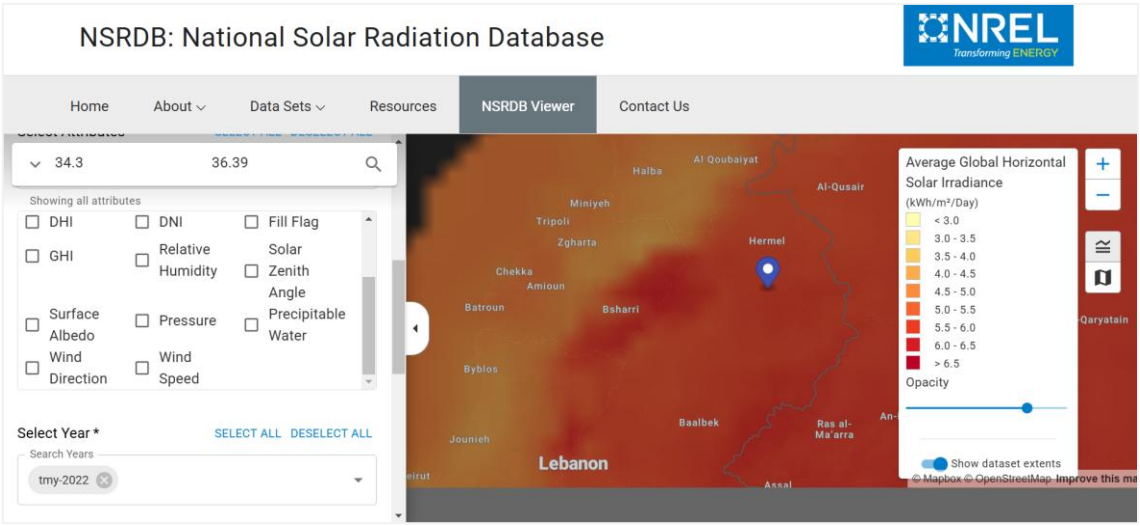

Figure 13. Screenshot from NSRDB tool to obtain meteorological data for selected sites

3.1.3. Design of Utility-Scale Solar PV and CSP Power Plants

The designed 50MW solar PV farm with BESS and both parabolic trough plant and power tower CSP power plants with TES will be modeled using SAM software by NREL at each of the selected sites. Modeling each proposed solar power plant in SAM follows a structured process that consists of three main subsections: system design, financial analysis, and performance simulation, as shown in Figure 14.

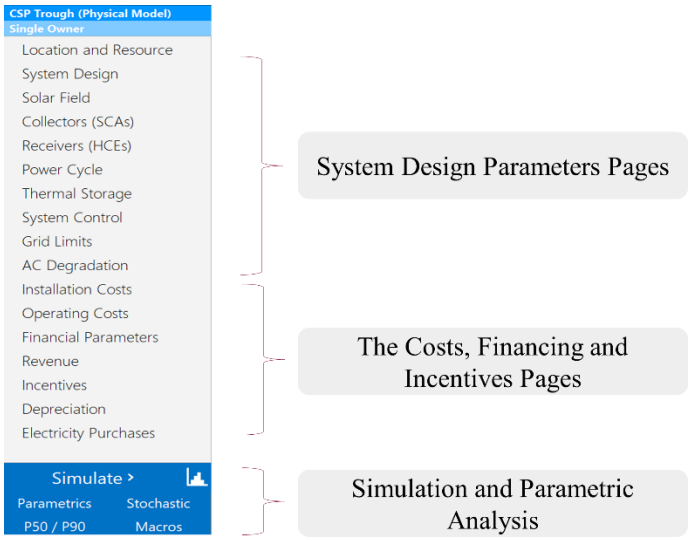

Figure 14. SAM modeling process

The system design process involves defining the technical parameters of the power plant studied. First, the location of the selected site is determined, and the resource data downloaded from the NSRDB database is added from SAM weather files to model the system. Next, the system components of the solar field design are configured.

For CSP power plants, the solar field design includes the solar collectors for parabolic trough plants and the heliostats for power tower plants, and the receiver design that will collect the solar heat. The solar field and receiver of the power tower is determined using an optimization approach by SolarPILOT to determine the position of heliostats in the field. The optimization algorithm automatically calculates heliostat positions and optimal values for the tower height, receiver height, and receiver diameter. Then, thermal energy storage and heat transfer fluid are explored for both plants to determine the best performing HTF type. SAM allows the selection of different types of HTF from the library: Solar salt, Caloria, Hitec XL, Therminol VP-1, Hitec salt, Dowtherm Q, Dowtherm RP, Therminol 59, and Therminol 66, in addition to a user-defined HTF fluid option. Finally, the power cycle is modeled with two options: Rankine cycle or user-defined cycle. The condenser type is also specified, with the following types: air-cooled condenser (dry cooling), evaporative cooling (wet cooling), or hybrid cooling system.

As for the solar PV farm, the system design components such as the PV modules and inverter type are selected accordingly. Once the PV module type is selected, the electrical output of the PV array is calculated by SAM based on the solar radiation obtained from the weather data file and the design parameters such as the number of modules, the orientation, tracking, shading, and other losses or parameters specified.

Next, the inverter type is specified from SAM database or from an inverter datasheet whose model is not available in the database. After the module and inverter type are chosen, SAM runs the system sizing optimization approach to determine the number of inverters and the PV module array configuration. Shading and layout and losses are also determined in this stage. Next, the battery system consisting of battery type, sizing, battery life and replacement and battery dispatch are determined. There are multiple battery types available on SAM depending on the battery chemistry: lithium ion, lead acid, or flow-battery.

After the selection of system design components, financial modeling is performed. Capital and operational cost data estimates are determined based on previous articles found in literature and are continuously updated to reflect continuous developments in the field. Also, the financial parameters such as the analysis period, inflation rate, discount rate, and project term debt are specified. The PPA price is calculated by SAM based on the specified internal rate of return (IRR). As for the incentives, Lebanon does not offer investment tax credits (ITCs) to support renewable energy development.

Afterwards, simulations are performed to predict the system performance. The results of these simulations will then be used to demonstrate the performance of implementing different utility-scale solar plant types, in particular, solar PV with BESS and parabolic trough and power tower CSP power plants using molten salt as HTF as explored in this study.

3.1.4. Optimization Analysis for CSP Power Plants and Simulation of Solar PV Farm

Unlike the simulations performed by SAM on solar PV power plants, the simulations of the CSP plants require an iterative optimization approach to achieve

maximum energy generation and minimum LCOE. After inputting modeling parameters such as solar field, power cycle, and TES into SAM, an initial simulation is performed to determine the initial energy production and costs. Next, an iterative optimization approach is implemented where the design parameters are repeatedly refined to simultaneously optimize multiple conflicting objectives, such as cost and efficiency. In this study, the input parameters involved are energy concentration, solar multiple (SM), and TES hours. The objective of the optimization analysis is to determine the highest annual energy yield and lowest possible LCOE possible for both sites and the effect of the design parameters. The optimization was constrained with a minimum capacity factor of 35% to ensure reliable energy generation and economic feasibility of the CSP plant.

After the optimization of both parabolic trough and power tower CSP power plants, a comparison will be conducted with the simulation results obtained for the solar PV farm in terms of system efficiency, annual electrical yield, and levelized cost of electricity. Based on the system's performance and costs, the optimal utility-scale solar plant configuration will be selected. Finally, conclusions are drawn regarding both technologies and the suitability of the selected sites in Lebanon.

3.2. SAM software by NREL

The System Advisor Model (SAM) simulates a variety of renewable energy systems, including but not limited to solar PV, CSP plants, wind, geothermal, biomass, and storage technologies. Developed by NREL, it enables users to assess the technical performance and economic returns of these systems across different locations, system configurations, and financing options. SAM features multiple financial models,

including residential/ commercial models, PPA, and third-party ownership. For each project, SAM allows users to model multiple variables, including system design specifications, financial parameters, and different incentive schemes, making it a powerful tool for feasibility studies and investment analysis in renewable energy (NREL, 2024b).

3.3. Limitations in Implementation

The study presents an optimal design and evaluates the feasibility of implementing a utility-scale solar plant in Lebanon. However, its implementation faces several limitations tied to Lebanon's economic, regulatory, and political challenges which unfortunately complicate the feasibility of the plant's deployment.

One limitation is the absence of a structured regulatory framework specific to long term renewable energy projects in Lebanon. This creates uncertainty when it comes to project implementation. Second, there are no established policies or financial incentives such as tax credits or subsidies that could offset the high capital costs of utility-scale solar plants, leading to higher energy generation costs thus limiting their economic competitiveness. Moreover, the country's economic crisis and political instability have stalled funding from major financial sources such as the IMF and World Bank funds. This instability not only limits investment opportunities and restricts funds for similar renewable energy projects, but also complicates potential financing avenues, and weakens investor's confidence due to the high economic uncertainty (Ayoub et al., 2021).

Another limitation of this study pertains to the environmental assessment of CSP projects. One of the challenges that CSP projects face is their huge ecological and

environmental impact, such as causing bird deaths, endangering wildlife habitats, inducing water pollution, and worsening water shortages (Yang, 2024). If this study is to be implemented, a life cycle assessment (LCA) is essential. The LCA will evaluate thoroughly the environmental and ecological impacts associated with CSP deployment over its entire life cycle. Hence, environmental concerns of stakeholders will be addressed, influencing positively the public's trust towards the project's developer.

CHAPTER 4

DESIGN OF UTILITY-SCALE SOLAR POWER PLANTS

4.1. Site Selection and Solar Resource Data

Selecting the appropriate site for CSP and PV power plants deployment is a key consideration to maximizing the plant's performance. As such, the economic feasibility of the plant highly depends on the DNI and GHI levels available at the chosen site. In addition to solar irradiation levels, other factors must be considered when choosing the site location of the plant, of which easy access to location, sufficient water supply (for CSP power plants), and proximity to electrical grid. Moreover, the site location is preferred to be in locations with the lowest population density.

In Lebanon, the North Bekaa area has high solar irradiation levels (DNI and GHI), as can be seen from the map of APPENDIX I. Moreover, the low population density in North Bekaa region, the availability of vast lands that are not used for agricultural purposes, and the freshwater supply from the Al-Asi River nearby played a significant role in site selection. Also, the 220kV HV transmission lines are at proximity as illustrated in the electrical transmission map presented in APPENDIX II. Hence generated electricity can be dispatched to the national grid line with minimal losses. All these factors make this region ideal for utility-scale solar plants deployment.

Based on the above requirements, the following sites have been selected to be modeled on SAM software:

- Site 1: Ras Baalbeck, Location: 34.30, 36.39
- Site 2: Baalbeck, Location: 34.16, 36.26

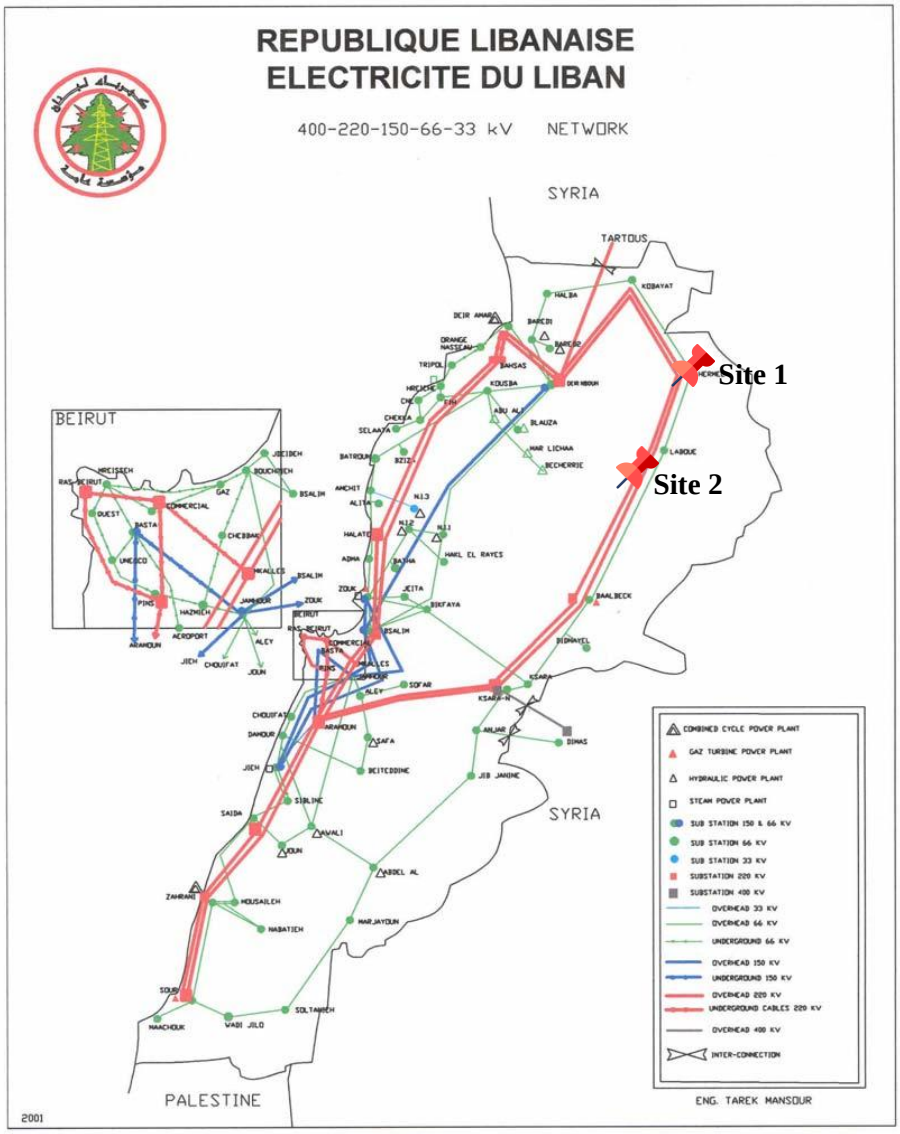

Figure 15. Selected locations of the CSP plant in Lebanon

The location specific parameters of the selected sites were gathered from the Global Atlas for Renewable Energy by IRENA (2025), shown in Table 1.

Table 1. Site Specific Parameters. Source: (IRENA, 2025)

	Solar irradiation DNI (kWh/m^2)	Distance to grid (km)	Distance to road (km)	Population density (ppl/km^2)	Distance to closest population center (km)	Elevation (m)	Land slope (°)
Site 1	2102.55	0.11	1.83	5.27	5.6	782	0.77
Site 2	1934.06	4.78	1.55	10.34	10.69	988	1.28

After site selection, the weather data files of both sites were retrieved from the NRSDB database provided by NREL. SAM software then uses the time zone, elevation, latitude and longitude to calculate the sun position during simulations.

The temperatures at both Sites 1 and 2 show very similar recordings. The maximum daily average temperature is recorded during the month of August, 28°C for Site 1 and 27°C for Site 2 respectively. The monthly average temperatures at the two representative sites are shown in Figure 16.

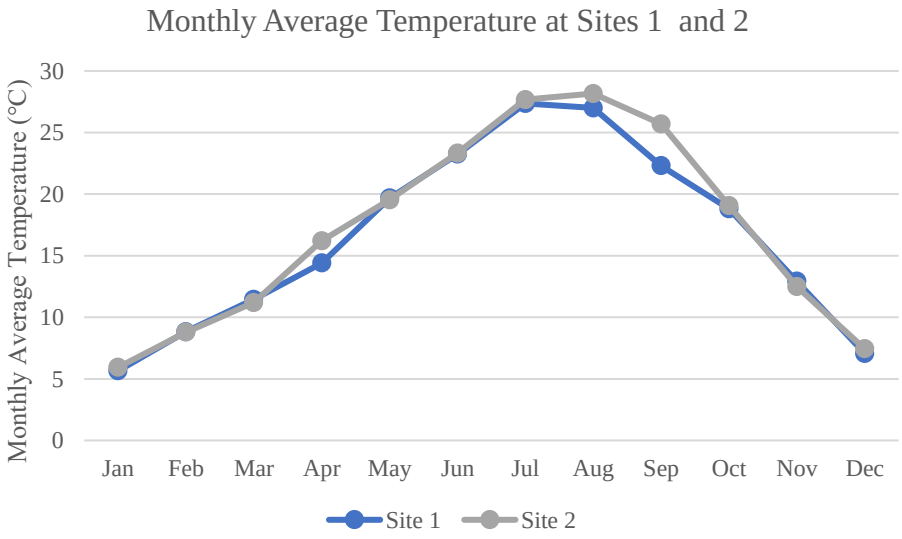

Figure 16. Average temperature at the two selected sites. Source: NRSDB Database

Both sites offer high DNI and GHI all year round, see Figure 17Figure 18. GHI and DNI at Site 2 and Figure 18. Given the similar temperatures and irradiation levels for the two sites, and given the proximity of both sites to one another, the performance of the plant is expected to yield similar results. Hence Site 1 will be selected to perform the simulation on SAM and conduct the comparative analysis of the 50MW utility-scale PV farm and parabolic trough and power tower CSP power plants.

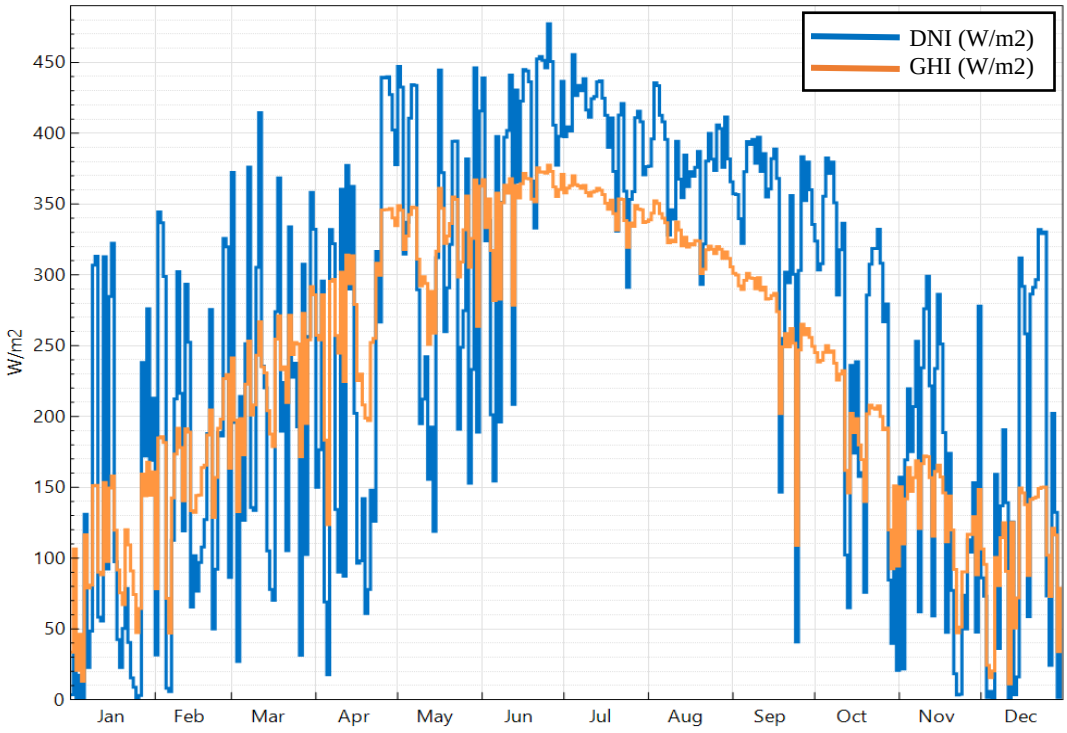

Figure 17. GHI and DNI at Site 1. Source: NRSDB Database

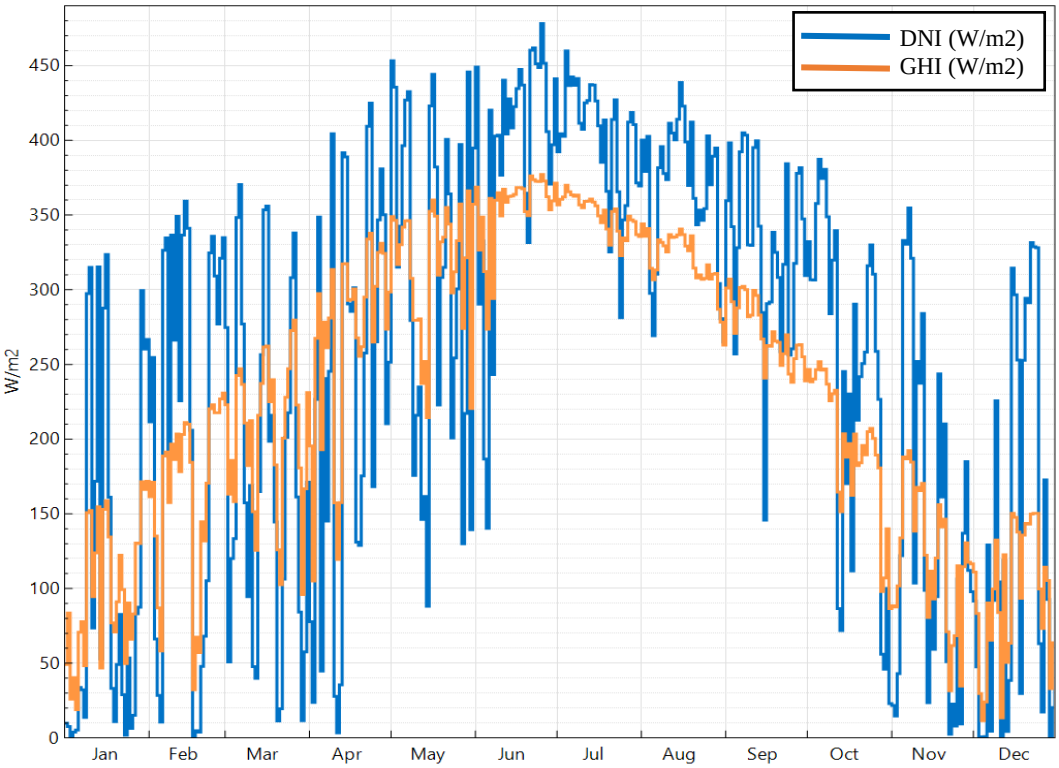

Figure 18. GHI and DNI at Site 2. Source: NRSDB Database

4.2. Modeling and Design of 50MW CSP Plant

The CSP plant consists of three main stages: the solar field, power block, and TES. The solar field consists of mirrors, reflectors, or heliostats that concentrate sunlight and a receiver that collects the concentrated heat. The HTF flowing through the receiver absorbs the solar heat to be transferred to the power block through Rankine cycle which in turn exchanges the heat with water to produce steam in the heat exchanger (Yang, 2024).

4.2.1. Selection of Common Design Points

The key parameters to consider while designing the solar field are design point DNI, solar multiple (SM), and design point temperature.

- *Design Point DNI* represents the DNI value at which the designed thermal power plant would achieve the desired thermal rating. Increasing the design point DNI implies that lesser number of heliostats are enough to achieve the rated output and vice versa. Hence selecting a higher DNI causes the solar field to be over-designed and the opposite is true. According to NREL (2017), the appropriate DNI is based on the most frequent DNI value. This is determined as the 90–95 % of the probability density function (PDF)/cumulative distribution function (CDF) value of DNI chart of the selected site using SAM software. The DNI is determined at 925W/m2, as shown in Figure 19.

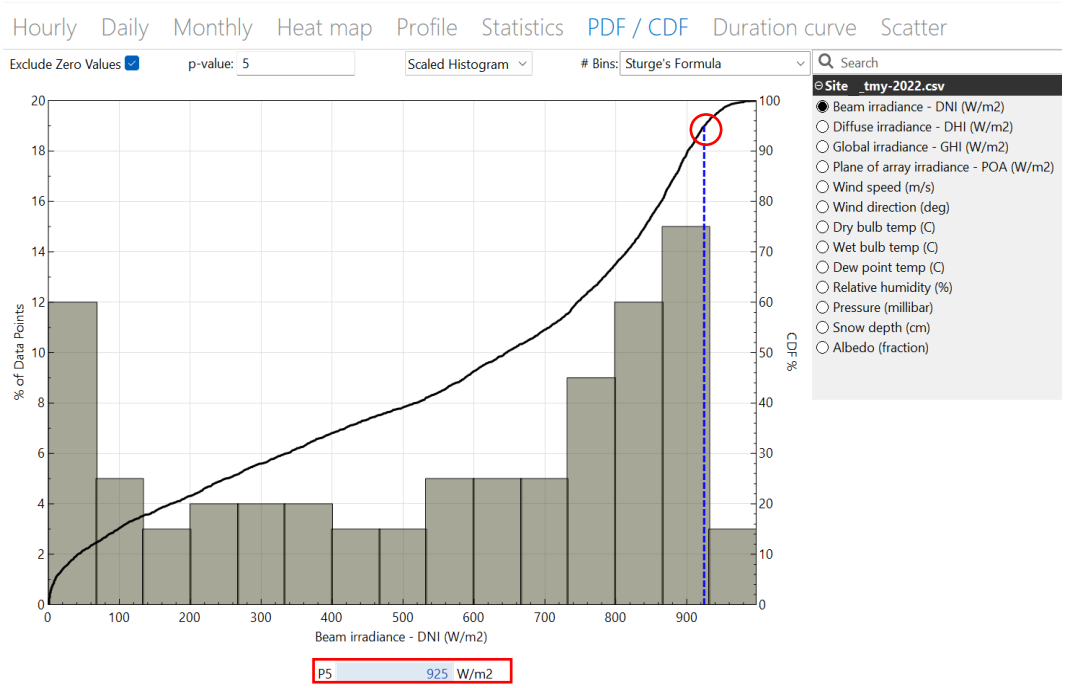

Figure 19. PDF/CDF of direct beam irradiance (DNI) for Site 1

- *Solar Multiple (SM)* is the ratio of thermal power generated by the solar field at the chosen design point and the thermal power needed for the power cycle at normal conditions.

$$SM = \frac{Capacity\ of\ Solar\ Field}{Capacity\ of\ Power\ Cycle} \quad \ldots (1)$$

The ideal SM of the CSP plant will be determined using an optimization approach to maximize annual energy generated and minimize LCOE.

- *Design Point Temperature* is the temperature at which the solar thermal power plant is designed to operate at its full potential. It is determined by considering the mean annual temperature of the location or taking the most frequent hourly temperature occurring annually (NREL, 2017). In this study, the design point temperature was determined by choosing the mean wet bulb temperature at the specified location. The design point temperature at site 1 is 10.6°C. See Figure 20.

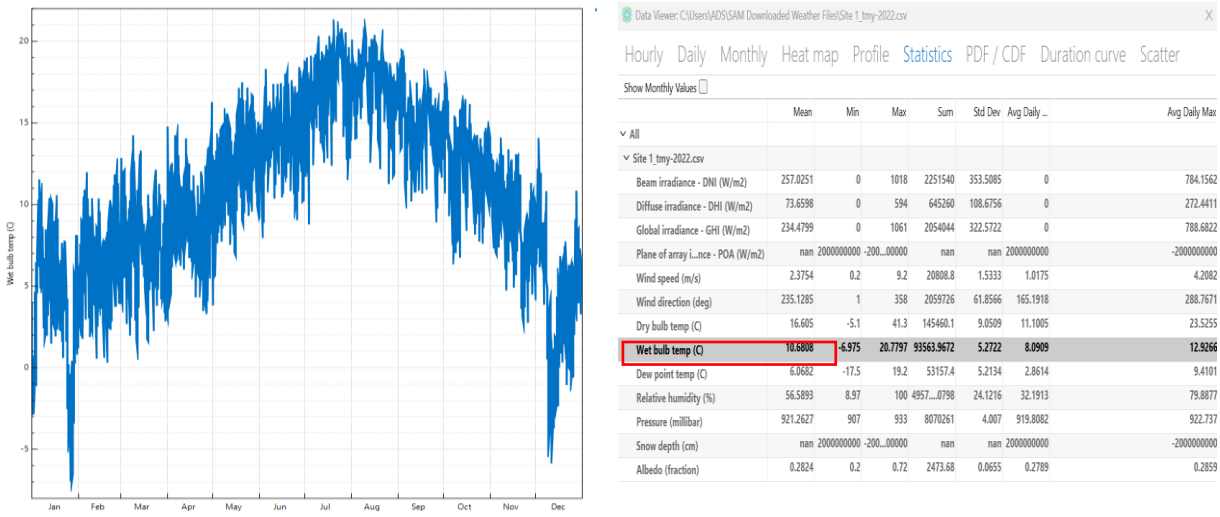

Figure 20. Selection of mean temperature (Design point temperature) at Site 1

4.2.2. Solar Field and Receiver Design of Proposed CSP Power Plants

4.2.2.1 Parabolic Trough Collector Solar Field and Receiver Design

In a parabolic trough CSP plant, the solar field consists of parabolic collectors lined in parallel rows that concentrate solar irradiation onto a receiver passing through their focal point. The collector used in this study is SkyFuel SkyTrough (with an 80-mm OD receiver). The solar collector is placed in rows and each row consists of 8 modules per assembly. The spacing between the rows is 15m to prevent shading from other collectors in the field at the selected location, taking into consideration worst case scenario: the winter solstice where the sun has low altitude (Awan et al., 2019).

The total solar field area for a 50MW parabolic trough CSP plant is 213 acres for a SM of 1, which is equivalent to 861,980m^2. However, the collector area is 244,588m^2, consisting of only 28% of the total solar area.

The receiver of the parabolic trough plant is a metal pipe enveloped by vacuum within a glass tube that runs through the focal point of the collector. In this study, a Schott PTR80 type receiver will be selected. The receiver is covered by anti-reflective

coatings on the glass tube to maximize the absorption of the solar radiation (NREL, 2024a). HTF flows through the receiver absorbing the concentrated heat and then transfers it to the power block. The velocity of the HTF is a key parameter that determines the rate of power generation. High velocity minimizes the receiver efficiency, so it is important to determine the optimal velocity depending on the type of HTF used to maximize performance. The minimum and maximum HTF flow velocities depend on the minimum and maximum HTF mass flow rates ($\dot{m}$), the HTF density at the design loop inlet and outlet temperatures (ρ), and the inner diameter of the absorber tube (D). The HTF flow velocities can be calculated using the following equation:

$$Minimum\ HTF\ flow\ velocity = \frac{\dot{m}_{loop,min} \times 4}{\rho_{HTF,in} \times \pi \times D^2_{tube,min}} \quad \ldots (2)$$

$$Maximum\ HTF\ flow\ velocity = \frac{\dot{m}_{loop,max} \times 4}{\rho_{HTF,out} \times \pi \times D^2_{tube,min}} \quad \ldots (3)$$

The detailed design parameters of the 50MW parabolic trough plant are presented in APPENDIX III.

4.2.2.2 Power Tower Heliostat Field and Receiver Design

The solar field of a power tower CSP plant consists of heliostats that concentrate sunlight into a receiver mounted on top of a tower. Unlike parabolic trough designs, power tower system designs require optimization of the heliostat distribution and the height of the receiver tower. The heliostats used in this study have square reflecting surface of a 144m^2 area. To minimize the shading effect from adjacent heliostats, the deploy and stow angles of the heliostats are selected at 8°. The optimization is run in SAM through SolarPILOT optimization algorithm which automatically calculates heliostat positions and optimal values for the tower height, receiver height, and receiver

diameter (NREL, 2024a). As for the receiver, the material type of the panel tubes used is stainless steel-alloy with an outer diameter of 40mm. The design parameters of the 50MW power tower plant are presented in APPENDIX III.

Proper positioning of heliostats and optimal tower height are important to minimize the thermal losses of the plant. The heliostat field for this study is optimized and designed using the solar field geometry optimization function of SAM. Figure 21 shows a model diagram of the heliostat positioning of the designed 50MW CSP plant using SAM.

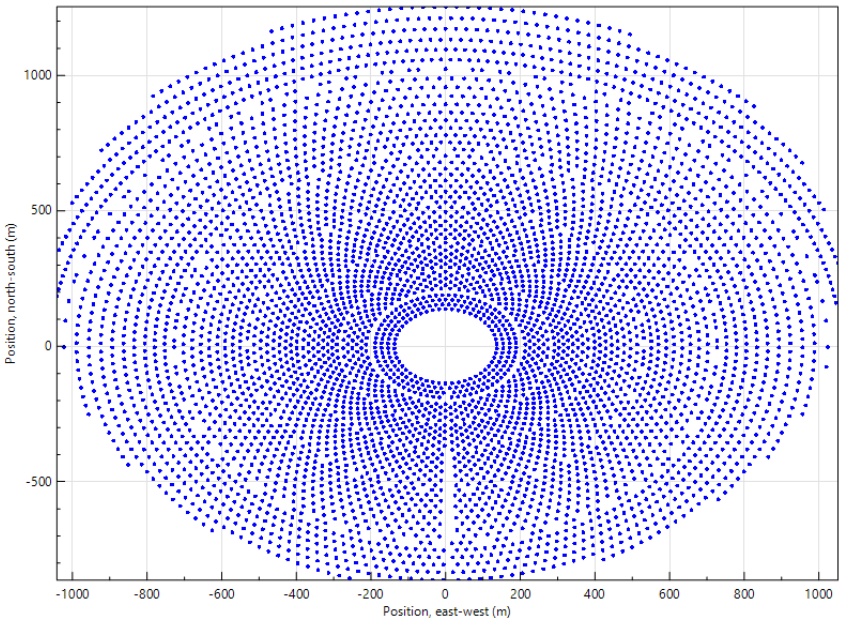

Figure 21. Typical model of heliostat positioning and receiver tower for 50MW plant

Figure 22 shows the variation of thermal power directed to the receiver tower. The receiver incident thermal power ranges from 0 to 420MWt in year 1.

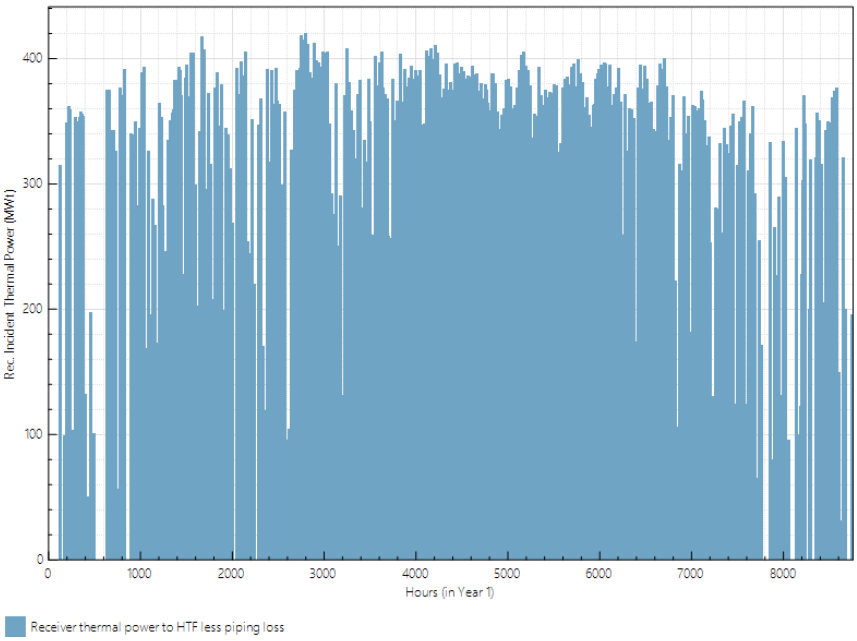

Figure 22. Receiver thermal power directed to receiver tower (MWt)

The design of the CSP plant must consider minimizing the thermal losses to maintain a receiver thermal efficiency of more than 90% at design (Shabbir et al., 2018). The TES thermal losses are illustrated in Figure 23, ranging from 610kWt to 690kWt. It is noted that the lowest losses are during summer season (July, August) since due to high temperatures in this season, a higher temperature can be achieved within shorter periods.

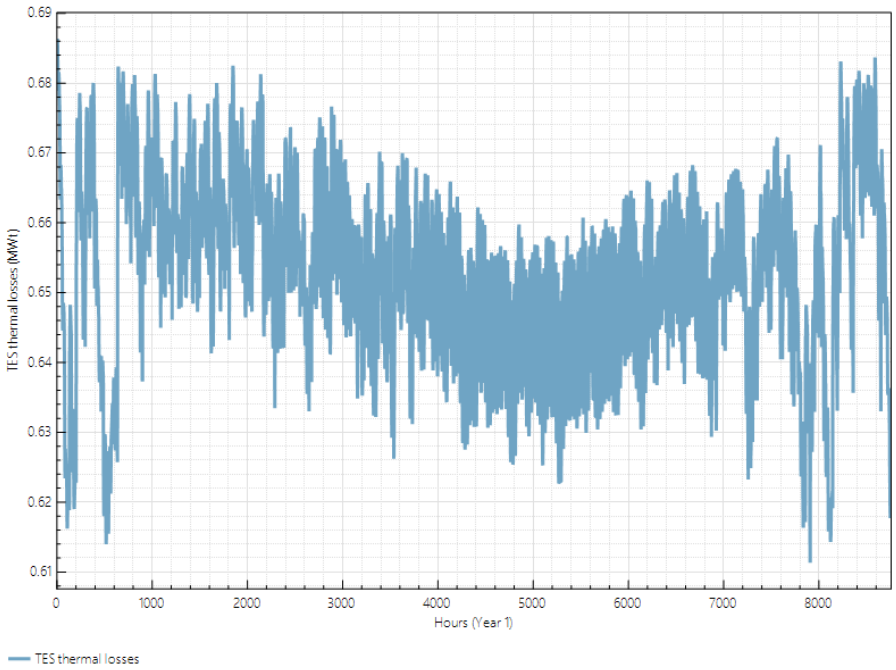

Figure 23. TES thermal losses

4.2.3. HTF and Thermal Energy Storage System

Choosing an appropriate HTF is essential for optimizing the performance and efficiency of the CSP plant. HTF has two roles in a CSP plant: as thermal fluid storage stored in well insulated tanks forming the TES or as a heat transfer medium that generates steam and drives the turbine to generate electricity. An ideal HTF should have the following specifications: high specific heat, non-combustible, high chemical stability, low maintenance. In addition, the method of production must have minimum CO_2 emission with minimum impurities (Hossain et al., 2024).

Thermal storage is a key feature of CSP technologies and has two main objectives. First, thermal storage maximizes electricity production when demand and prices are high by allowing hourly to daily storage. Second, thermal storage increases the plant's capacity factor by providing second to minute storage to smoothen the variability in sunlight and provide a reliable output. Direct storage systems using molten salt (nitrate

salt mixture 60% $NaNO_3$ + 40% KNO_3) are the most common storage system configuration. Using molten salt rather than air or oil allows for higher temperatures, smaller storage tanks, and higher steam cycle efficiency. For instance, molten salt reaches temperatures as high as 565℃ as compared to 550℃ for steam and 390℃ for oil (Yang, 2024). The melting point of molten salt is 223℃ and has high thermal stability up to 600℃. Hence, in this study, the HTF hot and cold temperatures will be 565℃ and 290℃ respectively.

In parabolic trough plants, aside from storage systems, HTF is used to circulate in the receiver to collect heat from the solar irradiation and transfer it to the power block. The most common HTF used are Theminol VP-1 synthetic oil and Hitec Solar Salt. Theminol VP-1 operates within a temperature range of 12℃ to 400℃, whereas Hitec Solar Salt operates between 238℃ and 593℃. A higher temperature range results in higher energy output. However, freezing protection must be used to ensure that HTF becomes solidified clogging the piping of the receiver. For instance, since salt becomes solidified below 238℃, the minimum loop inlet temperature is set at 290℃.

Both Theminol VP-1 and Hitec solar salt HTFs are evaluated in SAM for the 50MW parabolic trough CSP plant to select the best performing option. Simulations are performed using SAM for a SM of 2 and TES hours of 6. Results showed that the annual energy generated in year 1 using Theminol VP-1 as HTF is 82GWh as compared to 142GWh using Hitec Solar salt as HTF. Figure 24 shows the monthly energy produced of parabolic trough CSP plant using Theminol VP-1 vs that using Hitec solar salt as HTF.

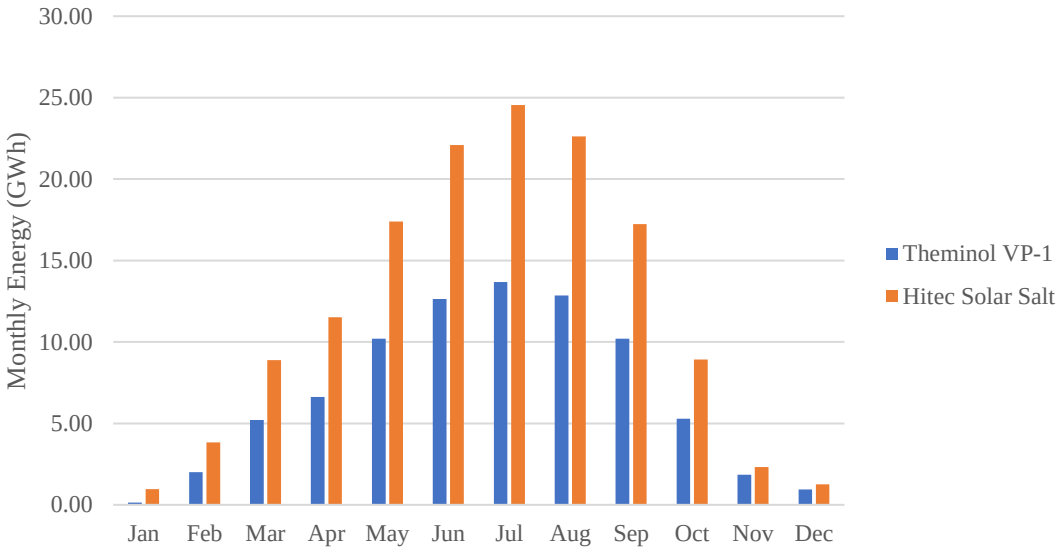

Figure 24. Monthly energy produced of parabolic trough CSP plant using Theminol VP-1 vs Hitec solar salt as HTF.

As illustrated in Figure 24, the energy output of the parabolic trough collector in year 1 using Hitec solar salt as HTF is 43% higher than that using Theminol-VP1. Moreover, the parabolic trough CSP plant using Theminol VP-1 is not technically feasible and has a poor performance, since this would result in a capacity factor of 18.6%. However, the capacity factor of the CSP power plant using Hitec solar salt is 32.2%. As a result, Hitec solar salt will be used at HTF for the parabolic trough CSP plant.

The number of hours of TES will be determined using an optimization approach like that used to determine the optimal solar multiple. A parametric analysis will be conducted using SAM software to explore the effect of varying TES hours on the energy produced and cost of the CSP plants.

4.2.4. Solar Field Control of CSP Power Plants

The main concern for a parabolic trough HTF system is the freezing of HTF in the solar field. A method proposed by Kearney et al. (2004) implemented an operational strategy that manages the circulation of the HTF to ensure safe and efficient operation. Due to the length of piping and receiver tubes, a large volume of HTF circulates in the receiver. During normal operation, the HTF enters the cold tank at design point temperature of 290℃, then flows through the solar field and into the hot tank to reach 565℃. During times of insufficient solar irradiation, the return temperature begins to drop. When the return temperature from the hot tank reaches lower than 500℃, HTF is circulated from cold tank to solar field and then back to the cold tank. This increases the average temperature of the cold tank to approximately 310 to 320 °C. However, if the temperature falls below 285℃ before sunrise, molten salt from the hot tank is then circulated to maintain the field outlet temperature at 285℃.

The HTF control of a power tower CSP power plant is similar to the solar field control of a parabolic trough. However, for a power tower, the receiver is drained when it is not in operation, making the control operation more complicated. There are three control operation modes for power tower CSP power plant. The first mode is the standby mode, when there is no sufficient DNI to begin operation, hence the receiver is drained from molten salt. The second mode of operation is the receiver tube preheating and recirculation. Operation in this mode starts when the DNI is larger than 50W/m^2 (Poole, 2017). The solar radiation from the heliostat fields heats up the receiver tubes. The receiver start-up delay time is set to 0.5 hours, during which the receiver tubes will be heated by the heliostat field to around 500℃. Then, the molten salt pumps are initiated to enable recirculation of the molten salt from the cold tank, up the riser

through the receiver tubes and then back down to the cold tank through the downcomer. When the outlet temperature of the receiver reached the design point hot temperature of 565℃, the third mode of operation is entered. In this mode, the HTF is diverted from the downcomer into the hot tank and the temperature is held constant at 565℃.

The major drawback of this method is the increased thermal losses in times of insufficient solar irradiation, such as nighttime and cloudy days. However, this method eliminates the need for inefficient electric heating resistance in the solar field during operation.

4.2.5. Power Cycle Modeling of the CSP Power Plant

In this study, the Rankine cycle will be modeled as the power cycle for the parabolic trough and solar tower CSP plants. The cooling system of the condenser plays an important role in condensing steam and maintaining cycle efficiency. There are two main condenser types, wet cooling that uses water for heat dissipation, and dry cooling which relies on air. The water consumption, efficiency, and cost differ according to the condenser type used. In a water-cooled CSP plant, the evaporative flows from Rankine cycle cooling are the primary source of water consumption, accounting for more than 90% of total water usage of the plant. In contrast, mirror washing represents only 1.4% of the plant's overall water demand (Wagner and Kutscher, 2010). According to the study done by Wagner and Kutscher (2010), while water consumption is reduced by 100% for dry-cooling systems, the annual penalty efficiency drops by 2.45% compared to wet-cooling systems. As a result, the condenser type selected is the evaporative cooling (wet cooling). Since the selected site is close to the Al-Assi River that provides

the plant with the freshwater required, the evaporative condenser system is preferred to maximize efficiency and enhance overall plant performance.

4.2.6. Efficiency of the CSP Plant

According to different studies explored by Hossain et al. (2024) and Praveen et al. (2018), the thermal power generation of the solar field largely depends on the incident thermal energy it receives. The energy collected by the collectors/ heliostat field is calculated using the following equation:

$$Q_{sf} = DNI \times A_h \quad \ldots (4)$$

Where DNI is the direct normal irradiance (W/m^2) and A_h is the total reflective area of the heliostats (in m^2). The solar field efficiency is calculated using equation 5:

$$\eta_{sf} = \frac{Thermal\ power\ incident\ on\ receiver\ (Q_{rec})}{Solar\ field\ thermal\ power\ (Q_{sf})} \quad \ldots (5)$$

The thermal efficiency of the receiver can be calculated using the following equation:

$$\eta_{rec} = \frac{Thermal\ power\ transferred\ to\ HTF\ (Q_{HTF})}{Thermal\ power\ incident\ on\ receiver\ (Q_{rec})} \quad \ldots (6)$$

Where Q_{HTF} is calculated by equation 7:

$$Q_{HTF} = m'_{HTF}(h_{out} - h_{in}) \quad \ldots (7)$$

The power cycle thermal efficiency is expressed by equation 8:

$$\eta_{pc} = \frac{Power\ cycle\ electrical\ energy\ output\ (Q_e)}{Power\ cycle\ thermal\ energy\ output\ (Q_{pc})} \quad \ldots (8)$$

The power plant efficiency is expressed by the following equation:

$$\eta_{plant} = \eta_{sf} \times \eta_{rec} \times \eta_{pc} \quad \ldots (9)$$

And finally, the capacity utilization factor is given by the following:

$$Capacity\ utilization\ factor\ CUF = \frac{annual\ energy\ generated\ (E_{net})}{plant\ nameplate\ capacity \times 8760} \quad \ldots (10)$$

4.2.7. CSP Plant Optimization Approach

In this study, an iterative multi-objective optimization approach will be conducted for the CSP plants, similar to the approach presented in a study conducted by Hossain et al. (2024). This involves continuously refining the design through optimizing the design parameters to reach conflicting objectives which are reducing costs and maximizing efficiency. The input variables analyzed were SM, TES hours and energy concentration. The energy concentration of the plant is expressed as follows:

$$Energy\ concentration = \frac{Annual\ net\ electrical\ energy\ (GWh)}{Solar\ land\ area\ (acres)} \quad \ldots (11)$$

The energy concentration represents the energy yield per unit of land occupied by the solar collectors. It indicates how efficiently the CSP plant converts solar energy into electricity relative to the area it occupies.

The optimization objective is to maximize annual energy production and minimize LCOE. As per (Hossain et al., 2024), the optimization was constrained with a minimum capacity factor of 35%. This is imposed to ensure reliable energy generation and economic viability of the CSP plant.

4.3. Design of 50MW PV Farm

The design of the 50MW solar PV farm follows a similar approach to that of Noor Abu Dhabi 1200MW solar PV farm, which served as a reference for component selection and provided guidance on key design choices (Noor Abu Dhabi, 2025). The main components of the solar PV farm are the PV modules, inverter, and BESS.

4.3.1. Characteristics and Design Parameters of the PV Modules

The type of PV module proposed for the 50MW PV farm is Longi monocrystalline silicon of 555kWp and is selected from SAM database. The output power of the PV module mainly depends on the GHI levels and cell temperature, which rarely operates at standard test conditions (STC). The characteristics of the PV module at reference conditions are shown Figure 25 in below. Refer to APPENDIX V for the detailed datasheet.

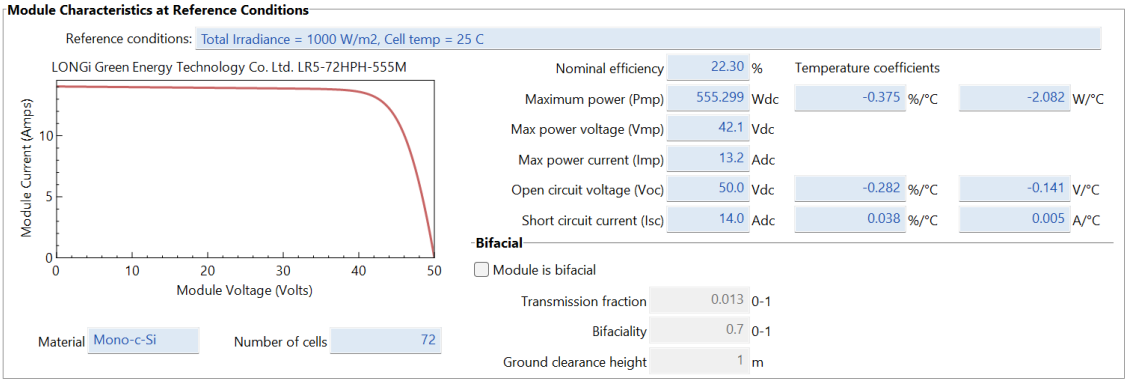

Figure 25. PV Module Characteristics

The maximum power (Pmp) represents when the PV generation reaches is maximum, occurring at maximum power voltage (Vmp) and maximum power current (Imp). Moreover, the open circuit voltage (Voc) and short circuit current (Isc) are the maximum voltage and current the PV module can produce. The efficiency of the PV module depends on the temperature. The temperature coefficients define the decrease in efficiency as the operating temperature increases.

In this study, the PV farm topology is ground-mounted installation of parallel PV arrays. A single axis tracking system is selected for better performance, given that the intensity of the solar irradiance can be maximized by proper positioning of PV modules in the Sun's direction. Also, it is recommended that the tilt angle of the PV modules

should be equal to the angle of latitude of the site, i.e. 34.1°, to maximize the annual energy generation of the PV farm.

The proposed 50MW PV farm has a total of 90,068 PV modules. Every 23 modules are connected in series to form a single string, and a total of 3,916 strings connected in parallel form the PV array.

Shading and losses must be carefully considered in the design of the solar PV farm. Given the above array dimensions, SAM calculates the spacing between the array rows at 13.7m to minimize mutual shading between adjacent rows in early morning and late evening hours, especially in winter solstice where the sun has low altitude (Gilman, 2015). The PV derating factor is another factor that affects the output power and includes shading, dust and soiling, and wiring losses. In this study, the soiling losses are assumed to be 3.5% (Awan et al., 2019).

4.3.2. Inverter Characteristics and Design Parameters

Another main component of the PV farm is the inverter, which converts DC to AC electricity to be fed into the power grid. During this conversion, a small power loss during conversion, defined by the efficiency η_{inv}, calculated by the following equation (Gilman, 2015):

$$\eta_{inv} = \frac{P_{AC}}{P_{DC}} \quad \ldots (12)$$

The inverter proposed for this study is INGECON SUN 1245TLU B480, whose datasheet is presented in APPENDIX V. The efficiency and the curve characteristics of the selected inverter are shown in Figure 26. The inverter has a rated output power of 1100kVA, maximum DC input voltage of 1500V, and an MPP voltage range of 895V to 1500V.

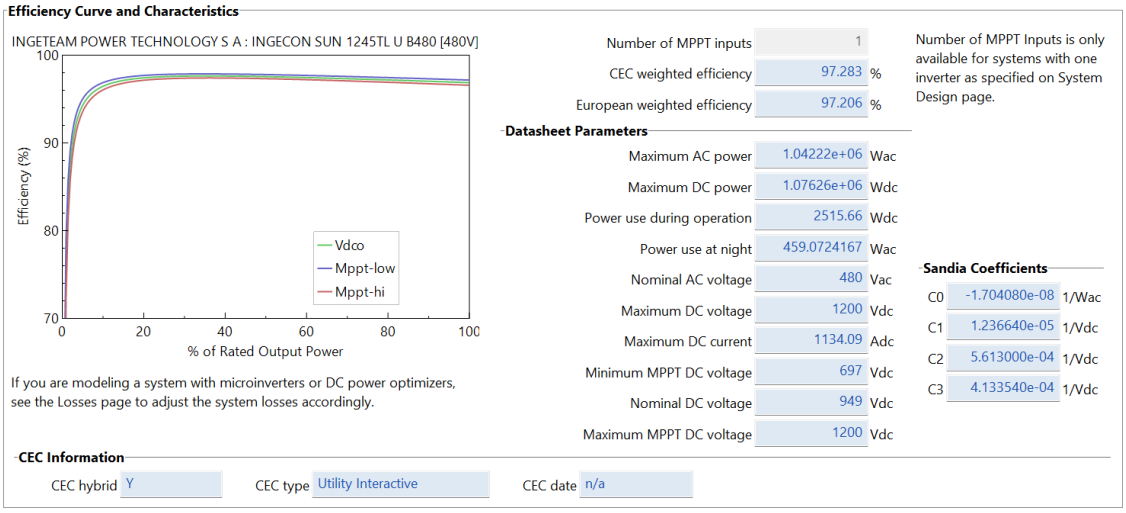

Figure 26. Inverter Characteristics

4.3.3. BESS Design Parameters

To make a fair comparison between the 50MW PV and CSP technologies with storage, a battery energy storage system (BESS) of 8hours capacity will be added to the designed PV farm.

The proposed battery type is a Lithium-ion Iron Phosphate ($LiFePO_4$). This battery type is characterized by a lower voltage cathode material with excellent safety properties but lower volumetric energy as compared to other lithium-ion battery types (NREL, 2024a). Utility-scale lithium-ion batteries are replaced at a specified schedule in SAM. The batteries are scheduled to be replaced in year 15, according to a technical report published by NREL on utility-scale batteries (Cole and Karmakar, 2023).

The storage dispatch strategy in SAM enables the users to specify detailed parameters, including discharge periods, discharge capacity, and the minimum state-of-charge (Diorio et al., 2015). Figure 27 Figure 27.displays the scheduled dispatch strategy applied in this study for the electricity market with uniform rates, given that the tariff scheme is Lebanon is uniform regardless of the amount or time of usage.

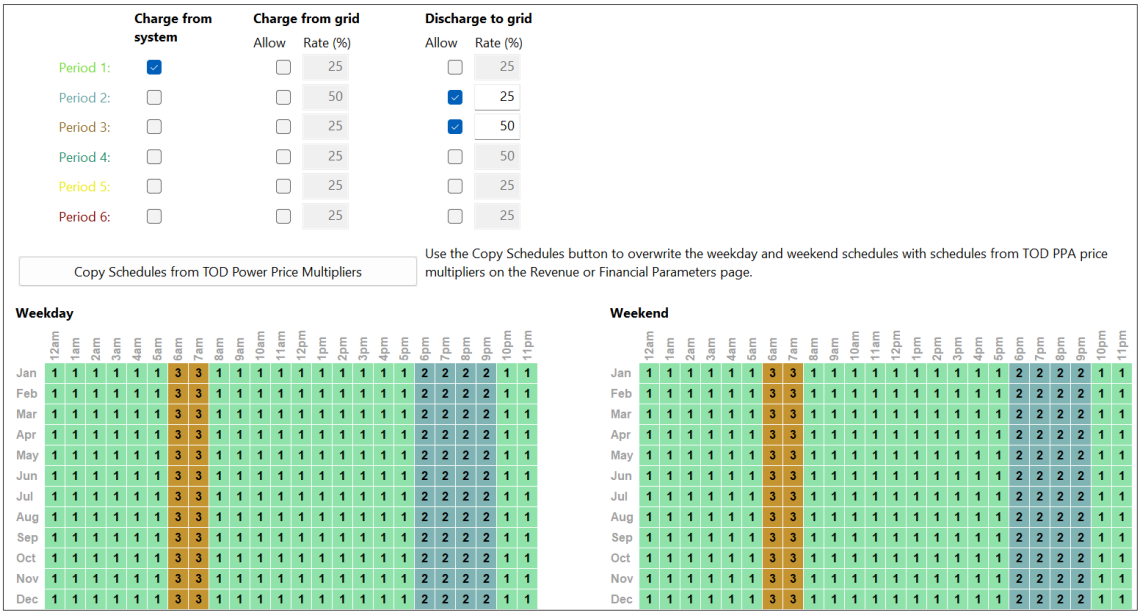

Figure 27. Manual dispatch strategy for the BESS

Period 1 only allows charging of the battery from the PV array. Period 2 is set to allow the battery to charge from excess PV energy, and at the same time, it allows discharge to meet the load if the load exceeds PV production. In this period, only 25% of the available capacity is allowed to be used every hour covering the four-hour evening period. Finally, Period 3 follows the same approach as Period 2, however, it allows 50% capacity to be used during every hour covering which covers the two-hour morning period. The battery dispatch schedule is designed to only allow the battery to discharge during typical peak usage hours. Refer to APPENDIX IV for the detailed PV farm design parameters.

4.4. Economic Modeling for Solar PV and CSP Power Plants

To study the economic feasibility of the proposed plants, the current energy laws and regulations and policy schemes in Lebanon are explored to determine the financial mechanism to finance these projects in Lebanon. However, Lebanon does not offer

direct tax credits or investment tax credits for utility-scale solar projects, like those seen in countries like USA or Spain (UNDP, 2017)

Unlike fossil fuel electricity generating plants, renewable energy plants have a high initial investment cost. However, the cost of operating and maintenance is low due to almost no fuel cost. In this study, and as per the financing scheme of utility scale solar plants in Lebanon, the single owner power purchase agreement (PPA) model will be used for economic modeling.

In this study, SAM will calculate the power purchase price (PPA) given the internal rate of return (IRR). The PPA has a fixed annual escalation rate of 1%. Next, the financial parameters, IRR and debt-service coverage ratio (DSCR) ratio, are determined to perform the economic analysis. The approach for calculating IRR in SAM will follow the method outlined in SAM webinar by Gilman (2015). First the inflation rate was set to zero so that the discount and nominal rates are equal. Then, a parametric analysis on the real discount rate using SAM was done with values ranging from 0 to 100% in increments of 10%. A value of 20% was obtained, as can be shown in Figure 28.

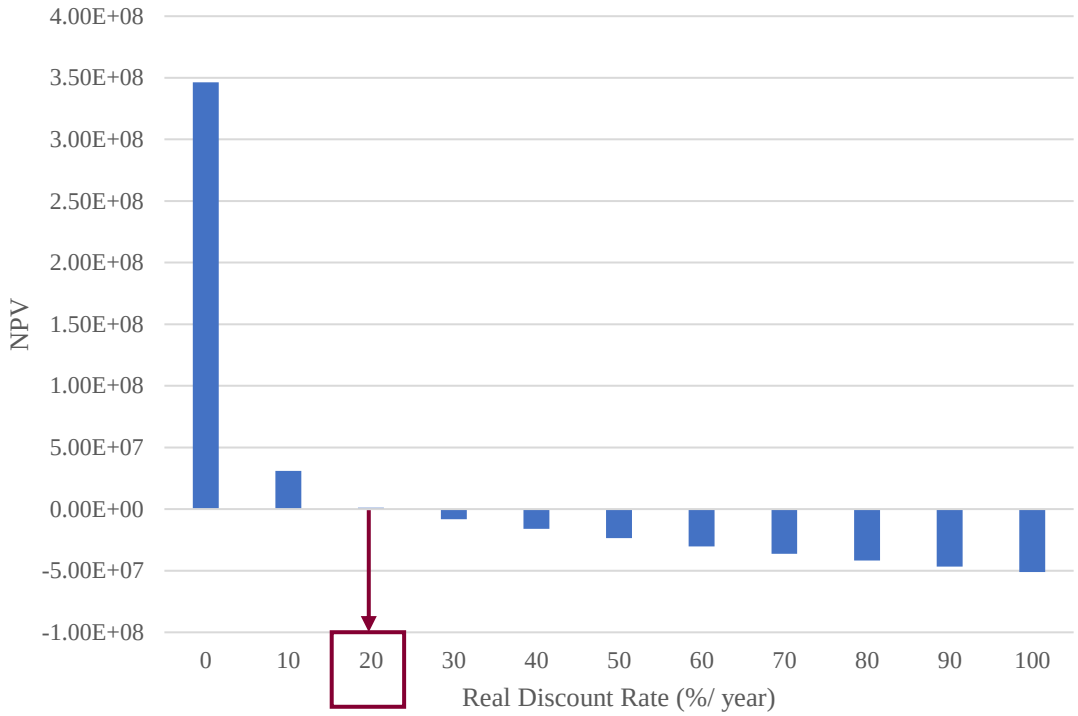

Figure 28. Parametric analysis on real discount rate

The DSCR is the ratio of annual cash flow available for debt service to the annual total debt service requirement. A value of DSCR above 1.2 is required to reduce investor risk, and it is recommended that this value should be considered between 1.3 and 1.4. Thus, the value of DSCR has been set at 1.4 in this study (NREL, 2024a).

One main indicator in this scheme is the levelized cost of energy (LCOE) which is the cost incurred to generate one unit of electricity from the plant over the entire analysis period. LCOE can be calculated using either real or nominal methods. Nominal LCOE method is usually used for shorter analysis periods and does not consider the inflation rate. However, given the long analysis period of utility-scale solar plants, the real LCOE method will be selected. This method considers long analysis periods and includes the inflation rate. Equation 13 is used to calculate real LCOE of the solar plants in this study, where C_o is the initial investment cost ($), C_n is the cash flow in year n

($), $d_{nominal}$ is the nominal discount rate (%),d_{real} is the real discount rate (%), and E_n is the total annual energy generated in year n.

$$LCOE_{real} = \frac{-C_o - \frac{\sum_{n=1}^{N} C_n}{(1+d_{nominal})^n}}{\frac{\sum_{n=1}^{N} E_n}{(1+d_{real})^n}} \quad \dots (13)$$

The analysis period for both utility-scale solar PV and CSP plants will be 25 years to make a fair comparison between both. The inflation rate is set at 2.5%, with a real discount rate of 10% and a nominal discount rate of 12.75% (IMF, 2025).

Another indicator of the financial analysis is the net present value (NPV), which assesses the profitability of a project by discounting future cash flows to present value, considering initial investment and operational costs. A positive NPV reflects the economic feasibility of the project, whereas a negative NPV indicates that the project will not be economically feasible. It is calculated using the following equation:

$$NPV = \sum_{n=0}^{N} \frac{C_n}{(1+d_{nominal})^n} \quad \dots (14)$$

Cost data estimates are determined by SAM based on previous articles found in literature and are continuously updated to reflect continuous developments in the field. Detailed costs for both PV and CSP plants are listed in APPENDIX III and APPENDIX IVAPPENDIX I respectively.

CHAPTER 5

RESULTS AND DISCUSSION

The feasibility of the 50MW utility-scale solar PV farm and the power tower and parabolic trough CSP plants is carried out using SAM software by NREL. The performance analysis and energy cost of the grid-connected plants were analyzed based on the annual energy production, capacity utilization factor, LCOE, NPV, plant efficiency and land use factor for each plant. As simulation was carried out for both selected sites, Ras Baalbeck and Baalbeck, SAM modeling showed very similar performances and costs in both proposed sites, given the location proximity and similar solar irradiation levels. Accordingly, the results for Site 1 Ras Baalbeck will be analyzed.

5.1. Optimization Results of CSP Plant

The optimization approach involves repeatedly refining design variables to simultaneously optimize multiple conflicting objectives, such as cost and efficiency. A parametric analysis will be performed using SAM through varying SM and TES hours to maximize energy production and minimize LCOE. The two later parameters were optimized based on energy concentration (GWh/acre), and LCOE. Energy concentration identifies the point where net electricity generation is maximized relative to land area, ensuring the most effective use of available land. The optimization process is constrained by achieving a minimum capacity factor of 35% (Hossain et al., 2024).

5.1.1. Optimization Analysis of Parabolic Trough CSP Plant

The variation of the capacity factor with respect to SM for the 50MW parabolic trough is shown in Figure 29. A minimum SM of 2.4 is required to achieve a capacity factor of more than 35%.

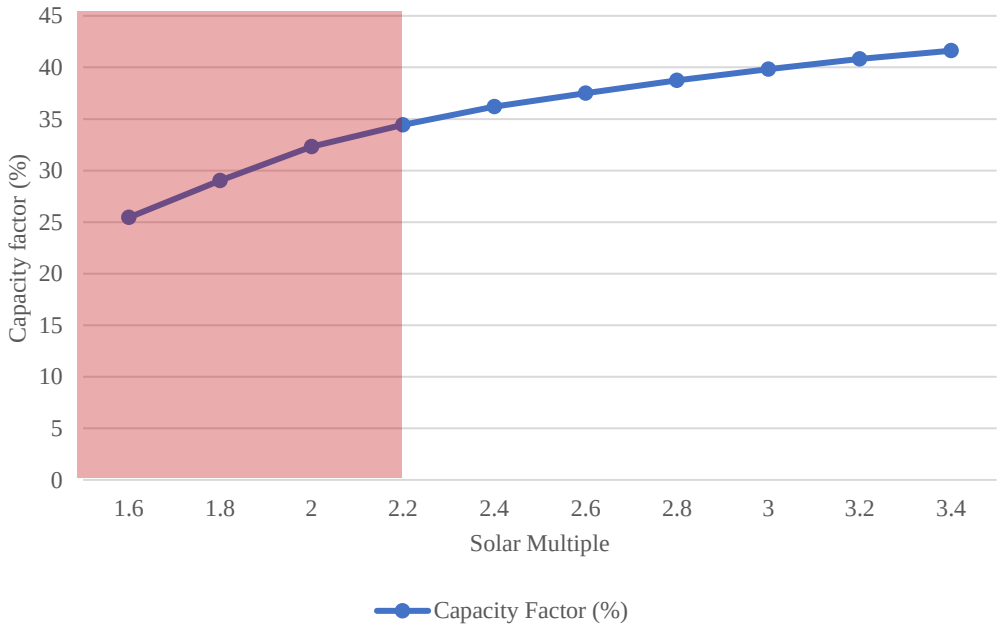

Figure 29. Variation of capacity factor based on different SMs for parabolic trough CSP plant

The energy concentration (GWh/acres) varies with SM so that the maximum energy concentration would be reached at the point where the annual net electricity generation and land area curves are farthest apart. This happens at SM 2.4, at which the annual energy generated is 159GWh, while the solar land area is 363 acres. Increasing SM to a value greater than 2.4 will increase land area linearly with a negligible increase in the annual energy generated that reaches a plateau at SM values larger than 3 as illustrated in Figure 30.

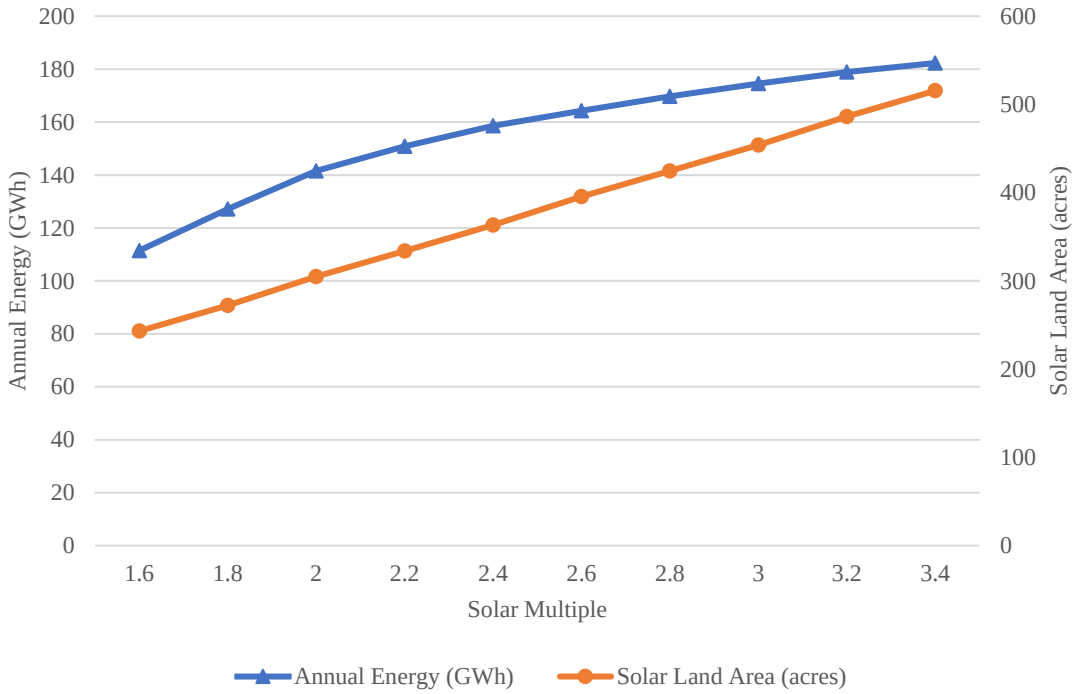

Figure 30. Variation of energy concentration based on different SMs for parabolic trough CSP plant

The sharp decrease in LCOE value happens when SM reached 2.4, where the LCOE reaches a minimum value of 18.81cents/kWh, as shown in Figure 31. Hence, SM 2.4 for the parabolic trough CSP plant will be selected.

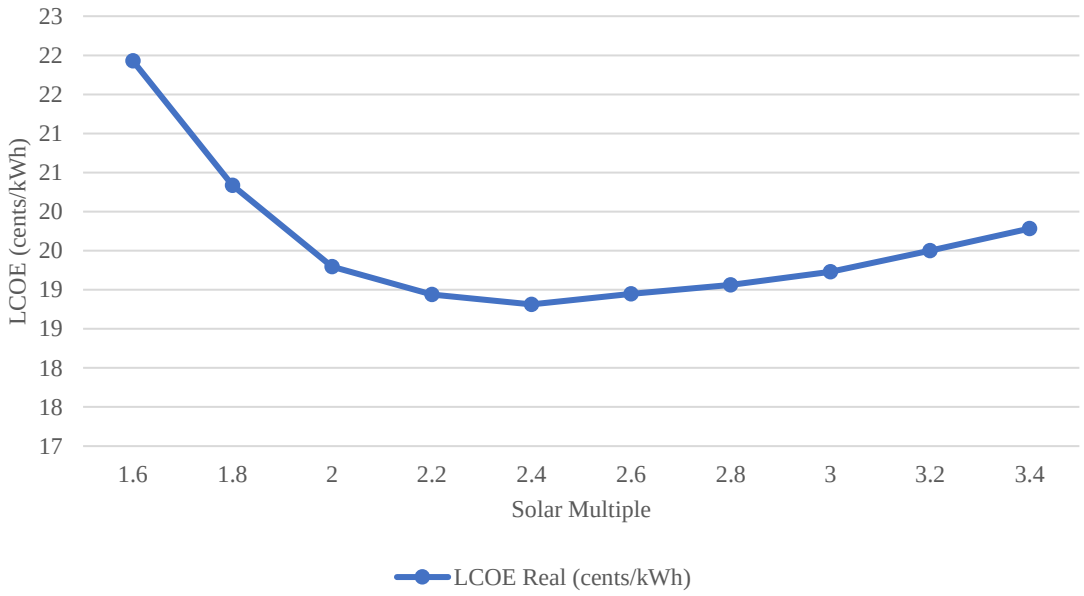

Figure 31. Variation of LCOE based on different SMs for parabolic trough CSP plant

After optimizing the solar multiple, the optimum full load storage hours for TES are determined to ensure optimal performance. The TES hours parameter is important to enhance the plant's efficiency and performance to allow longer operating time intervals. For the selected SM 2.4, the annual electricity generated and LCOE were analyzed for varying TES hours from 4 to 14 hours. Figure 32 shows the variation in the annual energy generated and LCOE with TES hours. The LCOE reaches a minimum value of 18.81cents/kWh at TES hours of 6 and then starts increasing sharply. Also, for TES of 6 hours, the annual energy generated is 159GWh. Further increasing the storage hours has little impact on annual energy generation, as it plateaus beyond this point.

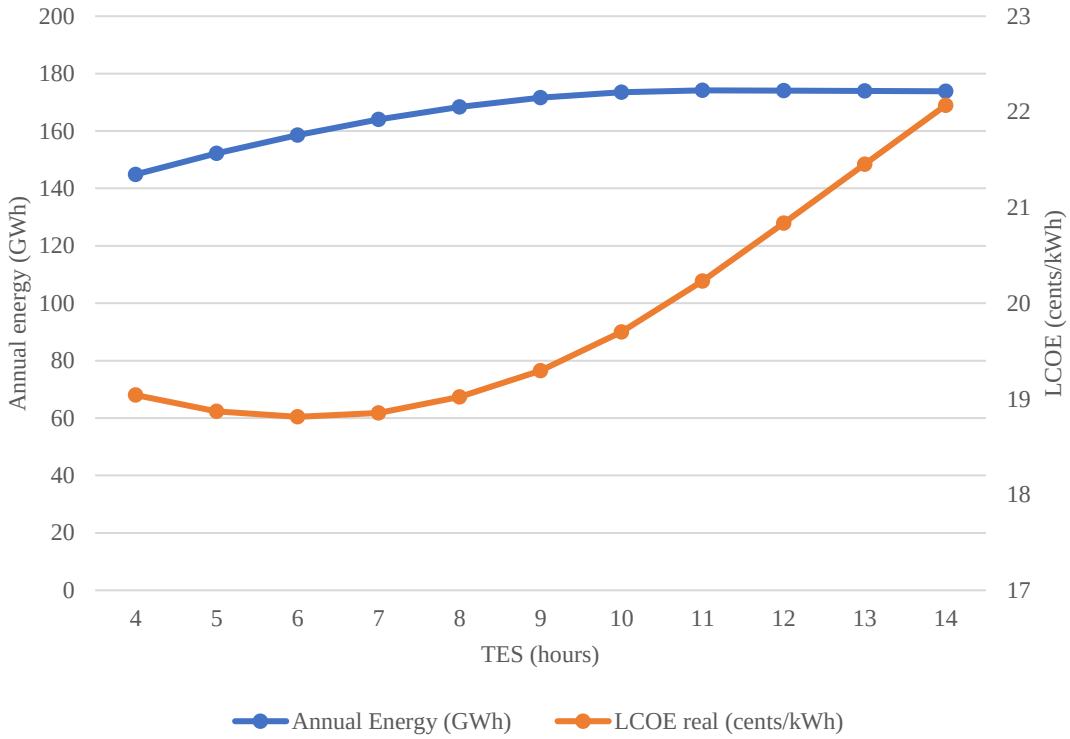

Figure 32. Annual energy and LCOE trend with varying TES hours for parabolic trough CSP plant

As a result, for a 50MWparabolic trough CSP plant, the maximum performance and minimum cost is achieved for a SM 2.4 and TES 6 hours.

5.1.2. Optimization Analysis of Power Tower CSP Plant

A similar approach was carried out for the power tower CSP plant. The variation of the capacity factor with respect to the solar multiple for the 50MW power tower CSP plant is shown in Figure 33. A minimum SM 1.8 is required to achieve a capacity factor of more than 35%.

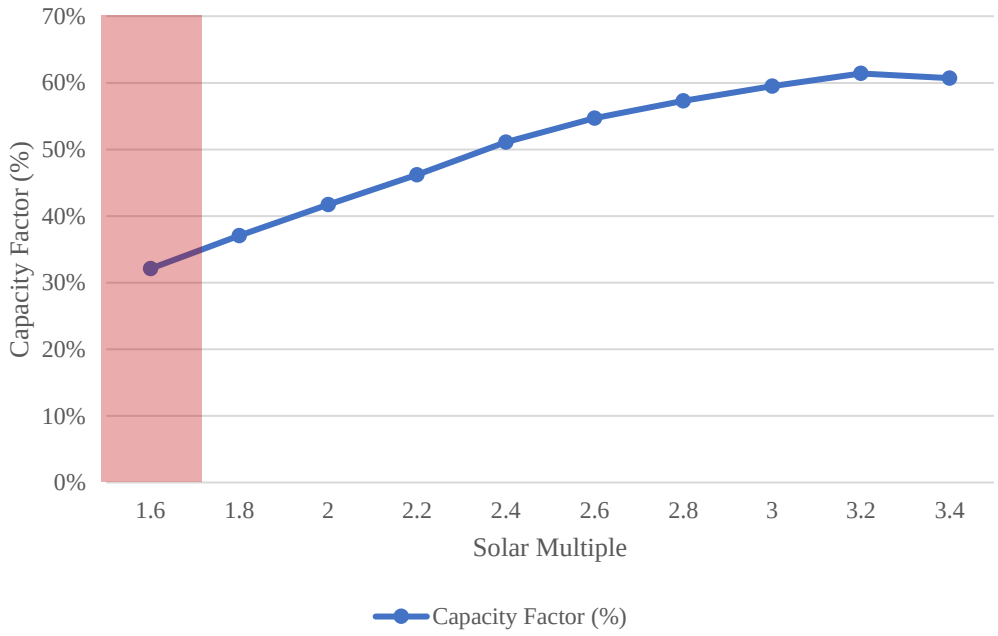

Figure 33. Variation of capacity factor based on different SMs for power tower CSP plant

The energy concentration maximizes at SM 2.2. At this value, the annual energy generated is 203GWh, while the solar land area is 748 acres, as shown in Figure 34. Increasing SM to a value greater than 2.2 will increase land area and annual energy generated linearly. The increase in annual energy production reaches a plateau beyond a SM 3, while the slope of the land area curve continues increasing linearly.

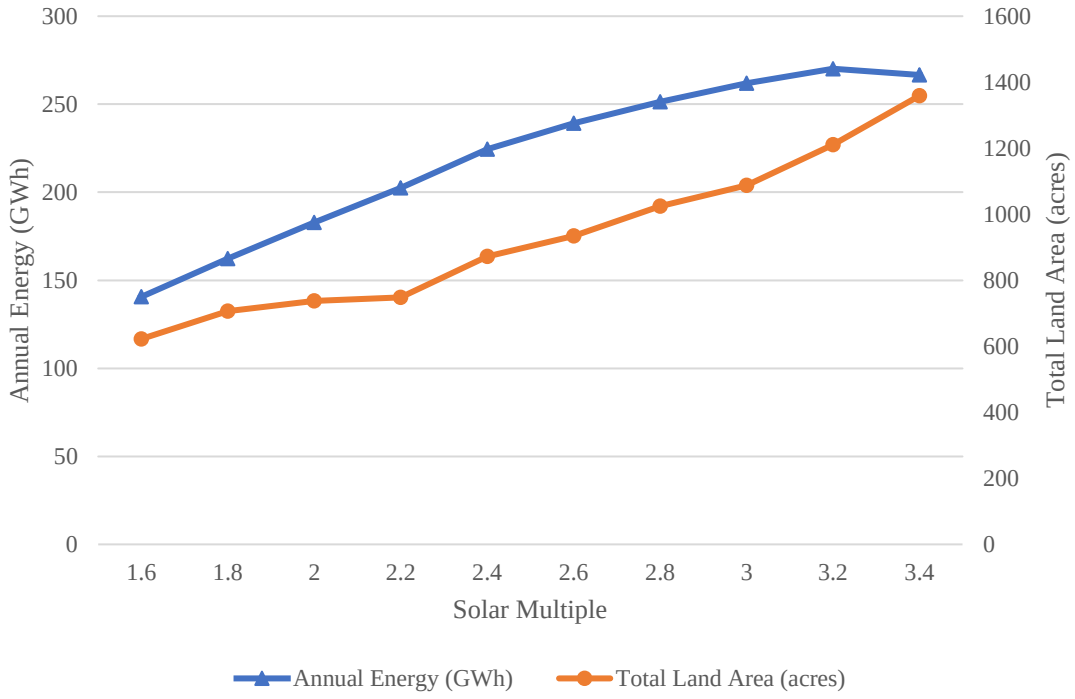

Figure 34. Variation of energy concentration based on different SMs for power tower CSP plant

While energy concentration is maximized at SM 2.2, the lowest LCOE ranges between SM 2.4 to 2.8, and reaches the minimum value at SM 2.6, as seen in Figure 35. Solar tower CSP plants require much larger area as compared to the parabolic trough CSP plant. At SM 2.2, the land area required for a power tower plant is 32% higher than that of parabolic trough plant with a SM 2.4. However, the results show that at SM 2.6, the solar field efficiency would not decrease despite the land area increase. Moreover, the energy generated for SM 2.6 is 18% higher than that for SM 2.2 and the LCOE is only 3% lower. Therefore, increasing SM to 2.6 would be technically and economically favorable. At this value of SM, the number of heliostats required is 5,322 with a power tower height of 183.1m, according to SolarPILOT optimization algorithm by SAM.

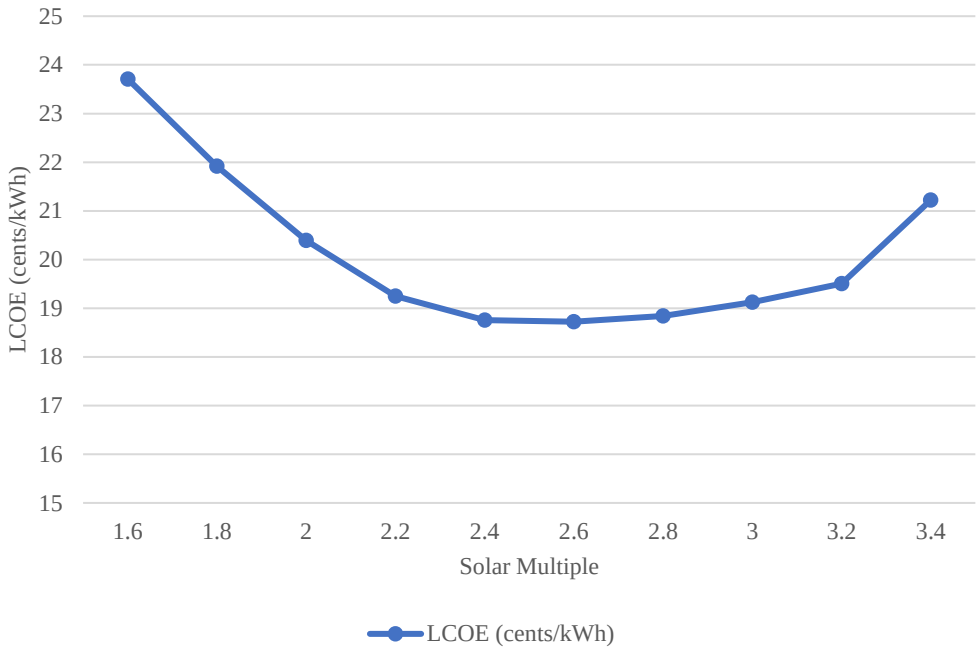

Figure 35. Variation of LCOE based on different SMs for power tower CSP plant

After the selection of the optimized SM, TES hours will be determined using the same parametric analysis in SAM. TES hours are varied ranging from 6 to 16 to determine the best performance and lowest LCOE of the power tower. Figure 36 shows the variation of annual energy generated and LCOE with respect to TES hours. The LCOE value drops until TES hours reach 12h, after which the cost reduction becomes minimal. However, a minimum LCOE value of 18.55cents/kWh is obtained with an annual energy generated of 242GWh at 13h TES hour capacity. If TES hours increase beyond 13h, LCOE value increases again with a negligible increase in the annual energy being generated from the plant. Therefore, a TES hour capacity range of 12h to 14h is recommended.

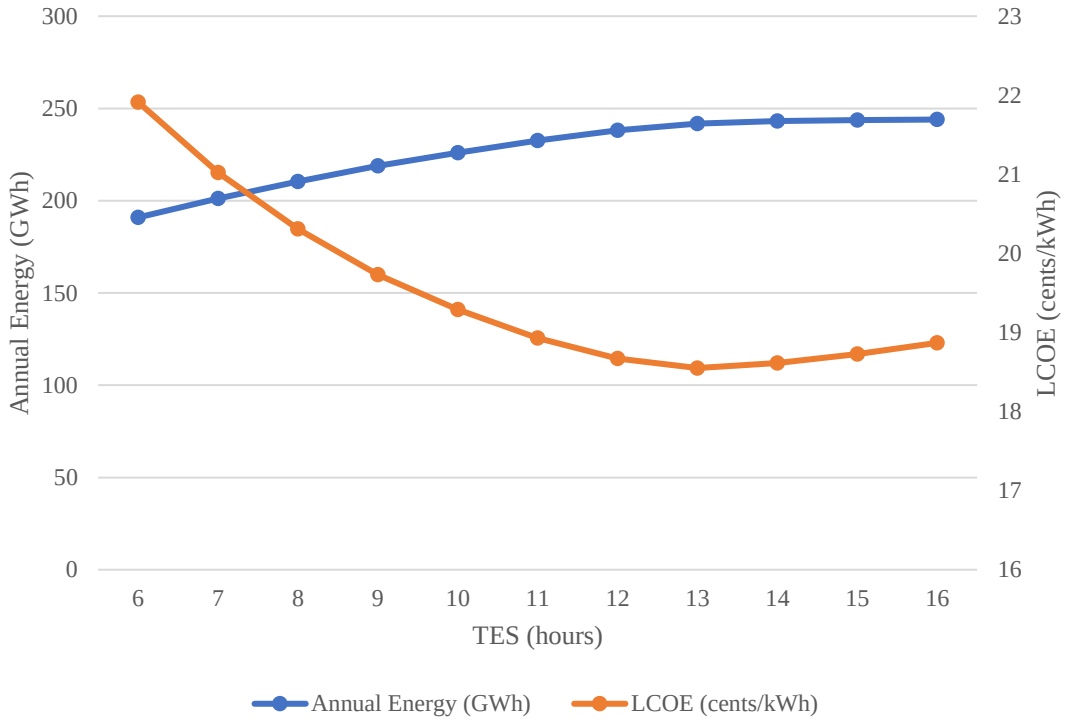

Figure 36. Annual energy and LCOE trend with varying TES hours for power tower CSP plant

Optimization analysis shows that for a 50MW power tower CSP plant, the optimum performance and minimum cost is achieved for a SM 2.6 and TES 13 hours.

5.2. Performance Analysis of the CSP Plants

After optimizing the key design parameters of the parabolic trough and power tower CSP plants, the annual energy produced, capacity utilization factor, and overall plant efficiency were analyzed to compare the performance of both plants. Additionally, the economic feasibility of the plants will be analyzed based on NPV and LCOE.

5.2.1. Technical Analysis of Proposed CSP Plants

Figure 37 shows the monthly energy generated for 50MW parabolic trough and power tower CSP plants. For SM 2.4 and TES of 6 hours, the annual energy generated from the parabolic trough CSP plant is 159GWh with a capacity factor of 36.2%. The monthly energy peaks during the month of July, reaching a value of 25.5GWh, while the monthly energy from the plant during January is minimum with a value of 1.4GWh. This seasonal difference is due to higher DNI levels and temperatures in summer, which helps meet the increased electricity load during summer.

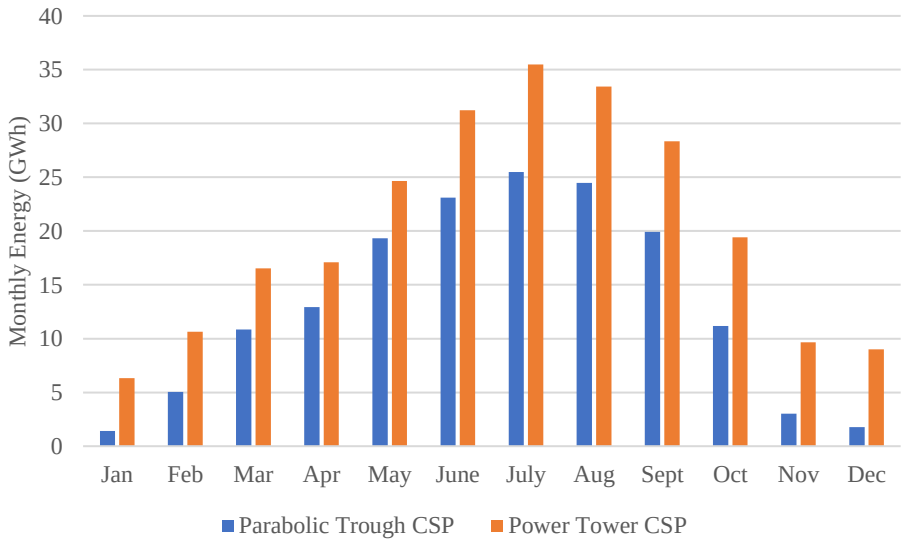

Figure 37. Monthly energy generated from parabolic trough vs power tower CSP plant

On the other hand, the annual energy output of the power tower CSP plant is 242GWh with a capacity factor of 55.21%, for a SM 2.6 and 13h TES hours. The maximum monthly energy produced is during July (35.5GWh), while the minimum monthly energy produced is obtained in January (6.33GWh).

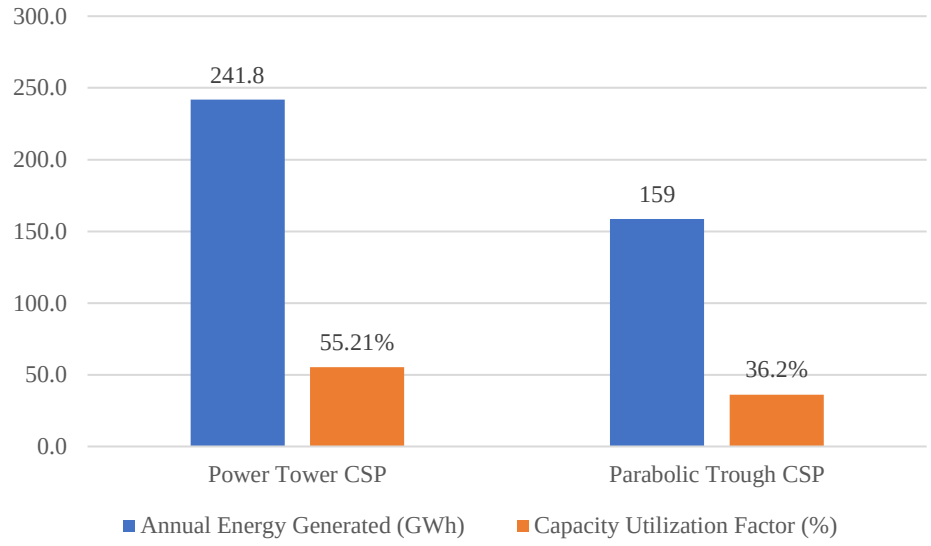

Figure 38. Performance comparison of power tower and parabolic trough CSP power plants

The annual energy generated in year 1 and the capacity utilization factor of both CSP power plants are shown in Figure 38. The annual energy produced for a power tower exceeds the energy produced of a parabolic trough CSP plant by 52.2%. This is owed to several factors. Parabolic trough plants experience higher thermal losses due to recirculation of HTF in the receiver during insufficient solar irradiation levels to prevent freezing. This eventually decreases the plant's performance. As for the power tower CSP power plant, the HTF is drained from the receiver when not in operation, resulting in reduced thermal losses and higher efficiency. Additionally, parabolic trough plants require more pumping power to circulate HTF, increasing auxiliary energy consumption. In contrast, power tower systems offer better storage integration, as molten salt serves both as the HTF and storage medium. This increases the thermal energy storage as compared to parabolic troughs, which need additional heat exchangers for storage purposes (NREL, 2003).

The solar field efficiency and overall plant efficiency are key parameters that must be analyzed to study the plant's technical performance. The efficiencies are obtained using equations… (4) to … (9). Figure 39 shows the overall plant and solar field efficiency of the CSP plants studied.

Figure 1

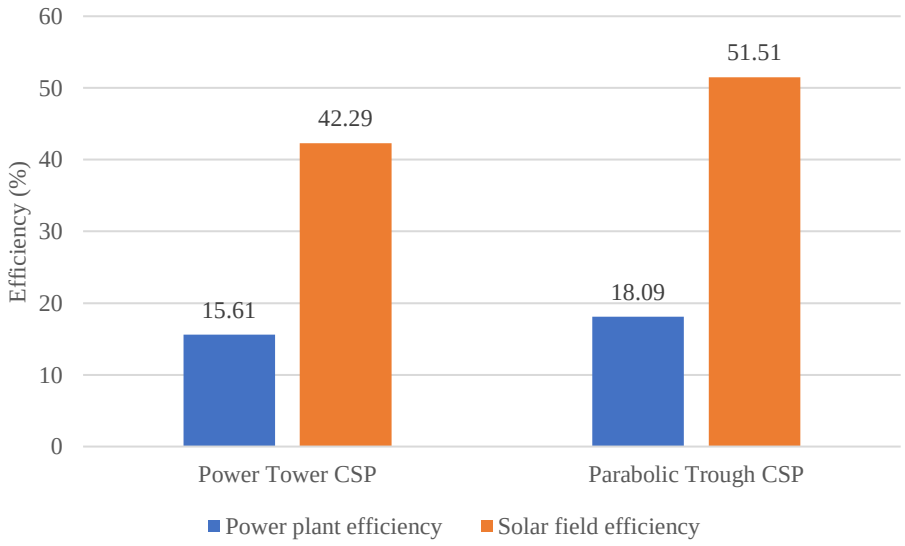

Figure 39. Comparison of CSP plants: power plant and solar field efficiency

Parabolic trough collectors result in higher annual solar field efficiency than the heliostat field of the power tower CSP power plant. This is primarily due to higher optical and atmospheric attenuation losses of the heliostats, in addition to the focusing error due to the large distance over which the energy is transmitted from the solar field to the receiver. As a result, the losses in the heliostat field of the power tower CSP are higher than the losses in the solar collectors of the parabolic trough CSP. The overall power plant efficiency follows a similar trend to that of solar field efficiency. The lower overall efficiency of the power tower CSP power plant can be explained from the inherent lower efficiency of the heliostat field compared to the parabolic trough collectors.

5.2.2. Economic Evaluation of CSP Plants

The analysis period of the parabolic trough and power tower CSP plant was determined at 25 years. The net capital cost (NCC) of the parabolic trough plant is 319,309,000$, with an 80% debt (255,326,400$) and 20% equity (63,982,748). However, the NCC of the power tower plant is higher than that of the parabolic trough (471,501,792$), with 80% debt and 20% equity. The PPA price of the plants is calculated by SAM based on the determined IRR value (20%). The PPA price at year 1 of the parabolic trough is 25.22 cents/kWh, which is close to that of the power tower 24.84 ¢/kWh, with an annual escalation rate of 1%. Figure 40 shows the annual after-tax cashflow of the proposed 50MW parabolic trough and power tower CSP plants. The huge negative cashflow in year 0 represents the NCC of the plant minus the project debt. The debt spans over 18 years, and after that, the net-positive cashflows of the plant increase by almost 3-fold.Figure 1

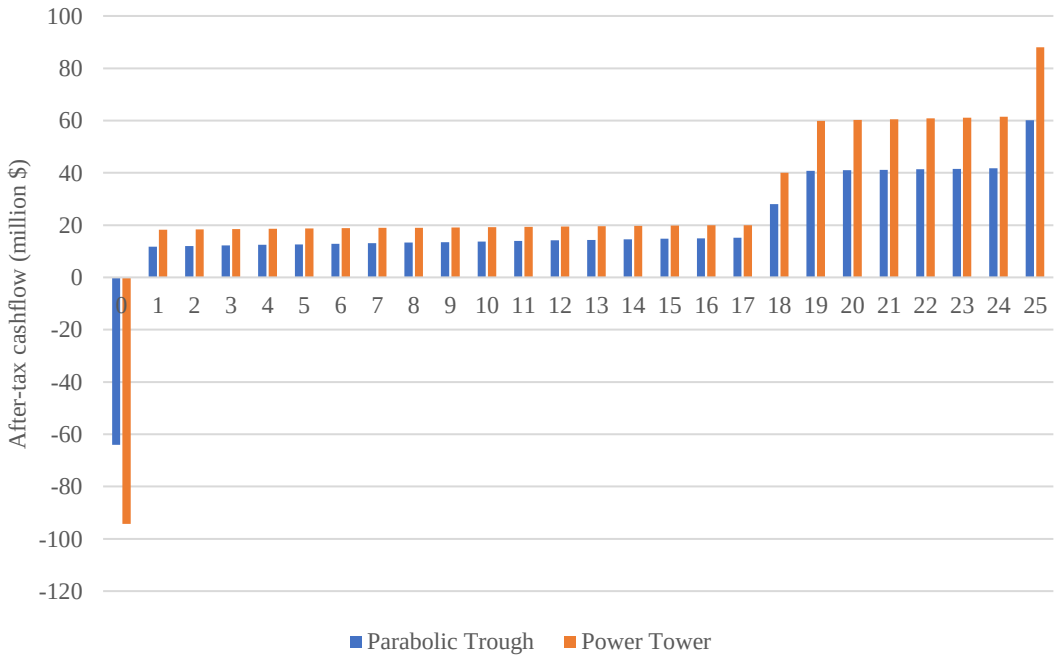

Figure 40. Annual after-tax cashflow of the proposed CSP plants

The LCOE of the parabolic trough and power tower CSP plants is 18.81cents/kWh and 14.85cents/kWh respectively. Additionally, the net present value (NPV) of the parabolic trough system is estimated at $49.6 million, which is lower than the $71 million NPV of the power tower system.

5.3. Performance Analysis of the PV Plant with BESS

5.3.1. Technical Analysis of the PV Plant

The 50MW utility-scale PV solar farm was designed and simulated using SAM. The performance of the PV farm was analyzed based on the annual energy produced and capacity utilization factor. Figure 41 shows the monthly energy generated for the proposed PV solar farm. The annual energy generated is 105GWh with a capacity factor of 24.01%. The monthly energy peaks during summer months, particularly in August as it reaches 11.4GWh. In contrast, the lowest monthly energy is produced during winter months, where it reaches a minimum value of 5.11GWh during December.

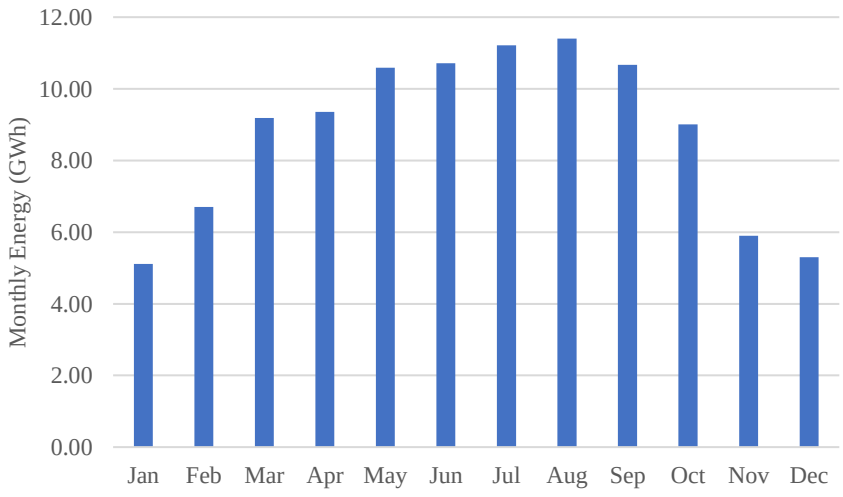

Figure 41. Monthly energy generated for PV solar farm + BESS

5.3.2. Economic Analysis of the PV Plant

The analysis period of the 50MW solar PV farm is determined at 25 years, similar to that of the CSP plants to have a fair comparison. The NCC of the PV farm is 240, 437,632$ with an 80% debt spanning over 18 years. Note that the NCC of the PV farm is much lower than that of the proposed CSP plants. The PPA price of the PV plant is calculated by SAM by setting the IRR to 20%. The PPA price is 27.67 cents/kWh with a 1% annual escalation. The NPV value obtained is 33.8$ million. Figure 42 shows that annual after-tax cashflow of the proposed 50MW PV farm. The initial investment cost is 48.1$ million. This cost includes the NCC minus the debt. The project generates a positive income in year 1 onwards at the calculated PPA price. After year 18 (the debt period), the cash flow increases by 3-fold. Note that the cashflow in years 14 and 15 is negative. This is because of the battery replacement cost in year 15.

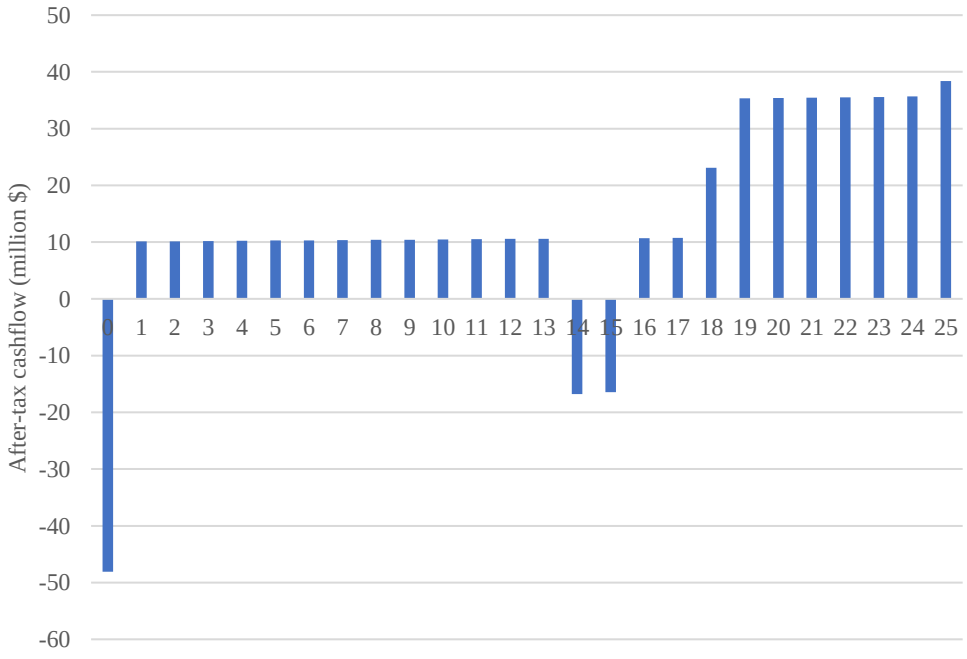

Figure 42. Annual after-tax cashflow of the proposed PV plant with Li-ion battery storage

5.4. Comparison between PV and CSP Plants

A performance evaluation of the proposed 50MW solar PV farm and parabolic trough and power tower CSP plants will be conducted by comparing key parameters such as annual energy generated, lifetime electrical output, capacity utilization factor, solar-to-electric efficiency, and land use factor. In addition, an economic comparison will be presented to study the proposed plants' feasibility.

5.4.1. Electrical Energy

Figure 43 presents the annual power generation of the proposed plants. The power tower CSP plant has the highest generation at 241.8 GWh, followed by the parabolic trough CSP plant at 159 GWh and the solar PV farm at 105.2 GWh. In year 1, the power tower CSP plant produces approximately 139% more energy than the solar PV farm and 52% more than the parabolic trough CSP plant.

The capacity utilization factor indicates how effectively a power plant operates compared to its maximum potential output. It is the ratio of the energy generated by the plant to the electrical energy that this plant generates operating at its full capacity. SAM calculates the capacity factor of the simulated plant as per equation … (10). The capacity utilization factor of the power tower CSP plant is the highest at 55.21%. In contrast, the capacity utilization factor of the parabolic trough CSP plant is 36.2% flowed by the PV farm at 24.01%. CSP plants have higher operational capacity than solar PV farms because of thermal energy storage systems, which allow continuous power generation during periods of low sunlight, such as at night or on cloudy days. However, utility-scale PV farms have a lower capacity utilization factor than CSP with an average of 20% (IRENA, 2024b).

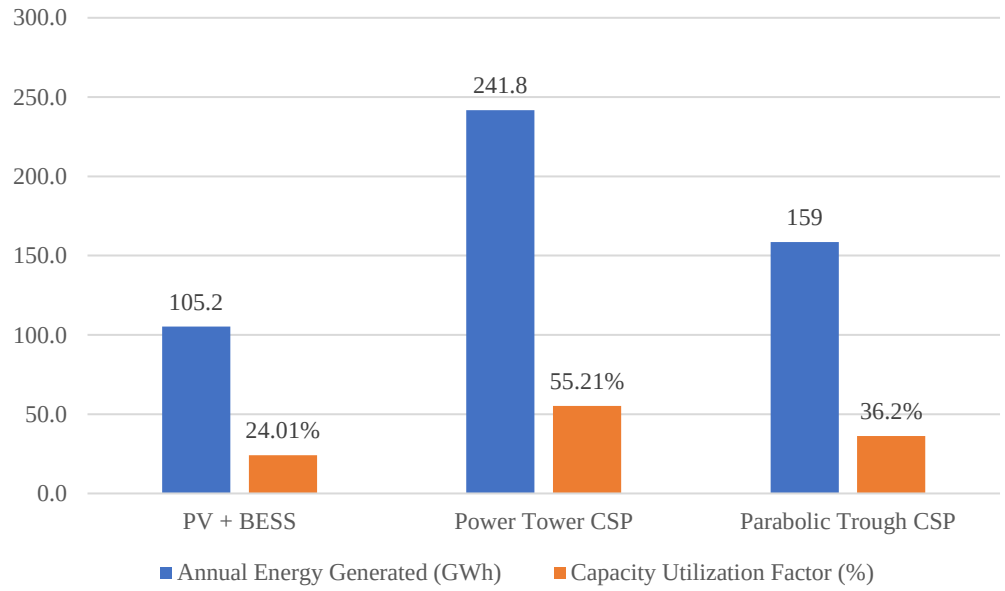

Figure 43. Annual energy produced and capacity factor for the proposed solar power plants

Moreover, as shown in Figure 44, the power tower CSP plant has better lifetime performance as compared to that of the parabolic trough CSP and PV farm. The gap between the cumulative energy generation curves of the CSP plant and the PV farm widens each year. This difference is attributed to the lower annual performance degradation of CSP plants due to aging (0.2%/year) as compared to PV farms (0.5%/year) (Awan et al., 2019). As a result, the power tower CSP plant generates 2.4 times more energy than the PV farm over its lifetime (25 years).

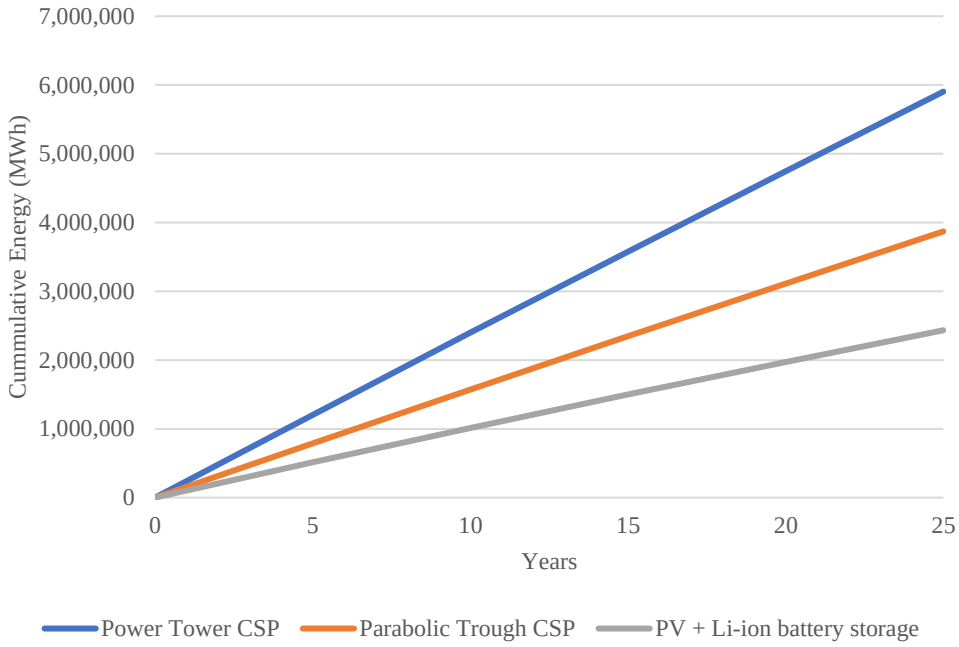

Figure 44. Cumulative energy produced by PV and CSP plants

5.4.2. Comparative Efficiency and Land Utilization of the Proposed Plants

A comparative analysis will be conducted to study the plants' efficiencies and land use factors, in addition to the annual energy generation and lifetime performance. Specifically, comparing land-use factor and solar-to-electric efficiency will provide more comprehensive assessment.

The solar to electric efficiency is another performance evaluation which refers to the percentage of solar energy that is converted into usable electrical energy by the proposed solar plants. It is the ratio of the amount of total electrical energy generated to the available solar energy received, calculated as per the following formula:

$$\eta_{SE} = \frac{E_{net}}{E_S} \quad \ldots (15)$$

Where E_S is the annual solar irradiation at the specified location multiplied by the total reflective area of the solar collectors. Figure 45 represents the solar to electric

efficiency of the solar power plants studied. The solar energy received by the solar field (E_S) is directly proportional to the total reflective area of the solar collectors. The power tower CSP plant has the largest solar field area and therefore has the highest E_S. In contrast, E_S of the solar PV farm is minimum given its smallest solar field area.

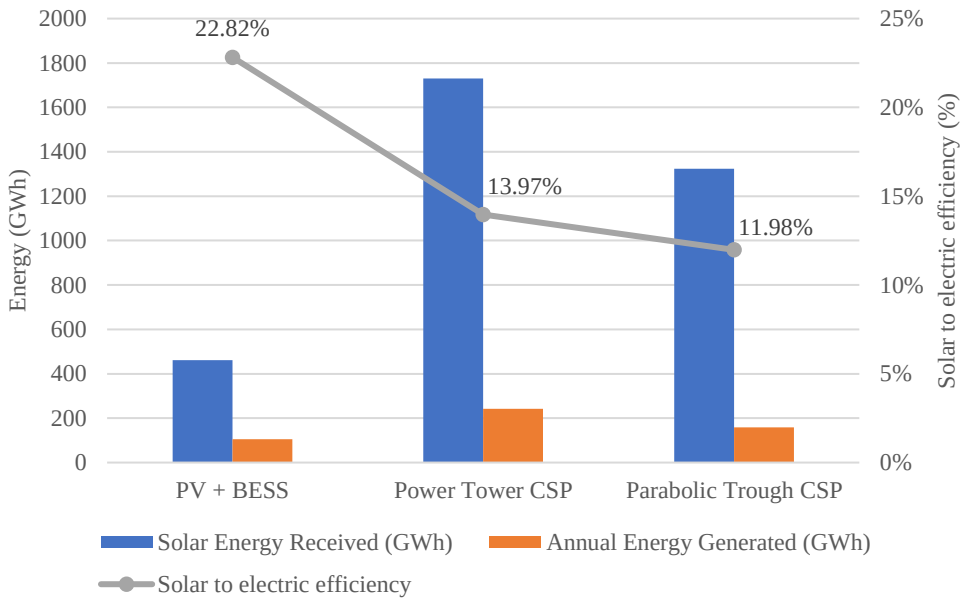

Figure 45. Solar to electric efficiency of the solar power plants

The solar to electric efficiency of the proposed solar PV farm leads with 22.82%, followed by the power tower CSP at 13.97%, and finally the parabolic trough CSP at 11.98%. The lower solar to electric efficiency of CSP power plants is mainly attributed to two main factors. First, CSP systems require larger heliostat aperture areas that concentrate sunlight, and this leads to higher optical losses. The second factor is the multiple energy conversion stages of CSP power plants unlike solar PV. These factors then result in lower solar-to-electric efficiencies for CSP power plants as compared to PV farms with BESS. However, as shown in Figure 43, CSP power plants have higher

capacity utilization factor than solar PV farms. The higher capacity factors are mainly driven by increased thermal storage capacity and increased operating temperatures due to continuous improvements.

Another important evaluation criteria to consider is the land use factor. The land use factor measures the spatial efficiency of solar power plants. It is the ratio of the active area of the solar field to the total area of the plant (Awan et al., 2019). It is expressed by the following equation:

$$L_F = \frac{A_{SF}}{A_T} \quad \ldots (16)$$

As seen in Figure 46, the parabolic trough CSP has the highest land use factor (0.29), followed by the PV farm (0.27), and finally the power tower CSP (0.21). Results show that the parabolic trough CSP plant has a better land use factor for collecting solar energy as compared to the power tower CSP for the determined key design parameters after optimization analysis. The relatively lower land use factor of power tower CSP is due to several key reasons. Heliostats have a larger collection area than the parabolic trough collectors. In addition, the positioning of the heliostats in the solar field requires wider spacing to avoid shading.

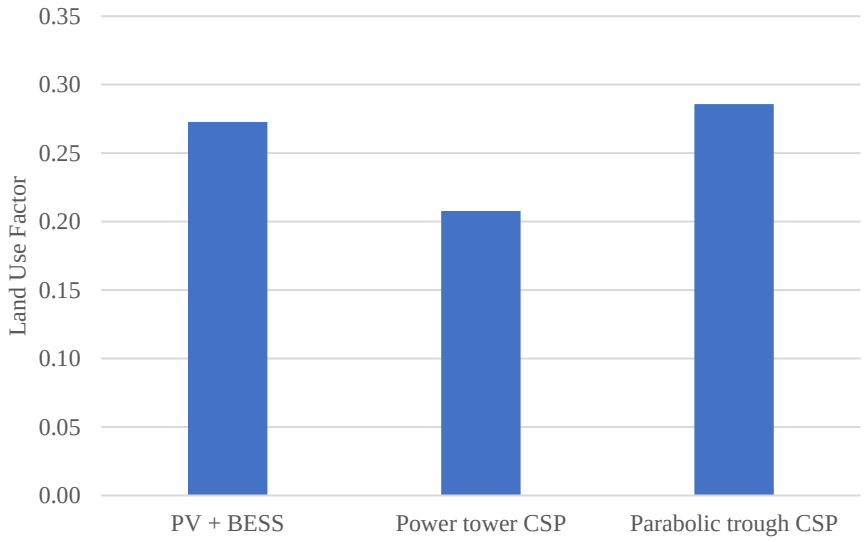

Figure 46. Land use factor of the proposed PV and CSP plants

5.4.3. Economic Assessment of the Proposed Plants

The NCC, NPV, and LCOE will be considered to evaluate the economic feasibility of the proposed PV and CSP plants. The details of the economics of the proposed solar PV and CSP power plants are shown in Table 2.

Table 2. Economic results of solar PV and CSP power plants

	PV+BESS	Power Tower CSP	Parabolic Trough CSP
Net Capital Cost (million $)	240	472	319
NPV (million $)	34	71	50
LCOE real (cents/kWh)	26.98	14.85	18.81

The net capital cost (NCC) is highest for the power tower CSP plant at $472 million, which is 1.5 times higher than that of the parabolic trough CSP plant and almost double times that of the solar PV farm. Similarly, the NPV of the power tower CSP plant is also the highest among the plants studied, at a value of $71 million. Moreover, SAM simulation results showed that the 50MW power tower CSP plant with

13 TES has the lowest LCOE of 14.85 cents/kWh. On the other hand, the 50MW solar PV farm with 8 hours of BESS has the highest LCOE at 26.98 cents/kWh. Note that the high LCOE of the solar PV farm is mainly attributed to the high costs of electrical energy storage (BESS). Despite having the highest NCC, the LCOE of the power tower is the lowest compared to the parabolic trough CSP and solar PV power plant. Power tower CSP plants have lower O&M costs over the power plant lifetime, unlike solar PV farms integrated with BESS, where the battery replacement costs over the plant's lifetime increases the LCOE significantly. Additionally, solar CSP plants have better capacity utilization factor that solar PV farms, resulting in higher energy generation and a lower cost per kWh.

In comparison, energy generation costs in Lebanon from traditional fossil fuels and private diesel generators are significantly higher than the LCOE of the proposed PV and CSP plants. Traditional fossil fuel-based power plants have a generation cost ranging from 13 to 21.44 cents/kWh (Ayoub et al., 2021) In contrast, the generation costs of private diesel generators reached 50 to 100 cents/kWh in 2021(Ayat, 2021). Therefore, the competitive LCOE of the proposed PV and CSP plants makes them an attractive alternative to traditional fossil fuel-based generation in Lebanon.

5.5. Performance Assessment and Key Outcomes

The results of the techno – economic comparison of the solar PV and CSP power plants at the selected sites in Lebanon are summarized in Table 3.

Table 3. Summary of key technical and economic results

	PV + BESS	Power Tower CSP	Parabolic Trough CSP
Annual energy generated in year 1 (GWh)	105.17	241.82	158.56
Lifetime electrical output (GWh)	2,433	5902.56	3870.31
Capacity utilization factor (%)	24.01%	55.21%	36.2%
Solar field efficiency (%)	-	42.3%	51.5%
Net Capital Cost (million $)	240.44	471.50	319.31
NPV ($)	33.82	71.32	49.56
LCOE real (cents/kWh)	26.98	14.85	18.81
Land Area (acres)	203	914	508

The results show that the power tower CSP power plant has the highest annual energy generated (241.82GWh), capacity utilization factor (55.21%), and the lowest LCOE (14.85cents/kWh) among all three power plants studied. Although the power tower CSP power plant has the highest net capital cost, the battery replacement costs of solar PV farms are substantial, increasing the LCOE significantly. However, one major advantage of the solar PV farm over both CSP power plants is the low land requirement (22% of the power tower CSP and 40% of the parabolic trough CSSP), where land availability is a major challenge in highly densely populated countries like Lebanon. In contrast, the parabolic trough collectors have higher solar field efficiency than the heliostat field of the power tower CSP power plant. This is mainly due to the high atmospheric attenuation losses of the heliostat field resulting in a decrease in solar field efficiency and therefore the overall plant efficiency.

The selection of the most feasible solar power plant in Lebanon depends on the priorities set by the government, investors, and policy makers. While the three proposed solar power plants proved their technical and economic feasibility, the deployment of

power tower CSP power plant is recommended if the main priority is high energy generation output and cheaper electricity. CSP technology offers higher efficiency by integrating thermal energy storage, therefore resulting in higher energy generation. However, if there is a constraint on the lower land area, the solar PV farm is recommended. PV solar farms require less land than CSP systems with the same nameplate capacity. In addition, the deployment of CSP plants poses an environmental challenge that must be thoroughly addressed through life cycle assessments. However, solar PV farms have lower environmental footprint and minimum water consumption favoring them over CSP plants.

CHAPTER 6

CONCLUSION

6.1. Summary of findings

Lebanon’s ongoing electricity crisis, driven by a heavy reliance on expensive and polluting fossil fuel imports, led to the sector’s collapse and imposed heavy financial burdens on the country. Consequently, people relied on expensive private diesel generators due to the frequent blackouts and unreliable electricity supply. The LCOE of energy generation in Lebanon from fossil fuel thermal and combined cycle plants ranges between 13 to 21.44 cents/kWh (Ayoub et al., 2021). The tariff of private generators reached a range of 50 to 100 cents/kWh after chronic blackouts by EDL and the removal of the fuel subsidies (Ayat, 2021). Lebanon's abundant solar resources present a valuable opportunity to invest in solar energy and diversify its energy mix to achieve energy diversification, security, and reliability.

This study explored the feasibility of deploying utility-scale solar plants. It conducted a comparative analysis of a 50MW utility scale solar PV farm with BESS and two types of CSP plants, power tower and parabolic trough with thermal energy storage. The key design parameters of the CSP plants were optimized to achieve maximum performance. The proposed solar plants were designed and simulated on SAM software by NREL. A technical and economic evaluation was performed to compare the performance of the proposed plants under Lebanon’s climatic conditions at the selected site.

The North Bekaa region in Lebanon is an ideal site due to several factors. The region has high solar irradiation, with a DNI of 2,252 W/m2 and a GHI of 2,045W/m2.

Also, the sites chosen for the deployment of the proposed solar plants have low population density. Additionally, the land is characterized as non-agricultural land and has access to freshwater from the Al-Asi River. Finally, the 220kV HV transmission lines are near which facilitate grid integration. All these factors make this region ideal for the deployment of utility-scale solar plants.

The proposed solar PV farm and power tower and parabolic trough CSP plants have the same nameplate capacity of 50MW. For the CSP plants, the key parameters were optimized using parametric analysis in SAM. The results indicated that the performance of the power tower system is maximized at SM of 2.6 and 13h TES, while the parabolic trough system performs best with an SM of 2.4 and 6h TES. The solar PV farm is coupled with an 8h BESS.

The technical comparison of the utility-scale solar PV farm and the optimized power tower and parabolic trough CSP plants was carried out based on the electrical output, capacity utilization factor, solar to electric efficiency, and land use factor. The analysis period was determined at 25 years. Power tower CSP had better performance than the parabolic trough CSP power plants. This is because in parabolic trough systems, the HTF continuously circulates in the receiver tubes to prevent freezing. As a result, thermal losses increase, and the thermal efficiency of the plant is reduced. However, unlike parabolic trough systems, the receiver of the power tower CSP plant is drained when not in operation, limiting thermal losses and increasing the output energy generated.

Results showed that the power tower CSP plant had the highest annual energy generation at 241.8GWh and a capacity utilization factor of 55.21%. However, the lowest annual energy generation and the capacity utilization factor were obtained for the

solar PV farm (105.2GWh and 24.01%). The solar to electric efficiency of the PV farm is the highest at 22.82%, as compared to 13.97% of the power tower CSP. In contrast, the parabolic trough system has the lowest efficiency of 11.98%.

The economic analysis of the proposed plants showed that the power tower CSP system has the highest NPV at $71 million, followed by the parabolic trough plant and then the solar PV farm ($50 million and $35 million respectively). In terms of LCOE, the power tower plant has also the lowest LCOE at 14.85cents/kWh, with the parabolic trough and PV systems following (18.81 cents/kWh and 26.98 cents/kWh respectively). The high LCOE of the solar PV farm is mainly due to high costs associated with the BESS.

6.2. Insights and Recommendations

The studied parabolic trough and power tower CSP power plants with TES systems and solar PV farm with BESS have demonstrated their technical and economic feasibility when compared to the LCOE of fossil fuel-based generation in Lebanon. Even under the absence of financial incentives such as tax credits and subsidies, the LCOE of utility-scale solar power plants remain competitive compared to that of fossil fuel-based plants especially when accounting for fuel import costs and price volatility.

As such, the selection of the most feasible solar power plant in Lebanon depends on the priorities set by the government, investors, and policy makers. CSP technology with thermal energy storage has better performance and higher economic returns compared to utility-scale solar PV with BESS. Therefore, the deployment of power tower CSP power plant is recommended if the main priority is high energy generation output and lower costs of electricity production. Additionally, the thermal energy

storage capability of CSP power plants is a major advantage as compared to solar PV technologies, even with BESS. However, a significant constraint of CSP power plant deployment is the higher land use required for CSP systems which limits their feasibility based on the land area availability. In this case, the solar PV farm is recommended.

Based on the comparative analysis conducted in this study, two key insights have emerged which are important to consider while determining the proper energy mix in Lebanon at the electricity production level.

First, the results of this study showed that both parabolic trough and power tower CSP power plants with TES system outperform solar PV farm with BESS, taking as reference equal installed capacity of 50MW. However, it would be interesting to consider assessing both solar PV and CSP power plants using net capital cost as the primary reference, knowing that it is a decisive factor from an investor's perspective.

Second, the LCOE of the PV farm can be reduced by around 25% if battery storage is excluded. This would significantly improve its economic competitiveness. Accordingly, it would be interesting to study the feasibility of a solar PV farm backed up by fossil fuel-based thermal power plant, forming a transitional energy mix. Rather than investing in costly storage technologies, the fossil fuel thermal plant will be used as backup to supply peak demand and ensure the system's stability during intermittency. However, this alternative should be evaluated carefully as fossil fuel thermal plants have several long-term concerns. First, the operating and maintenance costs of the fossil fuel thermal plant are significant. Second, fuel price volatility poses a major financial risk subject to international market fluctuations and geopolitical

instability. Lastly, GHG emissions associated with fossil fuel power plants must be considered since they undermine the goals of low-carbon energy transition.

APPENDIX I

LEBANON'S SOLAR IRRADIATION MAP

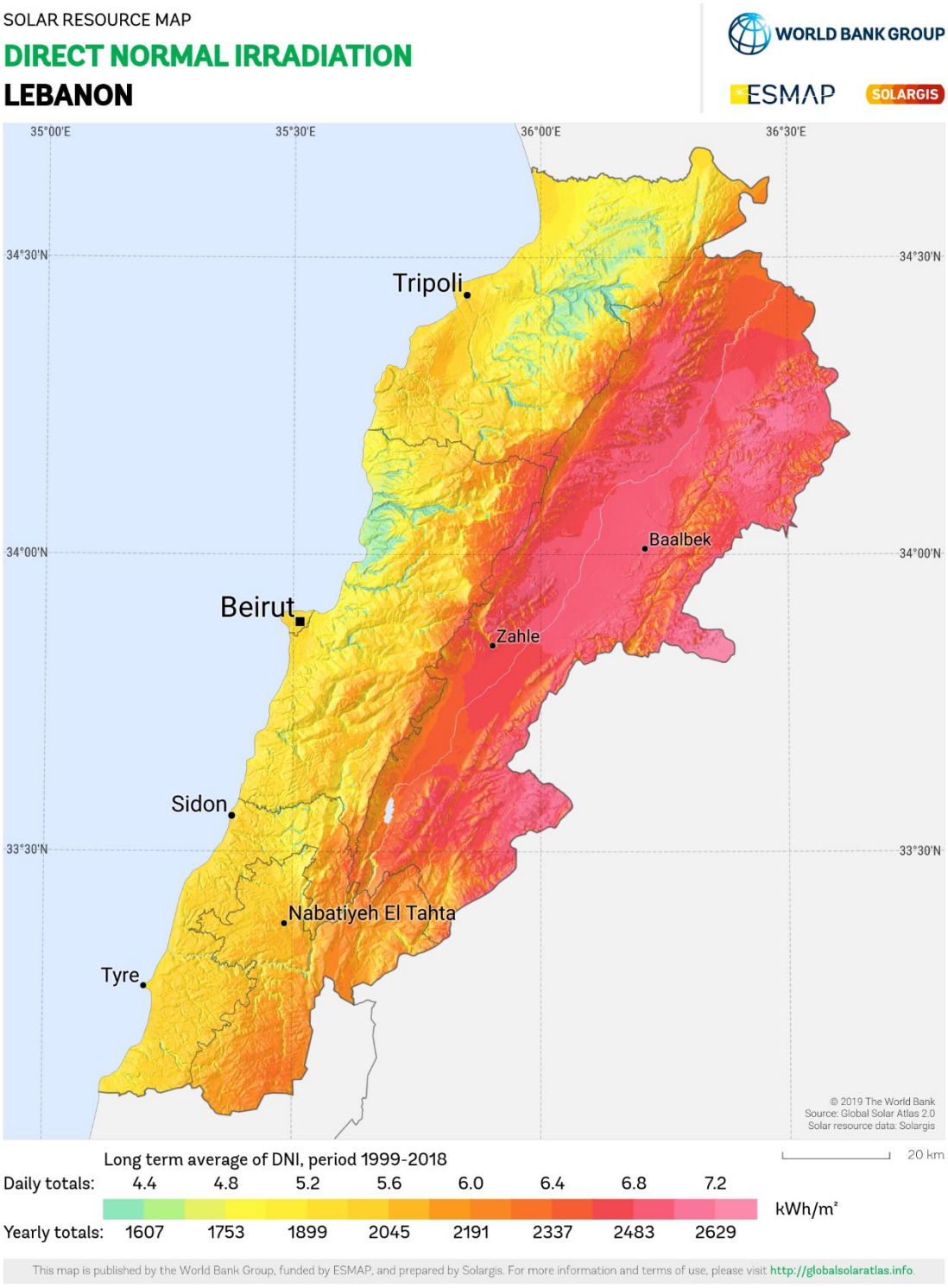

Figure 47. Lebanon's DNI Map. Source: Global Solar Atlas

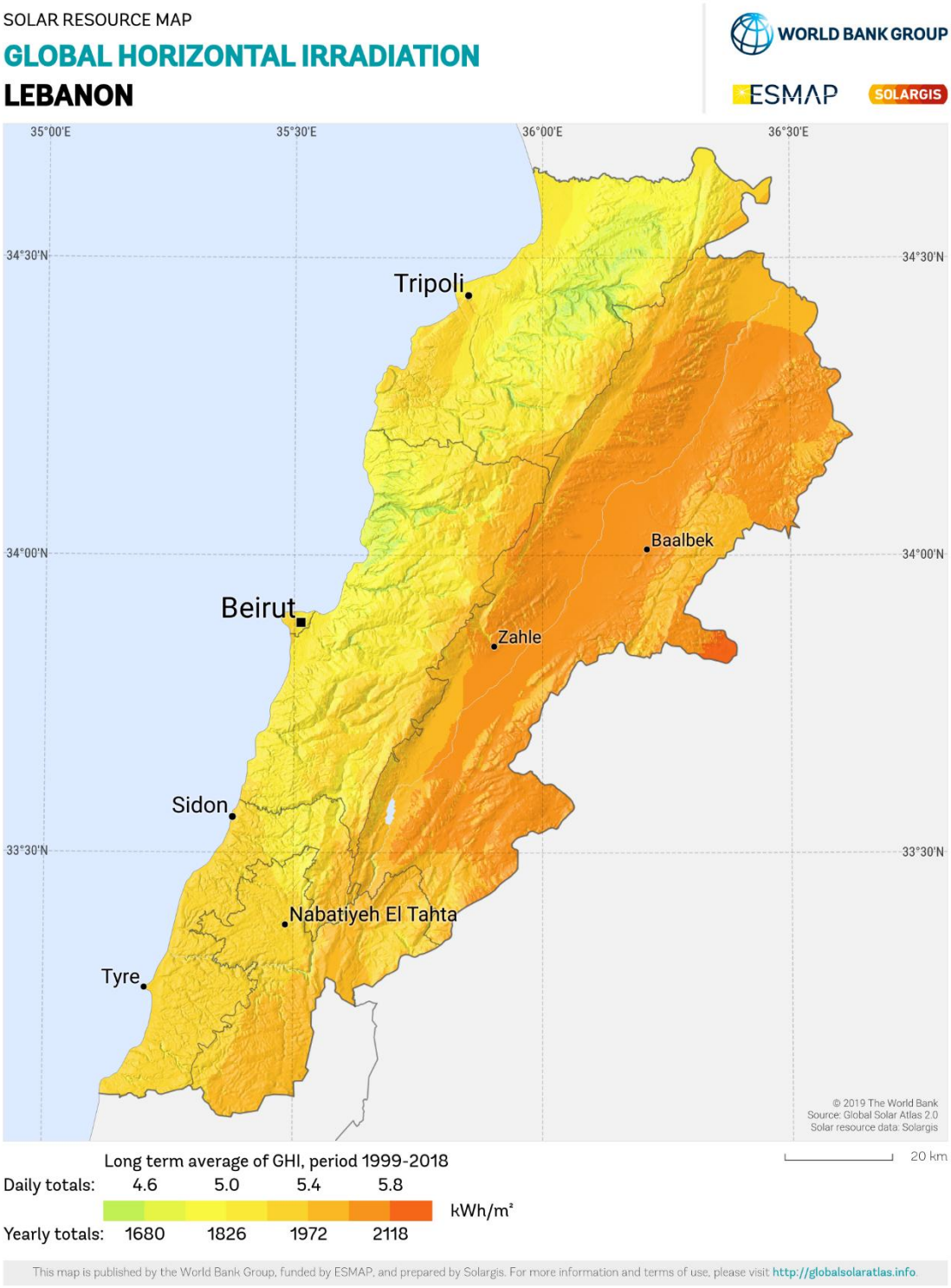

Figure 48. Lebanon's GHI Map. Source: Global Solar Atlas

APPENDIX II

ELECTRICAL TRANSMISSION NETWORK IN LEBANON

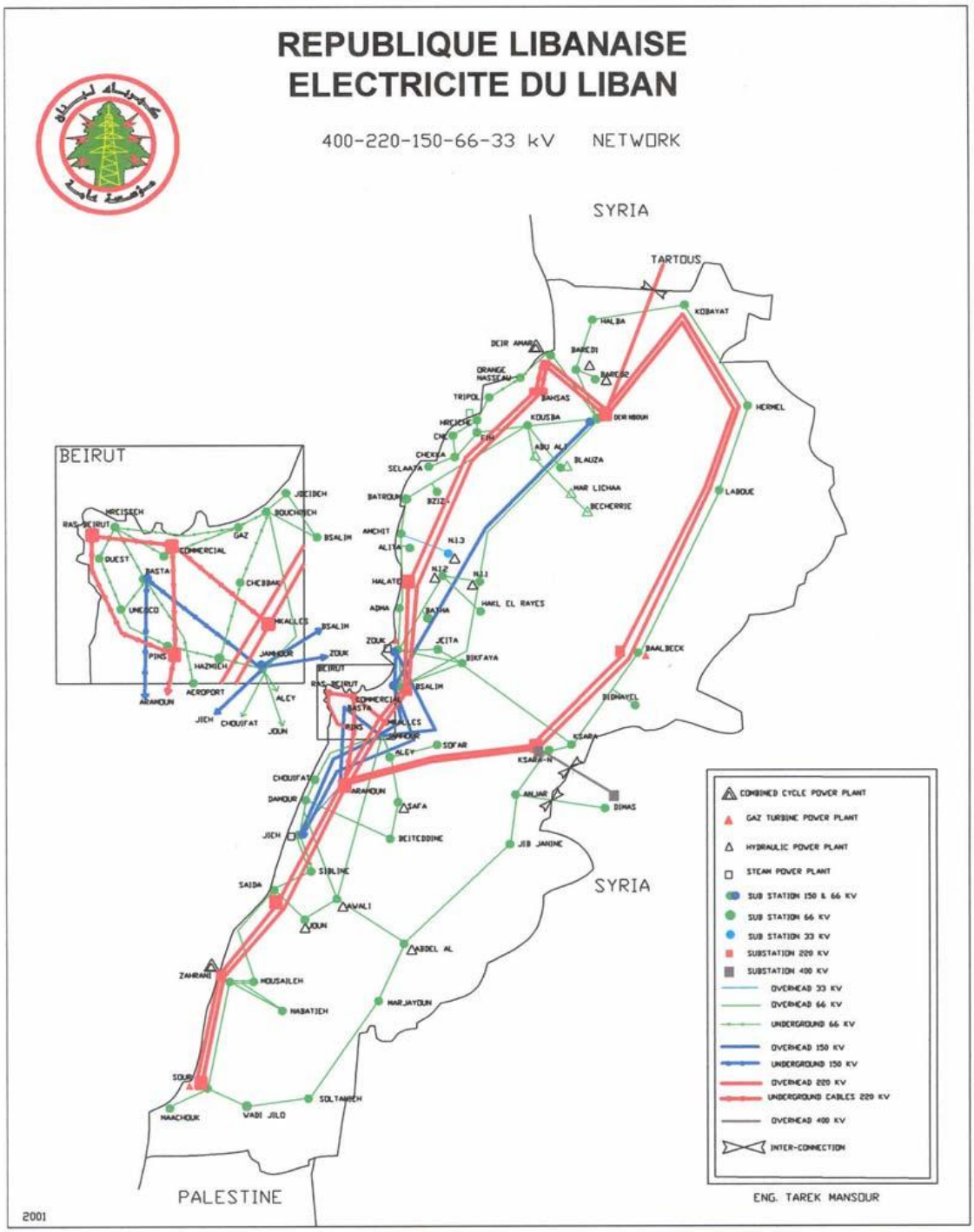

Figure 49. Electrical Transmission Network in Lebanon. Source: EDL

APPENDIX III

CSP PLANT DESIGN PARAMETERS

Table 4. Design Parameters of 50MW Parabolic Trough CSP plant

Category	**Variable**	**Value**
Plant Capacity	Plant Size	50MW
Solar Field	Solar multiple	2
	Number of loops	112
	Single loop aperture area	5,248 m^2
	Solar Field Area	363 acres
	Row Spacing (m)	15
	Number of field subsections	2
Solar Collector	Reflective aperture area	656 m2
	Width of aperture	6 m
	Length of each module	14.375 m
	Number of modules per collector assembly	8 m
	Collector assembly length	115 m
	Mirror reflectance	0.93
	Min single loop flow rate	1.75 kg/s
	Max single loop flow rate	12.8kg/s
	Min field flow velocity	0.2m/s
	Max field flow velocity	1.6m/s
Solar Collector	Surface to focal path length	2.15 m
	Optical efficiency	0.848
	Stow angle	170°
	Deploy angle	10°
Thermal Receiver	HTF Type	Hitec Solar Salt
	Minimum operating temperature of HTF	12℃
	Maximum operating temperature of HTF	400℃
	Design loop inlet temperature	290℃
	Design loop outlet temperature	565℃
Thermal Energy Storage (TES)	TES full load storage hours	6 h
	Storage fluid	Hitec Solar Salt
	Storage tanks	2
	Storage Volume	14,595.15 m3
	TES thermal capacity	936.40 MWht
Thermal Energy Storage (TES)	Storage HTF min operating temperature	238℃
	Storage HTF max operating temperature	593℃
	Storage tank heater efficiency	0.98
Power Block	Cycle thermal efficiency	0.356
	Design inlet temperature	391℃
	Design outlet temperature	293℃
	Cycle design HTF flow rate	648.6 kg/s

Power cycle	Power cycle	Rankine cycle
	Turbine inlet pressure control	Fixed pressure
	Condenser type	Evaporative
	Ambient temperature at design	10.6℃
Overall System	System AC degradation rate	0.2%

Table 5. Cost Parameters of 50MW Parabolic Trough CSP Plant

Category	**Parameter**	**Cost**	**Unit**
Direct Capital Costs	Site improvements	20	$/m2
	Solar field	120	$/m2
	HTF system	50	$/m2
	Storage	60	$/kWht
	Power plant	910	$/kWe
	Balance of plant	90	$/kWe
	Contingency	7	%
Indirect Capital Costs	Land cost	7	$/m2
	EPC and Owner cost	11	% of direct cost
	Sales tax	5	%
	Total installed cost	5,529.04	$/kW
Operational and Maintenance Costs	Fixed cost by capacity	44	$/kW-yr
	Variable cost by generation	3	$/MWhac

Table 6. System Design Parameters of 50MW Power Tower CSP Plant

Category	**Variable**	**Value**
Plant Capacity	Plant Size	50MW
System Design	Solar multiple	2
	Cycle thermal efficiency	0.38
	HTF hot temperature	565 ℃
	HTF cold temperature	290 ℃
	Full load storage hours	13 h
Heliostat Field	Heliostat width (m)	12.2
	Heliostat length (m)	12.2
	Water usage per wash (L/m2)	0.7
	Washes per year	63
Tower and Receiver	HTF Type	Salt (60% NaNO3 40% KNO3)
	Receiver Type	Stainless AISI 316
Power Cycle	Power Cycle Type	Rankine Cycle
	Condenser Type	Evaporative

	Ambient Temperature at design (℃)	10.6
	Reference condenser water dT (℃)	10
	Approach temperature (℃)	5
	Min Condenser pressure (inHg)	1.25
	Cooling system part loads levels	8
Thermal Storage	Tank height (m)	12
	Tank fluid minimum height (m)	1
	Parallel tank pairs	1
	HTF volume (m3)	8927
	Thermal energy capacity (MWt)	142
	Cold tank heater temperature set point (℃)	280
	Hot tank heater temperature set point (℃)	500

Table 7. Cost Parameters of 50MW Power Tower CSP Plant

Category	**Parameter**	**Cost**	**Unit**
Direct Capital Costs	Site Improvement Cost	16	$/m2
	Heliostat Field Cost	127	$
	Heliostat Field Cost, fixed	0	$
	Tower cost, fixed	3,000,000	$
	Receiver	56,431,155	$
	Thermal energy storage cost	22	$/kWht
	Heater cost	104	$/kWt
	Contingency	7	%
Indirect Capital Costs	Land cost	7	$/m2
	EPC and Owner cost	13	% of direct cost
	Sales tax	5	%
	Total installed cost	8,179.17	$/kW
Operational and Maintenance Costs	Fixed cost by capacity	66	$/kW-yr
	Variable cost by generation	3.5	$/MWhac

APPENDIX IV

PV PLANT DESIGN PARAMETERS

Table 8. Characteristics of the PV module, inverter, and battery

Variable	**Value**
PV Module Electrical Data at Standard Testing Conditions (STC)	
Nominal efficiency	22.3%
Max Power (Pmp)	555 Wdc
Max power voltage (Vmp)	42.1 Vdc
Max power current (Imp)	13.2 Adc
Open Circuit Voltage (Voc)	50 Vdc
Short Circuit Current (Isc)	14Adc
T_NOCT	46.6 ℃
Lifetime	25 years
Variable	Value
Inverter Characteristics	
Efficiency	97 %
Max AC power	1,042,220 Wac
Max DC power	1,076,260 Wdc
Nominal AC Voltage	480 Vac
Nominal DC Voltage	949 Vdc
Max DC voltage	1200 Vdc
Max DC current	1134.09 Adc
Min MPPT DC voltage	697 Vdc
Max MPPT DC voltage	1200 Vdc
Battery Characteristics	
Battery Type	Lithium ion (Lithium iron phosphate (LFP/ Graphite)
Desired bank power	50,000 kW
Desired bank capacity	8 h

Table 9. System Design Parameters of 50MW solar PV Farm

Category	**Variable**	**Value**
System Sizing	Nameplate DC capacity	50 MW
DC Sizing and Configuration	Number of PV modules	90,068
	Modules per string	23
	Strings in parallel	3,916
	Total module area	224,269.32m2
	String open circuit voltage	1,150 V
	String maximum power voltage	968.3 V
AC Sizing	Number of inverters	44
	DC to AC ratio	1.09

Shading and Layout	Module orientation	Portrait
	Number of modules along side row	2
	Number of modules along bottom row	23
Losses	Total DC power loss	4.44 %
	AC wiring losses	1%
	System AC degradation rate	0.5%

Table 10. Cost Parameters of 50MW Solar PV Farm

Category	**Parameter**	**Cost**	**Unit**
Direct Capital Costs	Module Cost	390	$/kWdc
	Inverter	50	$/kWdc
	Balance of System Equipment	270	$/kWdc
	Labor Cost	180	$/kWdc
	Installer Margin and Overhead	120	$/kWdc
	Contingency	3	%
Indirect Capital Costs	Land cost	7	$/m2
	Sales tax	5	%
	Total installed cost	2,840	$/kWdc
Operational and Maintenance Costs	PV Fixed cost by capacity	15	$/kWdc-yr
	Battery Fixed cost by capacity	5.3	$/kWhdc
	Battery replacement cost	323	$/kWhdc

APPENDIX V

PV MODULE AND INVERTER DATASHEETS

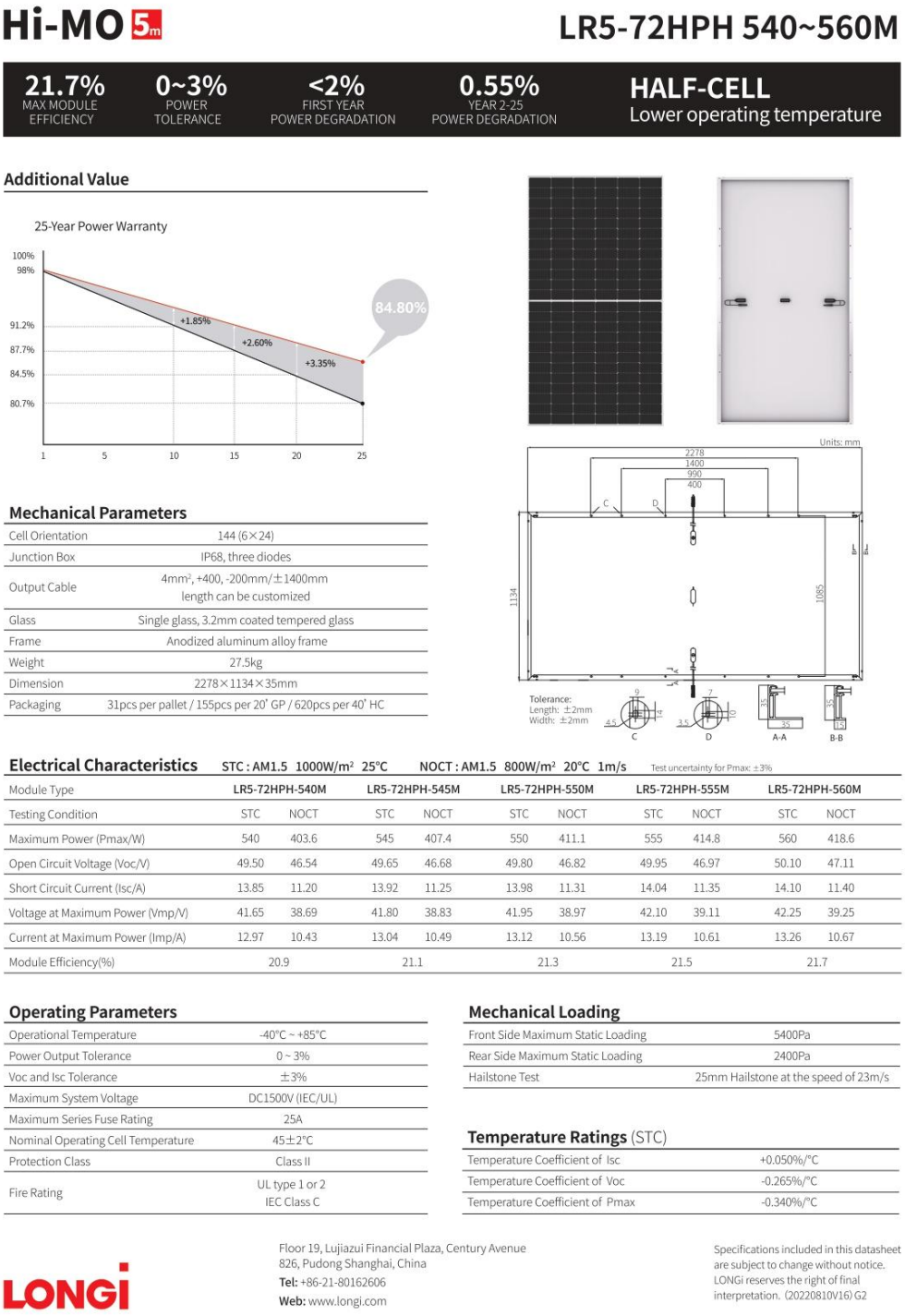

Hi-MO 5m

LR5-72HPH 540~560M

21.7%	0~3%	<2%	0.55%	HALF-CELL
MAX MODULE EFFICIENCY	POWER TOLERANCE	FIRST YEAR POWER DEGRADATION	YEAR 2-25 POWER DEGRADATION	Lower operating temperature

Additional Value

25-Year Power Warranty

Mechanical Parameters

Cell Orientation	144 (6×24)
Junction Box	IP68, three diodes
Output Cable	4mm², +400, -200mm/±1400mm length can be customized
Glass	Single glass, 3.2mm coated tempered glass
Frame	Anodized aluminum alloy frame
Weight	27.5kg
Dimension	2278×1134×35mm
Packaging	31pcs per pallet / 155pcs per 20' GP / 620pcs per 40' HC

Electrical Characteristics STC : AM1.5 1000W/m² 25°C NOCT : AM1.5 800W/m² 20°C 1m/s Test uncertainty for Pmax: ±3%

Module Type	LR5-72HPH-540M		LR5-72HPH-545M		LR5-72HPH-550M		LR5-72HPH-555M		LR5-72HPH-560M	
Testing Condition	STC	NOCT	STC	NOCT	STC	NOCT	STC	NOCT	STC	NOCT
Maximum Power (Pmax/W)	540	403.6	545	407.4	550	411.1	555	414.8	560	418.6
Open Circuit Voltage (Voc/V)	49.50	46.54	49.65	46.68	49.80	46.82	49.95	46.97	50.10	47.11
Short Circuit Current (Isc/A)	13.85	11.20	13.92	11.25	13.98	11.31	14.04	11.35	14.10	11.40
Voltage at Maximum Power (Vmp/V)	41.65	38.69	41.80	38.83	41.95	38.97	42.10	39.11	42.25	39.25
Current at Maximum Power (Imp/A)	12.97	10.43	13.04	10.49	13.12	10.56	13.19	10.61	13.26	10.67
Module Efficiency(%)	20.9		21.1		21.3		21.5		21.7	

Operating Parameters

Operational Temperature	-40°C ~ +85°C
Power Output Tolerance	0 ~ 3%
Voc and Isc Tolerance	±3%
Maximum System Voltage	DC1500V (IEC/UL)
Maximum Series Fuse Rating	25A
Nominal Operating Cell Temperature	45±2°C
Protection Class	Class II
Fire Rating	UL type 1 or 2 IEC Class C

Mechanical Loading

Front Side Maximum Static Loading	5400Pa
Rear Side Maximum Static Loading	2400Pa
Hailstone Test	25mm Hailstone at the speed of 23m/s

Temperature Ratings (STC)

Temperature Coefficient of Isc	+0.050%/°C
Temperature Coefficient of Voc	-0.265%/°C
Temperature Coefficient of Pmax	-0.340%/°C

LONGi

Floor 19, Lujiazui Financial Plaza, Century Avenue 826, Pudong Shanghai, China
Tel: +86-21-80162606
Web: www.longi.com

Specifications included in this datasheet are subject to change without notice. LONGi reserves the right of final interpretation. (20220810V16) G2

Figure 50. Selected PV module datasheet

INGECON SUN — Power B Series 1,500 Vdc

	1170TL U B450	1245TL U B480	1400TL U B540	1500TL U B578	1560TL U B600	1600TL U B615
Input (DC)						
Recommended PV array power range[1]	1,157 - 1,520 kWp	1,234 - 1,622 kWp	1,389 - 1,824 kWp	1,486 - 1,952 kWp	1,543 - 2,027 kWp	1,581 - 2,077 kWp
Voltage Range MPP[2]	645 - 1,300 V	686 - 1,300 V	769 - 1,300 V	822 - 1,300 V	853 - 1,300 V	873 - 1,300 V
Maximum voltage[3]	1,500 V					
Maximum current	1,870 A					
Nº inputs with fuse-holders	6 up to 12 (up to 15 if the combiner box is not integrated)					
Fuse dimensions	63 A / 1,500 V to 500 A / 1,500 V fuses (optional)					
Type of connection	Connection to copper bars					
Power blocks	1					
MPPT	1					
Input protections						
Overvoltage protections	Type II surge arresters					
DC switch	Motorized DC load break disconnect					
Other protections	Integrated DC combiner box / Up to 12 pairs of DC fuses (optional) / Reverse polarity / Insulation failure monitoring / Anti-islanding protection / Emergency pushbutton					
Output (AC)						
Power @86 ºF / @122 ºF	1,169 kVA / 1,052 kVA	1,247 kVA / 1,122 kVA	1,403 kVA / 1,263 kVA	1,502 kVA / 1,352 kVA	1,559 kVA / 1,403 kVA	1,598 kVA / 1,438 kVA
Current @86 ºF / @122 ºF	1,500 A / 1,350 A					
Rated voltage	450 V IT System	480 V IT System	540 V IT System	578 V IT System	600 V IT System	615 V IT System
Frequency	50 / 60 Hz					
Power Factor[4]	1					
Power Factor adjustable	Yes, 0-1 (leading / lagging)					
THD (Total Harmonic Distortion)[5]	<3%					
Output protections						
Overvoltage protections	Type II surge arresters					
AC breaker	Motorized AC circuit breaker					
Anti-islanding protection	Yes, with automatic disconnection					
Other protections	AC short-circuits and overloads					
Features						
Maximum efficiency	98.9%					
CEC	98.5%					
Max. consumption aux. services	4,700 W (25 A)					
Stand-by or night consumption[6]	90 W					
Average power consumption per day	2,000 W					
General Information						
Operational temperature range	-4 ºF to +135 ºF (operational temperature range expandable from -40 ºF to +135 ºF)					
Relative humidity (non-condensing)	0-100%					
Protection class	NEMA 3R (NEMA 3 with the sand trap kit)					
Maximum altitude	14,770 ft (for installations beyond 3,300 ft, please contact Ingeteam's solar sales department)					
Cooling system	Air forced with temperature control (230 V phase+ neutral power supply)					
Air flow range	0 - 84 ft³/s (0 - 7,800 m³/h)					
Average air flow	45 ft³/s (4,200 m³/h)					
Acoustic emission (100% / 50% load)	<66 dB(A) at 33 ft / <54.5 dB(A) at 33 ft					
Marking	CE, SGS					
EMC and security standards	UL1741, FCC Part 15, IEEE C37.90.1, IEEE C37.90.2, CSA22.2 No107					
Grid connection standards	IEC 62116, UL1741SA, IEEE1547, IEEE1547.1, NEC CODE, Rule 21, Rule 14H, CSA22.2 No107					

Notes: [1] Depending on the type of installation and geographical location. Data for STC conditions [2] Vmpp.min is for rated conditions (Vac=1 p.u. and Power Factor=1) and floating PV systems [3] Consider the voltage increase of the 'Voc' at low temperatures [4] For Pout>25% of the rated power [5] For Pout>25% of the rated power and voltage in accordance with IEC 61000-3-4 [6] Consumption from PV field when there is PV power available.

Ingeteam

Figure 51. Selected inverter datasheet

REFERENCES

Ahmad, M., Zeeshan, M., 2022. Multi-objective optimization of concentrated solar power plants from an energy-water-environment nexus perspective under distinct climatic conditions – Part A: Techno-economic analysis. J Clean Prod 375. https://doi.org/10.1016/j.jclepro.2022.134099

Awan, A.B., Zubair, M., Praveen, R.P., Bhatti, A.R., 2019. Design and comparative analysis of photovoltaic and parabolic trough based CSP plants. Solar Energy 183, 551–565. https://doi.org/10.1016/j.solener.2019.03.037

Ayat, C., 2021. Bridging the Banking Crisis to Crowdfund Electricity Reform in Lebanon.

Ayoub, M., Rizkallah, P., Haidar, C.A., 2021. Unbundling Lebanon's Electricity Sector Research Report About the Institute for Global Prosperity.

Berjawi, A.H., Najem, S., Faour, G., Abdallah, C., Ahmad, A., 2016. ASSESSING SOLAR PV's Potential in Lebanon.

BouKather, C.A., 2023. Re-energize Lebanon: 5 Action Steps to Rebuilding Lebanon's Collapsed Electricity Sector.

CEDRO, 2016. Solar PV Grid Interconnection Code for Lebanon: Recommendations And Guidelines.

CEDRO, 2013. Concentrated Solar Plants.

Cole, W., Karmakar, A., 2023. Cost Projections for Utility-Scale Battery Storage: 2023 Update. Golden, CO.

Darbha, D., Jha, M., Kanodia, A., Imam, R., 2023. Comparative Study of Concentrated Solar Power Technologies for Storage and Location. International Journal of High School Research 5, 17–21. https://doi.org/10.36838/v5i3.4

Diorio, N., Dobos, A., Janzou, S., Nelson, A., Lundstrom, B., 2015. Technoeconomic Modeling of Battery Energy Storage in SAM.

Gilman, P., 2015. SAM Photovoltaic Model Technical Reference.

Hossain, Md.S., Rahat, Md.A.I., Khan, Md.S.H., Shajid, S., Salehin, S., Karim, Md.R., 2024. Techno-economic assessment of various concentrating solar power (CSP) technologies for large-scale sustainable power generation in Bangladesh. Energy Convers Manag 321, 119079. https://doi.org/10.1016/j.enconman.2024.119079

IEA, 2025. Solar PV power capacity in the Net Zero Scenario, 2015-2030 [WWW Document]. URL https://www.iea.org/data-and-statistics/charts/solar-pv-power-capacity-in-the-net-zero-scenario-2015-2030 (accessed 2.4.25).

IEA, 2011. Solar energy perspectives. OECD/IEA.

Imam, A.A., Abusorrah, A., Marzband, M., 2024. Potentials and opportunities of solar PV and wind energy sources in Saudi Arabia: Land suitability, techno-socio-economic feasibility, and future variability. Results in Engineering 21. https://doi.org/10.1016/j.rineng.2024.101785

IMF, 2025. https://data.imf.org/ [WWW Document].

IRENA, 2025. Global Atlas for Renwable Energy [WWW Document]. URL https://globalatlas.irena.org/workspace (accessed 2.11.25).

IRENA, 2024a. Renewable Capacity Statistics 2024.

IRENA, 2024b. Renewable Power Generation Costs in 2023.

IRENA, 2016. The Power to Change: Solar and Wind Cost Reduction Potential to 2025.

Kearney, D., Kelly, B., Herrmann, U., Cable, R., Pacheco, J., Mahoney, R., Price, H., Blake, D., Nava, P., Potrovitza, N., 2004. Engineering aspects of a molten salt heat

transfer fluid in a trough solar field. Energy 29, 861–870. https://doi.org/10.1016/S0360-5442(03)00191-9

Khan, M.I., Gutiérrez-Alvarez, R., Asfand, F., Bicer, Y., Sgouridis, S., Al-Ghamdi, S.G., Jouhara, H., Asif, M., Kurniawan, T.A., Abid, M., Pesyridis, A., Farooq, M., 2024. The economics of concentrating solar power (CSP): Assessing cost competitiveness and deployment potential. Renewable and Sustainable Energy Reviews. https://doi.org/10.1016/j.rser.2024.114551

LCEC, 2016. The National Renewable Energy Action Plan for the Republic of Lebanon NREAP 2016-2020.

LCEC, 2012. The National Energy Efficiency Action Plan for Lebanon NEEAP 2011-2015.

Liu, T., Yang, J., Yang, Z., Duan, Y., 2022. Techno-economic feasibility of solar power plants considering PV/CSP with electrical/thermal energy storage system. Energy Convers Manag 255. https://doi.org/10.1016/j.enconman.2022.115308

Noor Abu Dhabi, 2025. Noor Abu Dhabi [WWW Document]. URL https://noorabudhabi.ae/ (accessed 2.16.25).

NREL, 2024a. SAM Advisory Model Help [WWW Document]. URL https://sam.nrel.gov/financial-models/utility-scale-ppa (accessed 8.2.24).

NREL, 2024b. System Advisor Model (SAM) [WWW Document]. URL https://sam.nrel.gov/ (accessed 11.4.24).

NREL, 2017. Modeling Molten Salt Power Tower Systems in SAM 2017.

NREL, 2003. Assessment of Parabolic Trough and Power Tower Solar Technology Cost and Performance Forecasts. Chicago, Illinois.

Poole, I.V., 2017. Concentrating solar power in South Africa-a comparison between parabolic trough and power tower technologies with molten salt as heat transfer fluid. Stellenbosch University, Stellenbosch, South Africa.

Praveen, R.P., Abdul Baseer, M., Nampoothiri, S.K., 2018. Design, Performance Analysis and Optimization of a 100 MW Concentrated Solar Power Plant with Thermal Energy Storage. Institute of Electrical and Electronics Engineers.

Shabbir, M.N.S.K., Chowdhury, M.S.A., Liang, X., 2018. A guideline of feasibility analysis and design for concentrated solar power plants. Canadian Journal of Electrical and Computer Engineering. https://doi.org/10.1109/CJECE.2018.2885016

UNDP, 2017. Lebanon: Derisking Renewable Energy Investment. New York, NY.

UNFCC, 2020. Lebanon's Nationally Determined Contribution Updated 2020 Version.

US Department of Commerce, African Development Bank, 2013. Understanding Power Purchase Agreements.

Wagner, M.J., Kutscher, C., 2010. The impact of hybrid Wet/Dry cooling on concentrating solar power plant performance, in: ASME 2010 4th International Conference on Energy Sustainability, ES 2010. pp. 675–682. https://doi.org/10.1115/ES2010-90442

World Bank, 2021. Concentrating Solar Power: Clean Power on Demand 24/7. Washington, DC.

Yang, P., 2024. Renewable energy: Challenges and solutions, Renewable Energy: Challenges and Solutions. Springer International Publishing. https://doi.org/10.1007/978-3-031-49125-2

Yuan, X., Zuo, J., Ma, C., 2011. Social acceptance of solar energy technologies in China—End users' perspective. Energy Policy 39, 1031–1036. https://doi.org/10.1016/J.ENPOL.2011.01.003